MODELLING OF AIRGAP ECCENTRICITY IN INDUCTION MOTOR

A thesis is submitted to fulfil the requirement of the degree

Master in Electrical Engineering

Submitted by

Mohammad Aadil Hasan

Examination Roll no. – **M4ELE23017**

Registration no. – **160166** of **2021-2022**

Under the guidance of

Dr. Susanta Ray

and

Prof. Arabinda Das

Electrical Engineering Department

Jadavpur University

Kolkata – 700 032

Faculty of Engineering and Technology
Jadavpur University, Kolkata – 700032

Certificate

This is to certify that the thesis entitled **'Modelling of Air Gap Eccentricity in Induction Motor'**, submitted by **Mr. Mohammad Aadil Hasan** (Examination Roll No. M4ELE23017), under our supervision and guidance during the session of 2021-23 in the department of Electrical Engineering, Jadavpur University. We are satisfied with his work, which is being presented for the partial fulfilment of the degree of **Master in Electrical Engineering** from Jadavpur University, Kolkata-700 032.

Susanta Ray 12/06/23

Dr. Susanta Ray
Associate Professor
Department of Electrical Engineering
Jadavpur University
Kolkata- 700032

Associate Professor
Electrical Engg. Dept.
Jadavpur University
Kolkata - 700 032

Arabinda Das 12/06/23

Dr. Arabinda Das
Professor
Department of Electrical Engineering
Jadavpur University
Kolkata- 700 032

Professor
Electrical Engineering Department
JADAVPUR UNIVERSITY
Kolkata - 700 032

Ardhendu Ghoshal 14/06/23

Prof. Ardhendu Ghoshal
Dean of Faculty Council of
Engineering and Technology
Jadavpur University
Kolkata- 700032

DEAN
Faculty of Engineering & Technology
JADAVPUR UNIVERSITY
KOLKATA-700 032

14/06/2023

Prof. Biswanath Roy
Head of the Department of
Electrical Engineering
Jadavpur University
Kolkata- 700032

Head
Electrical Engineering Department
JADAVPUR UNIVERSITY
Kolkata - 700 032

Faculty of Engineering and Technology
Jadavpur University, Kolkata - 700032

Certificate of Approval

The forgoing thesis entitled **'Modelling of Air Gap Eccentricity in Induction Motor'** is hereby approved as a creditable study of an Engineering subject carried out and presented in a manner that fulfils its acceptance as a prerequisite to the degree for which it is submitted. It is understood that by this approval, the undersigned does not necessarily endorse or approve any statement made, opinion expressed, or conclusion drawn therein but approves the thesis only for the purpose for which it is submitted.

The final examination for evaluation of the thesis

Signature of the examiners

……

……

……

Declaration of Originality

I hereby declare that this thesis contains a literature survey and original research work done by me. All the information in this document has been obtained and presented according to academic rules and ethical conduct. I also declare that, as required by these rules and conduct, I have fully cited and referenced all material and results that are not original to this work.

Name: Mohammad Aadil Hasan

Examination Roll No: M4ELE23017

Thesis Title: Modelling of Air Gap Eccentricity in Induction Motor

ACKNOWLEDGEMENTS

I express my sincere gratitude to my supervisor, **Dr. Susanta Ray** for his encouragement, suggestion and advice, without which it would not have been possible to complete my thesis successfully. I would like to thank **Prof. Arabinda Das** for being a constant source of encouragement, inspiration and for his valuable suggestions coupled with his technical expertise throughout my research work. It was a great honour for me to pursue my research under his supervision.

I would also like to thank my co-worker Tapas Sadhukhan, and all the staff of the Drives and Simulation laboratory, and the research scholars of our department for providing constant encouragement throughout my thesis work.

Last but not least I extend my words of gratitude to my parents for personally motivating me to carry out the work smoothly.

Signature with Date: Md. Aadil Hasan 12/06/23

ABSTRACT

The thesis Models Air Gap Eccentricity of Induction Motor under simple eccentricity profiles viz. Elliptical, Sinusoidal and Stepped profiles. First of all a model of Induction Motor is developed under transient state and then a Thevenin Equivalent Circuit is developed from Steady State Circuit Articulated by IEEE using simple Circuit Analysis technique and then Induction Motor model is developed under Steady state at No Load condition. For Induction Motor development all the equations are derived using DQ transformation from the scratch and their Torque and Rotor Angular speed are plotted. Afterwards of Induction Motor model development, simple eccentricity profiles are studied. Their basic code is written by applying eccentricity at rotor side and plotting stator and rotor current difference for the sake of profile understanding. Then these models are deployed in the dynamic model of Induction Motor and the variance in parameters are observed with variance of eccentricity profile. The order magnitude of Eccentricity profiles are adjusted to get relevant results**. All the coding and plotting is done in MATLAB2023a environment. Whenever acronyms are used they are specified also plots are given figure number in proper sequence in relevant place.**

Chapter No.	CONTENTS	Page No.
	Acknowledgment	
	Abstract	
1	**Introduction and Literature Review**	**1-4**
1.1	History of Induction Motor	1
1.2	Motivation of Work	2
1.3	Literature Review	3-4
1.4	Organization of the Thesis	4
2	**Induction Motor**	**5-22**
2.1	Construction of Induction Motor	6-7
2.1.1	Stator Construction	7-10
2.1.2	Rotor Construction	11-12
2.1.3	Stator frame, Fan and Fan Cover	14-15
2.2	Working Principle Induction Motor	16-18
2.3	Faults in Induction Motor	19-22
3	**DQ Modelling**	**23-44**
3.1	Introduction	23
3.2	Purpose of DQ Modelling	23-24
3.3.1	Induction Motor Dynamic Equation Derivation of DQ Modelling	25-29
3.3.2	MATLAB Implementation of DQ Modelling under transient condition	30-35
3.3.3	Induction Motor Stead State Model at No Load Torque	36-40
3.3.4	MATLAB Implementation of Induction Motor at steady state	41-44
4	**Air Gap Eccentricity**	**45-61**
4.1	Types of Air Gap Eccentricity	46
4.2	Causes of Air Gap Eccentricity	47-48
4.3	Significance of Air Gap Eccentricity	49
4.4	Detection of Air Gap Eccentricity	50-51
4.5	Air Gap Eccentricity Profiles	52-61
5	**Modelling of Air Gap Eccentricity in Induction Motor**	**62-86**

Chapter 1

Introduction and Literature Review

Introduction

Several industries, including power generation, transportation, and industrial automation, depend heavily on electrical machinery. The most common type of electrical machine utilized in industry is the induction motor. Air gap eccentricity is one of several parameters that affect an induction motor's performance and dependability. The term "air gap eccentricity" describes the displacement of the rotor's location from the stator's center, which results in a non-uniform air gap between the two components. The goal of this literature review is to examine the research that has already been done on electrical machine air gap eccentricity, emphasizing its sources, impacts, detection techniques, and mitigation approaches.

1.1 History of Induction Motor

François Arago, a French physicist, proposed the presence of rotating magnetic fields in 1824. These rotations were known as Arago's rotations. Walter Baily showed the first rudimentary induction motor in 1879 by manually turning switches on and off. Ottó Bláthy, a Hungarian engineer, created the first single-phase AC induction motor without a commutator, which he used to power his creation, the electricity meter. Galileo Ferraris and Nikola Tesla separately developed the first AC commutator-free poly-phase induction motors, with the former demonstrating a functional motor model in 1885 and the latter in 1887. In October and November 1887, Tesla submitted applications for US patents; some of these applications were accepted in May 1888. Ferraris's study on his AC poly-phase motor, which outlined the principles of motor functioning, was published in April 1888 by the Royal Academy of Science of Turin. Tesla presented three different types of four-stator, four-pole motors to the American Institute of Electrical Engineers (AIEE) in May 1888. The first type had a four-pole rotor that formed a non-self-starting reluctance motor, the second type had a wound rotor that formed a self-starting induction motor, and the third type was a true synchronous motor with a separately excited DC supply to the rotor winding. In 1888, George Westinghouse, who was then working on an AC power system, bought a US patent option on Ferraris' induction motor design and licenced Tesla's patents. Tesla worked as a consultant for one year as well. C. F. Scott, a Westinghouse employee, was tasked with helping Tesla and

eventually took over Westinghouse's induction motor research. Mikhail Dolivo-Dobrovolsky created the cage-rotor induction motor in 1889 and the three-limb transformer in 1890 while steadfastly advocating for three-phase advancement. Additionally, he asserted that Tesla's motor was impractical due to two-phase pulsations, which led him to continue working on three-phase systems. Despite creating the first workable induction motor in 1892 and creating a series of polyphase 60 hertz induction motors in 1893, Westinghouse's early motors had winded two-phase rotors until B. G. Lamme created a revolving bar winding rotor. Induction motors with three phases were first developed by the General Electric Company (GE) in 1891. A cross-licensing deal for the bar-winding-rotor design, subsequently known as the squirrel-cage rotor, was struck by General Electric and Westinghouse in 1896. In order to identify the 90o rotation operator in the analysis of AC issues, Arthur E. Kennelly was the first to fully realise the relevance of complex numbers (using j to denote the square root of negative one). Application of AC complex values was substantially advanced by Charles Proteus Steinmetz of GE, who also created an analytical model known as the induction motor Steinmetz equivalent circuit. A 100-horsepower induction motor today has the same mounting dimensions as a 7.5-horsepower motor in 1897 thanks to advancements in induction motor technology brought about by these breakthroughs and discoveries.

1.2 Motivation of Work

The induction despite being rugged and hard to breakdown are prone to mechanical faults and these mechanical faults can produced unwanted results. The mechanical fault of induction motor may have several reasons like construction fault, misalignment of machinery parts. Air Gap Eccentricity is a problem that is prevalent.

Although, there are many researches done to detect Air Gap Eccentricity and mitigate its effect. They are hardly any modelling of Air Gap Eccentricity on Induction Motor is done. Which motivates researcher to formulate Air Gap Eccentricity in mathematical profile, Model them and then analyze motor parameters.

This thesis work is all about simple eccentric profile Implementation in Induction Motor and seeing the variance of parameters with respect to the eccentricity. The eccentricity profile are adjusted mathematically to obtain the relevant plots. So the value of eccentricity are take in accordance order of magnitude.

1.3 Literature Review

Numerous factors, including as production flaws, thermal expansion, bearing wear, or outside mechanical forces, can cause air gap eccentricity. Eccentricity can be caused by differences in the alignment of the rotor and stator, which can occur as a result of manufacturing faults during the building of electrical machines. Temperature variations can also alter the relative locations of the rotor and stator due to differential thermal expansion between them. Air gap eccentricity can also be a result of bearing or other mechanical component wear.

Induction Motor' dependability and performance can be significantly impacted by air gap eccentricity. It causes magnetic asymmetry, which modifies the distribution of the magnetic field in the air gap. Uneven flux density, higher iron losses, and localized heating are the effects of this magnetic asymmetry. Air gap eccentricity results in imbalanced radial and tangential magnetic forces, which can result in mechanical strains, vibrations, and noise. The machine's electromagnetic performance, including torque ripple, efficiency, and power factor, is also impacted by the modified magnetic field distribution.

For the purpose of avoiding equipment failures and enhancing performance, accurate air gap eccentricity detection and diagnosis are essential. For the detection of air gap eccentricity, a number of approaches have been suggested and investigated. Traditional methods include shaft displacement monitoring, air gap flux density measuring, and vibration analysis. Vibration analysis makes use of variations in vibration patterns to spot eccentricity. Sensors are utilised to monitor the magnetic field distribution and spot variations brought on by eccentricity during the air gap flux density measuring process. Displacement sensors are used in shaft displacement monitoring to track the relative movement of the rotor and stator.

In order to lessen the impacts of air gap eccentricity in electrical devices, a number of techniques have been put forth. Active approaches use extra control algorithms or change the Motor's settings to actively regulate the eccentricity. These techniques frequently rely on in-the-moment feedback and monitoring devices to continually adjust the eccentricity. To reduce the effects of eccentricity, passive solutions emphasize improving the machine's mechanical and structural design. This may entail enhancing bearing system performance, dampening method implementation, or better alignment precision during production.

In Induction Motor, air gap eccentricity is a serious problem that can have an impact on reliability, performance, and efficiency. An overview of the origins,

consequences, and various approaches for detection and mitigating air gap eccentricity have been presented in this literature review. In order to improve the performance and reliability of electrical machines in the presence of air gap eccentricity, more study is required to create sophisticated detection systems and strong mitigation tactics.

1.4 Organization of the thesis

Entire thesis is organized in 6 chapter.

- Chapter 1 is all about introduction, history of Induction Motor and literature related to research area of thesis.
- Chapter 2 is all about Induction Motor construction, working principle, faults, and faults detection method discussion.
- Chapter 3 is all about DQ Methodology of axial transformation. Which is then applied to model dynamic simulation of Induction Motor under transient as well as under Steady State at No Load condition.
- Chapter 4 is all about Air Gap Eccentricity types, causes, significance, detection techniques and simple eccentricity profiles
- Chapter 5 is all about Modelling of Air Gap Eccentricity in Induction Motor using simple eccentricity profiles and plotting its parameters.
- Chapter 6 is all about contribution towards the work and future scope of work that can be done in the related area.

Chapter 2

Induction Motor

Electrical Machines are an essential component of daily living. They are utilised in several industries, including power generation, the paper industry, the oil fields, manufacturing, etc., as crucial components in electromechanical energy conversion. Because of its robust design, low price, superior speed regulation, strong start torque, high efficiency, and adaptability, induction motors are the electrical devices that are utilised in industry the most. About 30 to 40 percent of the electrical energy produced is used by induction motors. Induction motors are frequently referred to as the workhorse of the industry due to their significant contributions.

2.1. Construction of Induction Motor

A three-phase AC supply is used to power a three-phase induction motor, which operates on the basis of Faraday's law of electromagnetic induction and, because it is a motor, transforms electrical energy into mechanical energy. These are the key components of a three-phase induction motor. Where its numerous sections are divided, which are likewise depicted in figure 2.1.

1. **Stator**
2. **Rotor**
3. **Stator Frame or Motor Body**
4. **Fan**
5. **Fan Cover**

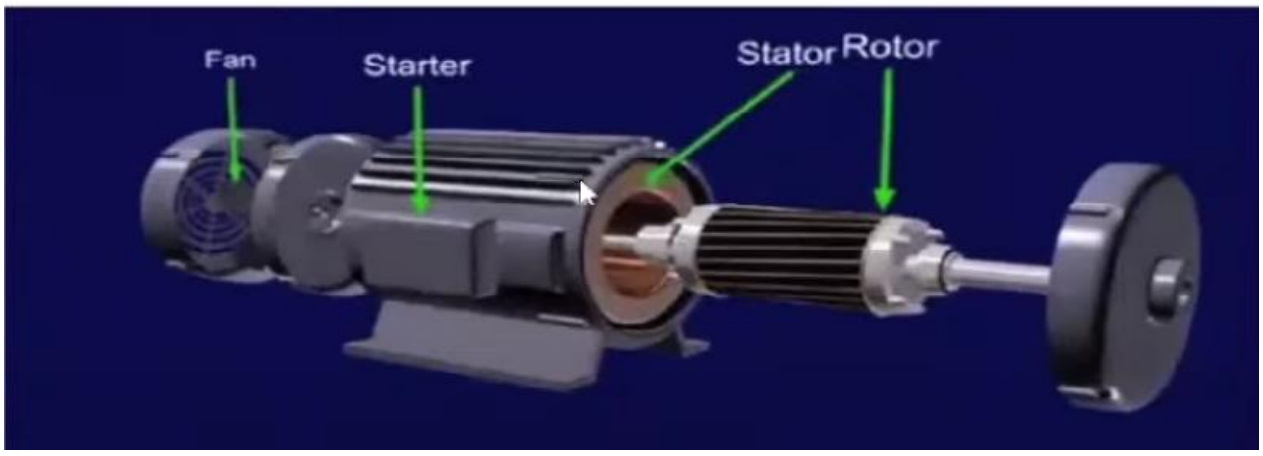

Figure 2.1

2.1.1. Stator

Figure 2.1.1

The stator, as its name implies, is the motor's immovable component. To minimize eddy current losses, it is composed of high-grade alloy steel lamination. Figure 2.1.1 depicts the steel lamination that is layered up. A presser machine is used to bind these laminations together. A stator frame or motor body constructed of cast iron or manufactured steel supports these steel laminations. As the length of the stack increases, resistance will likewise rise, which will lead to a decrease in eddy current because resistance is directly proportional to length. As a result, as the number of laminations grows, the conductor's length increases and its resistance rises. This decreases eddy current and, thus, eddy current losses. These laminations have inner peripheral slots. The number of slots in the internal peripheral is depicted in the figure. The

stator frame or motor body, which we saw in the preceding illustration, supports these laminations. Cast iron or steel-fabricated components make up the stator frame and motor body. The stator is really supported or strengthened by this motor body. Additionally, it aids in protecting the stator from harm. The slots are filled with the insulated stator conductors. They are constructed of copper, however they can also be made of Aluminium. However, copper is mostly utilized for industrial purposes. These conductors are isolated from one another before being inserted into the slots to create the three phase windings. These windings can now be joined in a star or a delta configuration. So, this is the stator's fundamental design and the material that it is made of.

2.1.2 Rotor

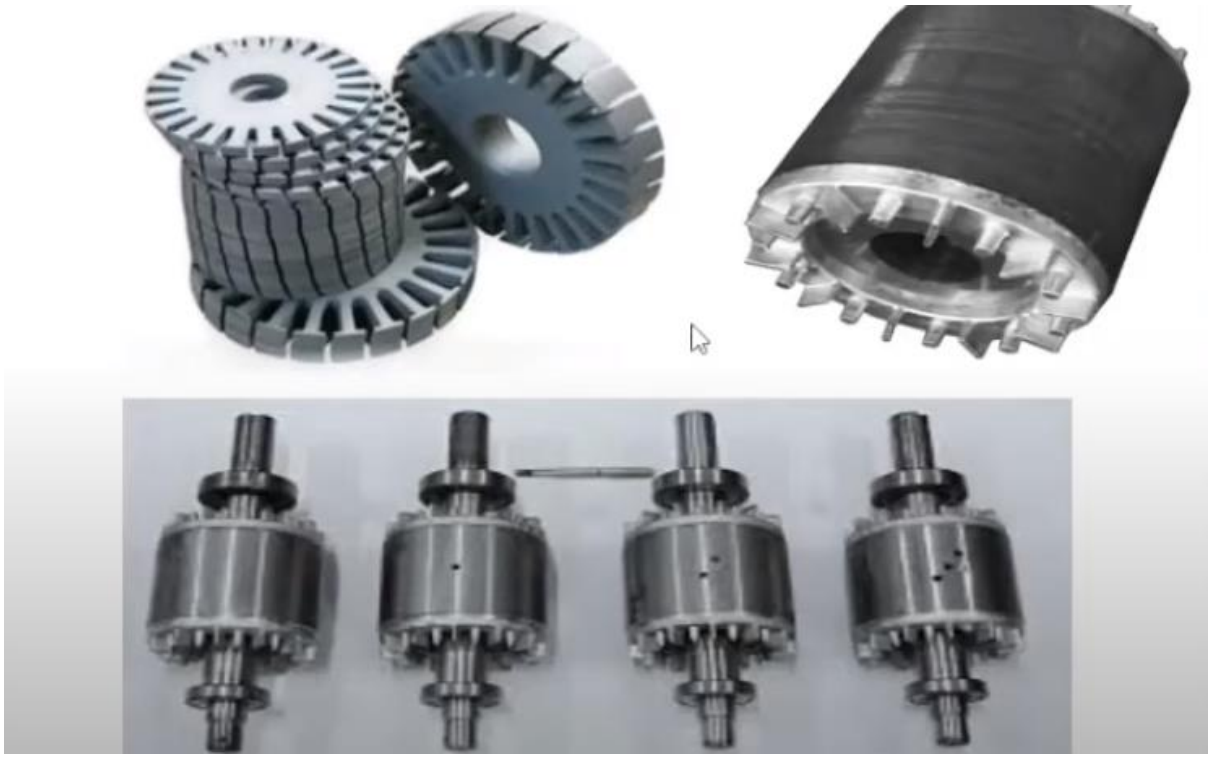

Figure 2.1.2(a)

Rotor is the component of an induction motor that rotates. Additionally, thin lamination is being built up, as shown in figure 2.1.2(a). The same materials that are utilized for stator production are also used for lamination production. The laminated cylindrical core is directly installed on the shaft, as can be seen in the image. The rotor will resemble the one in the diagram once these laminations have been pushed together. This is how the rotor appears after it has been manufactured, and the shaft is immediately pushed against the laminated cylindrical core of the rotor. Stainless steel is used to make the shaft. Additionally slotted in the outer periphery are these laminations. Within this

lamination are the rotor conductors. Copper or aluminium can also be used to make the rotor conductors.

The Induction motor uses one of two different types of rotor. The first is the squirrel cage rotor, often called the simple cage rotor. The second is a wrapped rotor, sometimes known as a sleep ring rotor.

Figure 2.1.2(b) below illustrates two types of rotors based on construction. Both the Squirrel Cage Rotor and the Slip Ring Rotor are displayed.

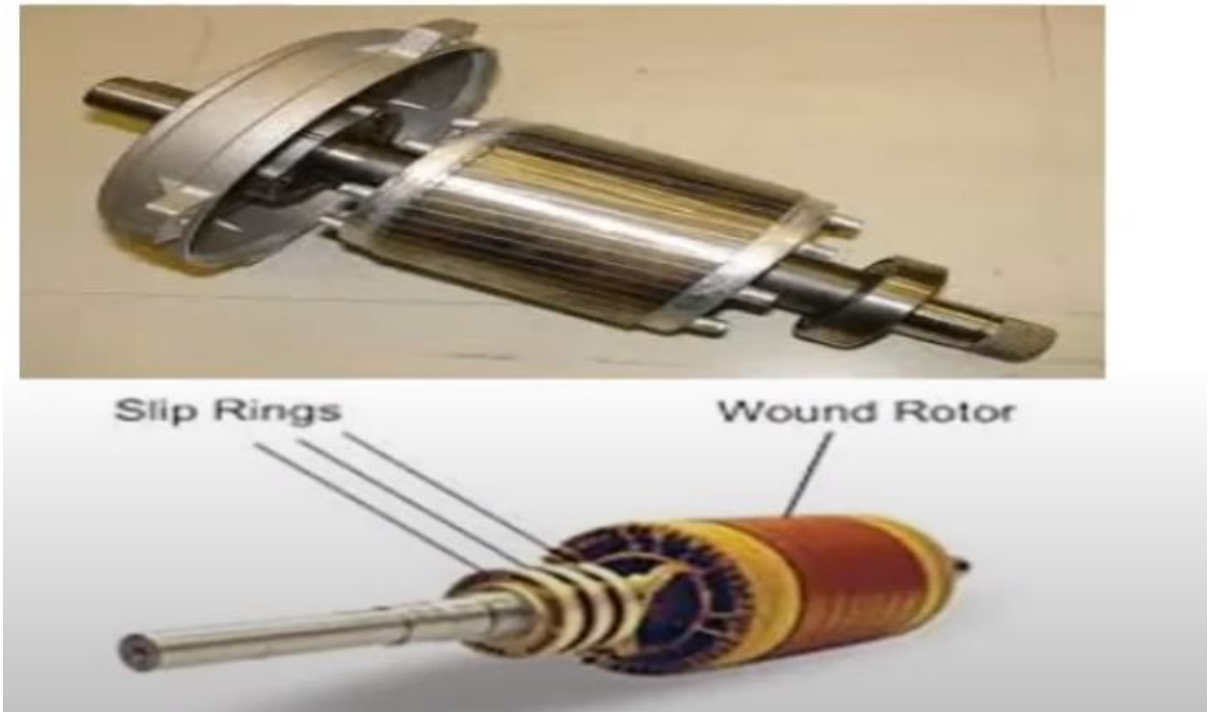

Figure 2.1.2(b)

Wound induction motors or slip ring rotors are the two names for induction motors that utilise these rotor types. In a similar vein, an induction motor with a squirrel cage is called a squirrel cage induction motor.

The cylindrical laminated core of the squirrel induction motor has slots that are almost exactly parallel to the shaft axis. It is also known as skewing. The illustration depicts the skewed end rings and rotor bars. Although parallel to one another, these rotor bars are not perpendicular to one another. Always there is an angle, and that angle is skewing. In the image 2.1.2(c) below, we can see a squirrel cage's induction rotor bars and how they are positioned in relation to the end rings.

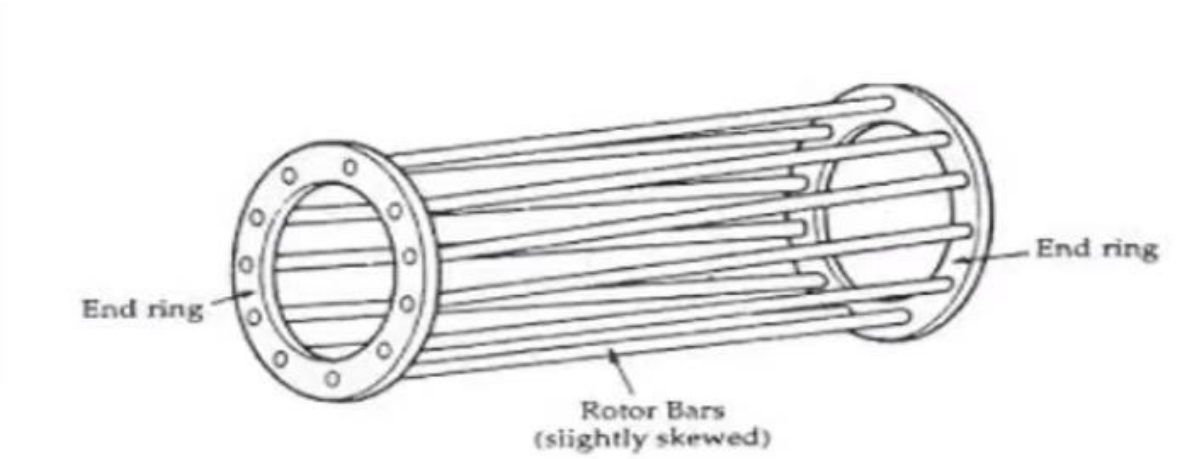

Figure 2.1.2(c)

H The hefty end rings, which are always constructed of the same material, short circuit the rotor bar conductors at either end of the rotor. The rotor's construction when it is mounted to the shaft is visible. In the picture 2.1.2(d) below, the black object is a laminated iron core, and the silver lines are conductor Aluminium bars. Aluminium bars are parallel to one another, but not perpendicular to the end rings, if we have good vision. The conductors of the rotor are skewed to provide more consistent torque, lessen operating noise, and lessen the likelihood of the rotor to lock up. Two ends make up the shaft. One end is used to extract mechanical power, while the other end is attached to a cooling fan. The complete set-up is housed inside the stator, which encircles the rotor bar on all sides.

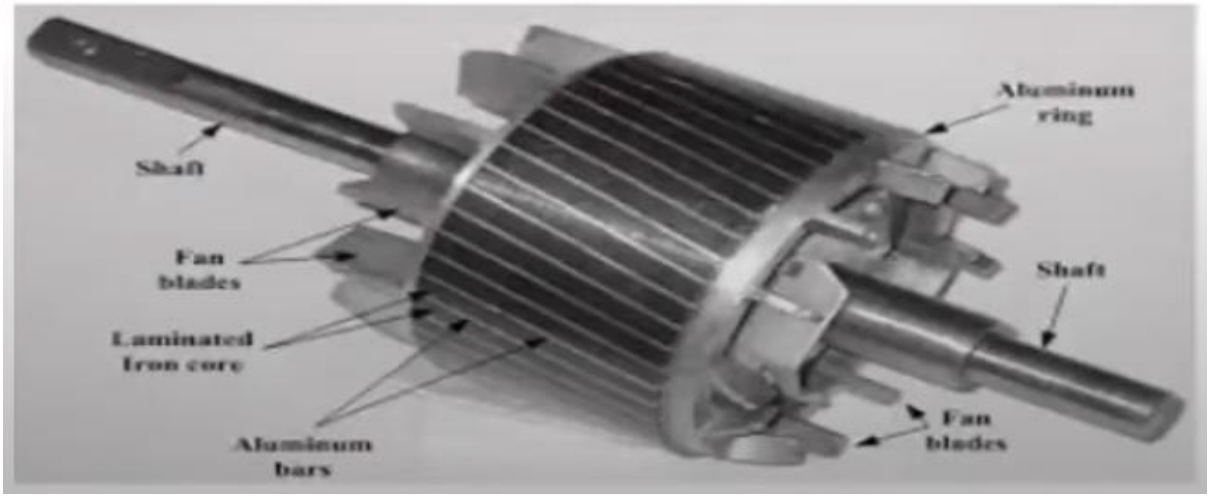

Figure 2.1.2(d)

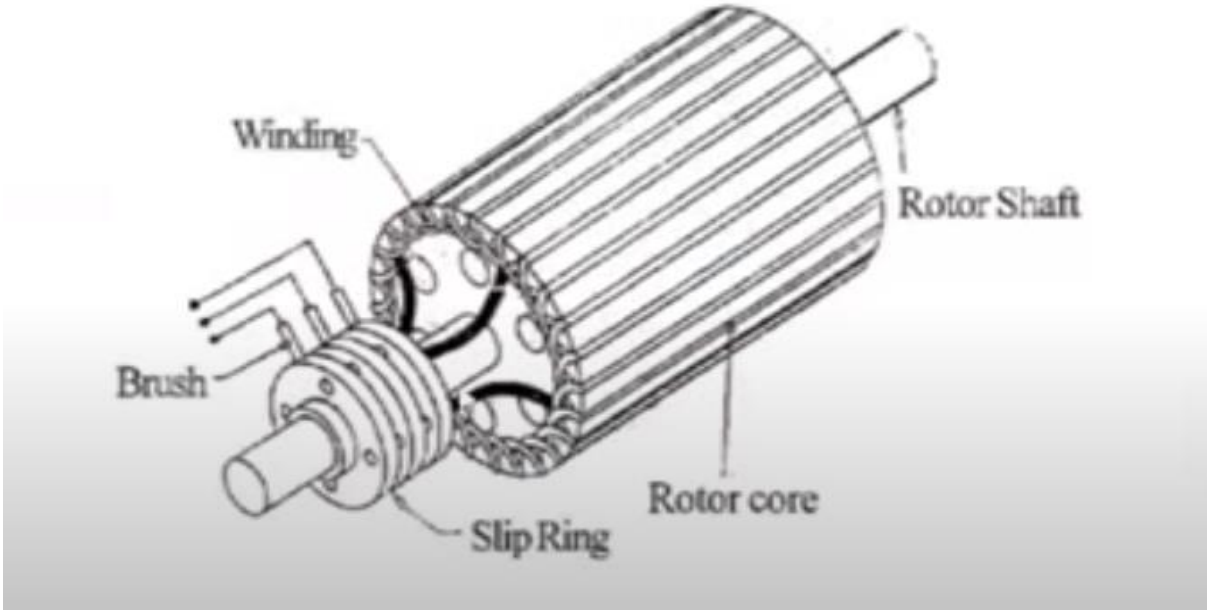

Figure 2.1.2(e)

H The slotted armature that makes up the wound rotor. As seen in figure 2.1.2(e) above, a wrapped rotor. The rotor alone makes up the armature. As a result, the rotor's structure is extremely similar to that of the prior rotor. However, copper is also used in the slip ring rotor's conductor. They create a three phase dispersed double layer winding and are also isolated from one another. These windings resemble the stator windings in appearance, and the rotor winding is always coupled in a star pattern. In this scenario, the rotor winding is always linked in star, even if the stator winding can be connected in either star or delta. According to figure 2.1.2(f) below, the open ends of the star circuit are transported outside the rotor and attached to the slip rings.

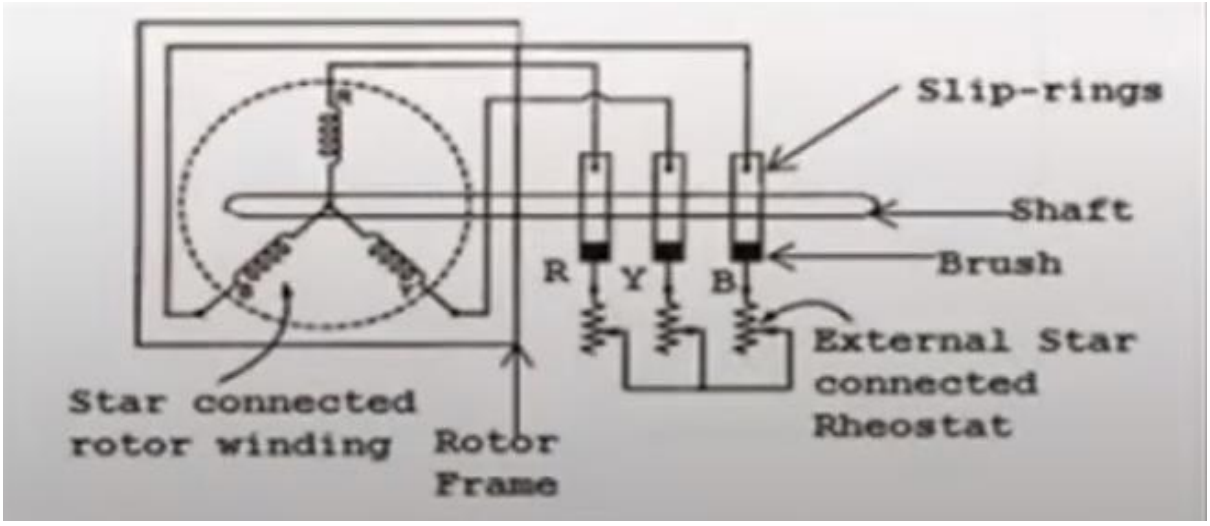

Figure 2.1.2(f)

Brushes rest on the slip rings, which are fixed in the shaft. Three variable resistors are arranged in a star pattern and linked to the brushes. Slip rings and brushes serve as a conduit for attaching an external resistor to the rotor current. The resistor makes it possible to achieve the following goals by varying each rotor phase resistance. To improve beginning torque and lower starting current as well as for motor speed control. The positioning of the armature winding on the rotor is seen in figure 2.1.2(g) below. Armature winding is positioned over the rotor precisely like this.

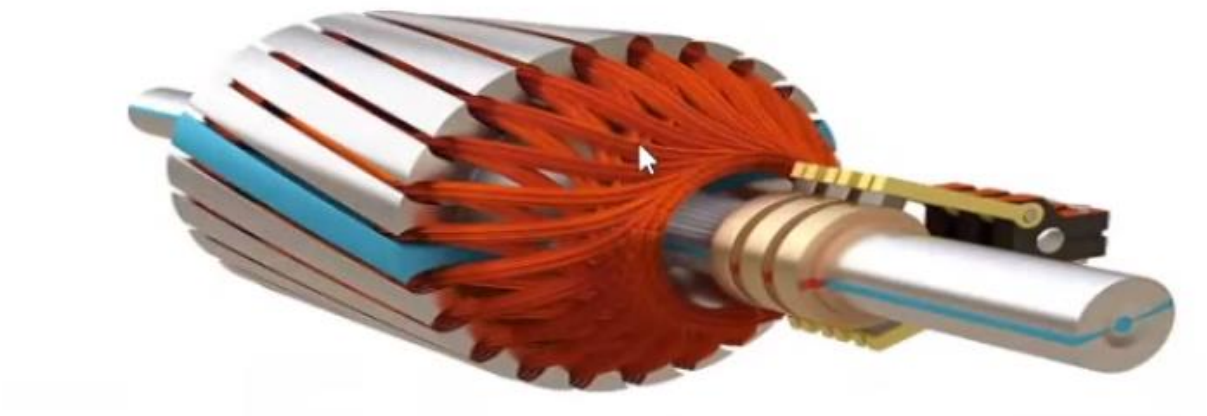

Figure 2.1.2(g)

2.1.3 Stator frame or Motor Body

Figure 2.1.3(a)

The stator is mounted on the Stator frame or Motor body as seen in figure 2.1.3(a) above. It serves to safeguard the motor. The stator rotor is positioned

within. We shall go into detail regarding the stator frame's design, key characteristics, use, and requirement for a motor. The stator frame, sometimes referred to as the motor body, is a crucial component of an induction motor. It acts as a structural housing for the motor's parts and physically supports and safeguards the stator core and windings. Typically, strong, high-quality materials like cast iron, steel, or aluminium are used to build the stator frame. These materials offer great mechanical strength, thermal conductivity, and durability to withstand the motor's operating conditions. The specific material depends on the use, the type of application, and environmental concerns. The stator core and windings are supported and protected primarily by the stator frame. The stator core is a laminated structure made of thin, insulated steel sheets that are stacked on top of one another. By providing a path for the magnetic flux generated by the stator windings, it facilitates efficient energy conversion in the motor. The stator windings, which are normally made of copper or aluminium conductors, are securely housed in the perforations on the stator core. These electrically insulated windings exactly align to provide the needed magnetic field when an alternating current passes through them. The stator frame, which provides mechanical rigidity and weather protection, encloses these crucial components. The stator frame assists in heat dissipation during motor running as well as serving a protective function. The frame acts as a heat sink, conducting heat out of the stator core and windings and into the surrounding air. The motor's performance and longevity are maximized, and the temperature is kept within safe ranges. The stator construction is designed to provide adequate airflow for cooling requirements. It has cooling fins, ducts, or other cooling systems to effectively dissipate heat. Ample cooling is necessary to prevent overheating, which can lead to the degradation of insulation, increased losses, and motor failures. On the stator frame, mounting options are also included for installing the motor to its intended use. It frequently features mounting feet or flanges in numerous applications, allowing for safe installation and precise motor alignment. The stability and vibration-reduction provided by these mounting arrangements improves the motor's overall performance and dependability. Additionally, the stator frame could have terminal boxes or connecting places for wiring. These make it simpler to connect the power supply wires to the stator windings and provide as a convenient interface for external electrical connections. Induction motors' stator core and windings require installation, structural support, protection, and heat dissipation, all of which are provided by the stator frame, also known as the motor body. It ensures efficient and dependable operation in a range of commercial and industrial applications by supporting the mechanical integrity, temperature regulation, and overall performance of the motor.

2.1.4 Fan

Figure 2.1.4(a)

The fan in figure 2.1.4(a) is there to provide cooling. Therefore, it is crucial to keep a machine cool since it produces heat as it operates, which might lead to a motor burn. The fan fulfils this function. The fan is an essential component of an induction motor because it keeps the motor cool and maintains its proper operating temperature. It is frequently mounted on the motor shaft and spins in unison with the motor to provide effective air circulation. The primary function of the fan is to draw outside cold air into the stator and rotor of the motor. The motor generates heat when it is operating as a result of mechanical friction and electrical losses. The fan assists in the dissipation of this heat by creating airflow that removes the hot air from the motor and replaces it with cooler outside air. The design of the fan is crucial for efficient cooling. Usually, the fan blades are angled or curved to provide an airflow that is swift and sufficient to cool the engine. The number and shape of the fan blades may vary depending on the size, power rating, and cooling requirements of the motor. It is common practice to cover or shroud fans to assist direct airflow to certain areas of the motor. The cover directs the rotor and stator windings, two essential components where heat dissipation is most required, to maximize overall cooling effectiveness. The fan serves purposes other than cooling. It helps to prevent insulation damage and functional issues by cleaning out any dust or debris that may have accumulated inside the motor. Reduced humidity, which can be detrimental to the induction motor, is another benefit of the fan's circulation. Some induction motors may employ an external fan that is housed outside the motor case to enhance cooling. This type of fan is frequently larger and has a greater airflow capacity. Since it is connected to the motor through a fan shaft, it rotates freely but in time with the motor's speed.

Figure 2.1.4(b)

The conventional positioning of a fan at the end of an induction motor is seen in Figure 2.1.4(b). However, the fan is not opened in this manner, and a fan cover is placed over them. So that the fan may operate without outside interference.

It's important to keep in mind how closely the engine and fan interact. As the motor power grows, the fan spins more swiftly, increasing airflow for better cooling. Conversely, when the motor is running slowly or at idle, the fan's ability to spin and cool the air may be reduced. Overall, keeping proper temperature regulation requires the fan of an induction motor. The fan promotes the exchange of hot air with cooler ambient air, guarantees the motor's dependable and effective functioning, and helps avoid overheating. It is crucial for extending the motor's lifespan and preventing excessive heat from reducing performance.

2.1.5 Fan Cover

Fan covers are used to protect fans when they are simply put as covers. Additionally, it shields the fan from outside harm.

The fan cover protects the fan assembly of an induction motor by enclosing it. It aims to improve the cooling system's efficiency by directing the fan's airflow onto specific motor components that require cooling. In order to guarantee effective heat dissipation, the fan cover's principal function is to guide airflow onto significant components including the rotor and stator windings. It functions as a shroud or casing that encloses the fan blades and creates a controlled airflow. By controlling airflow, the fan cover maximizes cooling effectiveness and improves the motor's overall thermal management. The design of the fan cover is crucial for maximizing cooling effectiveness. Its construction typically makes use of metals or high-temperature polymers with good heat conductivity

and mechanical strength. Air can flow smoothly and efficiently through the critical components of the motor because the cover is shaped and molded to match the airflow pattern created by the fan blades. Apertures or vents that allow the intake of fresh air from the outside and the exhaust of heated air are typically strategically positioned in fan covers. These holes are designed to allow for the proper airflow direction and to offer enough ventilation inside the motor. The precise design of the vents' size, shape, and placement achieves the optimal balance between efficient cooling and protection against the introduction of pollutants. In addition to regulating airflow, the fan cover protects the fan assembly from harm. It shields the blades of the fan from outside objects, preventing accidental collisions or other damage that can reduce the fan's efficiency. By assisting in preventing the accumulation of dust, dirt, or foreign particles on the fan blades, the cover guarantees that they can function properly and maintain their effectiveness over time. The fan cover is often fastened to the motor housing using bolts or mounting mechanisms, creating a strong and solid attachment. It is designed to withstand the mechanical vibrations and pressures caused by motor movement, maintaining its position and integrity even under trying conditions. Figure 2.1.5 below shows a typical induction motor fan cover and its arrangement over the induction motor.

Figure 2.1.5

The fan cover is ultimately necessary for an induction motor's cooling system to function properly. By guiding and maximising the airflow created by the fan, it improves the motor's thermal management, boosts cooling efficacy, and helps sustain the motor's performance and reliability. The fan cover also protects the fan assembly, ensuring both its longevity and proper operation.

2.2 Working Principle of Induction Motor.

Electric motors that use the electromagnetic induction theory include the widely used induction motor. Induction motors may be divided into two categories: single-phase induction motors and three-phase induction motors, depending on the power source utilised to run the motor.

1. Single-phase induction motors: Induction motors that run on one phase of electricity are known as single-phase induction motors. They are frequently utilised in small industrial applications as well as home appliances when three-phase electricity is not offered or necessary. There are two further categories of single-phase induction motors:

a. Split-phase induction motors: The main winding and the auxiliary winding are the two windings that make up the straightforward construction of split-phase induction motors. The main and auxiliary windings' currents are phased differently as a result of the auxiliary winding's series connection to a capacitor. A revolving magnetic field is created by this phase shift, enabling the motor to turn on and run.

b. Capacitor-start induction motors: Although they employ an auxiliary winding and a capacitor as well, capacitor-start induction motors start differently. When the motor reaches a specific speed, a centrifugal switch used in these motors disconnects the capacitor and auxiliary winding. When compared to split-phase motors, this arrangement offers a larger beginning torque and is employed in certain applications.

2. Three- phase induction motors: The most popular kind of induction motors are three-phase induction motors. They are made to work with three-phase power supplies, which are frequently used in commercial and industrial environments. Induction motors that operate in three phases provide a number of benefits, such as increased efficiency, improved power factor, and smoother operation. They fall into two types in particular**.**

a. Squirrel cage induction motors: The most prevalent kind of three-phase induction motors are squirrel cage motors. They have a rotor that resembles a squirrel cage and has conductive bars that have been shorted out. The three-phase power supply's revolving magnetic field causes currents in the rotor bars, creating torque and turning the motor. Due to its simplicity, durability, and little maintenance needs, squirrel cage motors are frequently employed in a variety of industrial applications.

b. Wound rotor induction motors: Induction motors with wound rotors feature windings on the rotor that are coupled to external resistors or slip rings. The rotor's resistance and reactance may be controlled by external resistors or slip rings, providing variable speed operation and better starting capabilities. These motors are frequently used in machinery such huge pumps, compressors, and mills that need to manage speed.

Based on the power source, these are the primary induction motor types. Each kind has unique benefits and uses, and the choice relies on the particular needs of the motor-driven system.

Since, the Three-Phase Squirrel Cage Induction Motor are most widely used Electrical Machine in the industry we will limit our discussion from ground level on the working principle of Three phase of induction motor only. The working principle of a three-phase induction motor is based on the concept of electromagnetic induction. It involves the interaction between a rotating magnetic field produced by the stator windings and the currents induced in the rotor windings. Here's a detailed explanation of the working principle:

1. Stator: The stator has a laminated core with three-phase windings arranged in slots that are uniformly spaced all the way around it. Typically, the windings are wired in a star (wye) or delta arrangement, and a balanced three-phase AC power source powers them.

2. Rotating Magnetic Field: A rotating magnetic field is produced when the stator windings are subjected to the three-phase AC supply. A magnetic field is created throughout each phase of an AC supply, and it changes over time in both direction and strength. A rotating magnetic field is produced when the three magnetic fields are 120 degrees apart in space.

3. Rotor: The motor's spinning component is known as the rotor. The core of a squirrel cage rotor is composed of laminated iron and is made up of conductive bars that are positioned parallel to the rotor axis. Conducting end rings short-circuit the bars at both ends. The term comes from how the conductive bars are arranged; they look like a squirrel cage. Due to its simplicity and durability, the squirrel cage rotor is the most popular kind used in three-phase induction motors.

4. Induction and Rotor Currents: By cutting through the rotor conductors as the stator's spinning magnetic field moves over the air gap, it induces voltage in accordance with Faraday's law of electromagnetic induction. Currents circulate in the conductors of the rotor as a result of this generated voltage. The short-circuited conductive bars in a squirrel cage rotor enable the induced currents to

flow in closed loops. In a wound rotor, the external resistors or slip rings receive the induced voltage, which controls the current passing through the rotor windings.

5. Rotor Magnetic Field: Their own magnetic field is produced by the rotor currents that pass through the conductive bars or windings. This magnetic field lines up with the revolving magnetic field of the stator in a squirrel cage rotor. The strength and direction of the rotor magnetic field may be changed in a wrapped rotor by adjusting the external resistors or slip rings, which govern the rotor's resistance and reactance.

6. Rotor Rotation: A torque is generated on the rotor as a result of the interaction between the revolving magnetic fields of the stator and the rotor. Lenz's law states that the rotor rotates in the opposite direction as the change in the magnetic field that causes the currents. The rotor begins rotating as a result of the torque and progressively accelerates towards a speed that is only a little slower than that of the revolving magnetic field.

7. Slip: Slip is the term for the discrepancy between the synchronous speed of the spinning magnetic field and the actual speed of the rotor. In order for the motor to produce torque, slip is required. The slip rises as the load on the motor does, enabling the motor to maintain torque and continue running. The slip also controls the motor's speed and effectiveness.

8. Motor Operation: Once the motor is in motion, the induced currents in the rotor and the spinning magnetic field of the stator continue to interact continuously, maintaining the rotor's rotation. As long as the three-phase power supply is available and the required load torque is within the motor's capability, the motor will continue to run.

This thorough explanation emphasizes the stator windings' development of a revolving magnetic field, the conductors' induction of currents, the formation of a rotor magnetic field, and the torque that results from this process, which propels the rotor's spinning. The motor's functionality and capacity to transform electrical energy into mechanical energy are guaranteed by the idea of slip and the ongoing contact between the stator and rotor fields. It demonstrates how the motor converts electrical energy into mechanical energy, resulting in rotational motion, by interacting with the revolving magnetic field of the stator and the induced currents in the rotor.

2.3 Faults in Induction Motor

Different defects that influence induction motor performance, efficiency, and dependability can occur. Here are a few typical induction motor flaws.

1. Stator Faults:

a. Stator Winding Insulation Failure: As a result of a variety of reasons, including thermal ageing, voltage spikes, moisture intrusion, and mechanical loads, the insulation in the stator windings may deteriorate with time. In the windings, insulation failure may result in short circuits or ground problems. These flaws may result in an increase in current flow, winding overheating, and eventually motor failure. Early symptoms of insulation degradation can be found via insulation testing, such as the insulation resistance measurement.

b. Stator Winding Inter-turn Short Circuit: When a short circuit forms between two turns of the stator winding, this issue happens. It may be brought on by deterioration of the insulation, mechanical strains, or manufacturing flaws. Increased current flow, localised heating, and decreased motor efficiency can all be caused by inter-turn short circuits. In extreme circumstances, they may result in winding burnout. Inter-turn short circuits can be found via electrical testing such as the surge test or winding resistance measurement.

c. Stator Core Lamination Faults: Laminations are piled one on top of the other to form the stator core. Vibrations in the core or shorted laminations are examples of faults. Shorted laminations can result from mechanical stress, moisture, or production flaws. Loose laminations or poor mechanical alignment can both cause core vibration. These flaws contribute to increased noise and vibration, as well as higher core losses and decreased motor efficiency. These flaws can be found and fixed with the use of routine visual inspections and core testing methods.

2. Rotor Faults:

a. Rotor Bar or End Ring Failure: The conductive bars and end rings of a squirrel cage rotor may develop issues. High rotor currents, mechanical stress, or fatigue might all be contributing factors to these failures. Rotor asymmetry, greater rotor losses, decreased motor performance, and increased noise and vibration can all result from broken or damaged rotor bars or end rings. Rotor defects can be diagnosed with the use of methods like vibration analysis and motor current signature analysis (MCSA).

b. Rotor Core Faults: The rotor core can also have issues like shorted laminations or core vibration, much like the stator core. Increased core losses,

decreased motor efficiency, and increased noise and vibration are all effects of these problems. Rotor core defects may be inspected and tested using the same techniques used for stator core problems.

3. Bearing Faults:

a. Bearing Wear or Failure: Over time, the bearings supporting the rotor shaft may experience wear. Bearing wear can be accelerated by elements including inadequate lubrication, contaminants, or excessive loading. Friction and heat production rise when the bearings degenerate, potentially resulting in bearing failure. Increased motor noise, vibration, and shorter motor life are all symptoms of bearing problems. To identify and prevent bearing failures, routine lubrication, visual inspections, and vibration monitoring are crucial.

4. External Faults:

a. Overvoltage or Under-voltage: Using the motor outside of its rated range can result in a number of problems. Increased motor current, excessive heating, insulation failure, and probable motor winding damage can all result from overvoltage. Reduced torque and motor performance can be caused by under-voltage. These failures can be reduced by keeping an eye on the motor's voltage levels and using safety tools like voltage relays.

b. Overcurrent or Overload: Overheating, insulation deterioration, and probable motor failure can occur when the motor is subjected to high currents or mechanical loads that are more than its specified capacity. For the purpose of avoiding damage brought on by overcurrent or overload circumstances, overcurrent protection devices such as thermal overloads and circuit breakers are crucial.

c. Single-Phasing: If one phase of the power supply is lost or disconnected in a three-phase motor, the motor may still function on the other two phases. Single-phasing is the phenomenon that causes imbalanced currents and torque. Single-phasing might potentially harm the motor windings and result in higher temperature and decreased torque. Single-phasing can be detected by phase monitoring devices and protective relays, which then start protective steps to stop motor damage.

Visual inspections, electrical testing, and condition monitoring methods like vibration analysis, thermal imaging, or motor current signature analysis (MCSA) are frequently combined to find and diagnose motor defects. Regular maintenance is essential for avoiding problems or spotting them early on, including insulation testing, bearing lubrication, and visual checks.

These can be tabulated as,

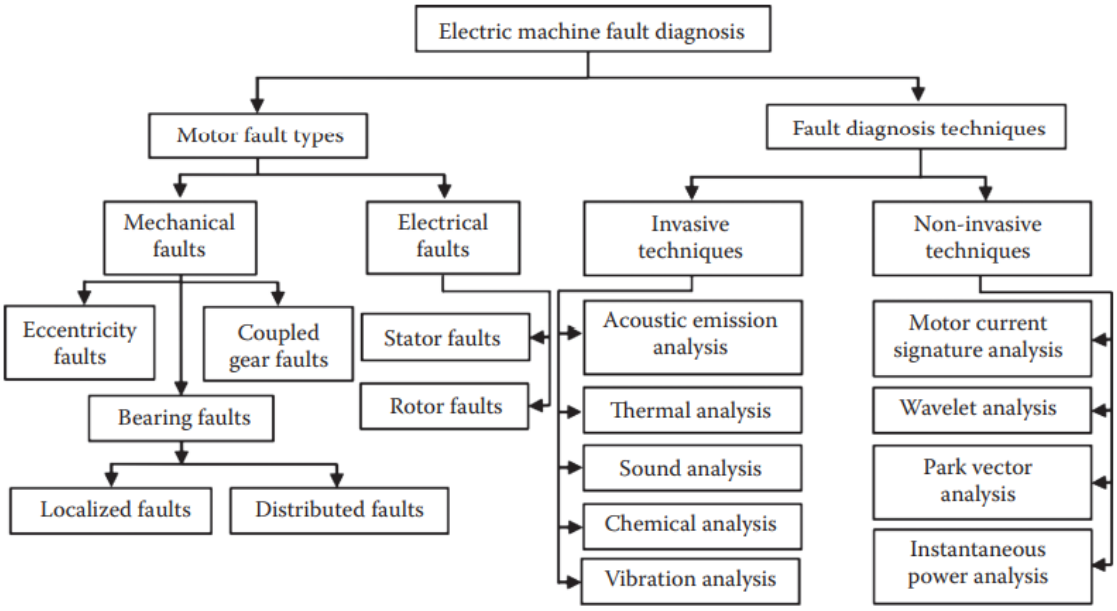

These are several types of faults that may occur in induction motors. According to a 1982 EPRI survey, bearing defects account for around 40% of all induction motor failures, stator faults for 38%, rotor faults for 10%, and other faults for 12%

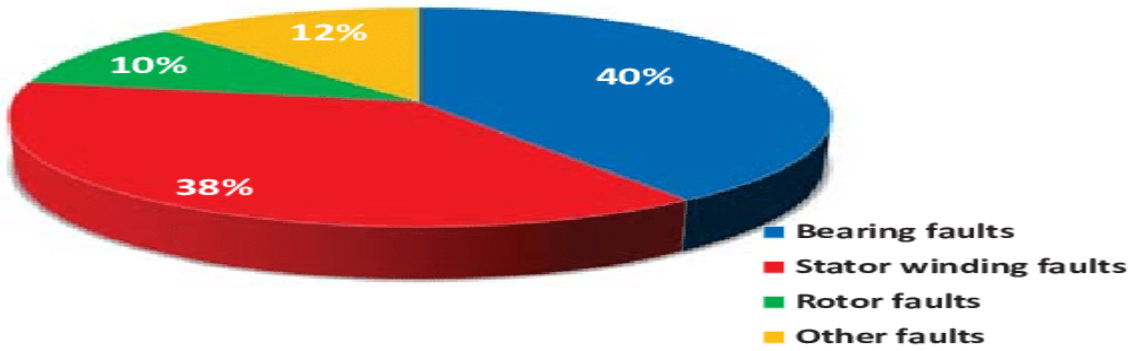

Bearing faults are categorized as inner race faults and outer race faults by the location of occurrences. The most common causes of bearing faults include contamination of lubricant, loss of lubricant, over-loading, and excess heating. The ultimate result is either extreme vibration leading to catastrophic failure, or a complete seizure of the bearing.

Stator faults are basically caused by a breakdown of winding insulation, which may result from excess thermal or voltage stress, mechanical vibration, or even an abrasion between the stator and rotor. The weakness of winding insulation may further result in a turn-to-turn short circuit and eventually a winding-to-ground short circuit.

There are two types of rotor faults. One is associated with the rotor itself, such as a bar defect or bar breakage. This type of fault occurs from thermal stresses, hot spots, or fatigue stresses during transient operations such as start-up, especially in large motors. A broken bar changes torque significantly and is dangerous to the safe and consistent operation of electric machines.

The second type of rotor fault is related to air gap eccentricity. Air gap eccentricity is a common effect arising from a range of mechanical problems in induction motors such as load unbalance or shaft misalignment. Long-term load unbalance can cause damage of the bearings and the bearing housing, which will influence air gap symmetry. Shaft misalignment means horizontal, vertical, or radial misalignment between a shaft and its coupled load. With shaft misalignment, the rotor will be displaced from its normal position because of a constant radial force.

Chapter 3

DQ Modelling

3.1 Introduction

DQ modelling, often referred to as the Park's transformation or Clarke's transformation, is a mathematical approach used to make three-phase systems, especially induction motors, easier to analyse and manage. Voltage and current, which are three-phase variables, are converted into the D-axis and the Q-axis, two orthogonal reference frames.

The direct axis of the system, which symbolises the magnetic field produced by the system, is lined up with the D-axis. The quadrature axis of the system, the Q-axis, is perpendicular to the D-axis. The analysis and management of the system may be separated into two distinct components—the D-component and the Q-component—by converting the three-phase variables into DQ variables.

3.2 Purpose of DQ Modelling

Primarily, the motive of DQ modelling is to render the overall calculation of a system. It also helps in lucid designing of a system. The following are few purposes of DQ modelling.

1. Simplified Analysis: By reducing three-phase systems to two disconnected components, DQ modelling makes it easier to analyse three-phase systems. The DQ transformation enables examining the system's behaviour and performance in a simpler and more logical way rather of having to cope with the intricate interactions among the three-phase variables. It makes the system easier to comprehend and use by simplifying the mathematical representation and analysis of the system.

2. Control Design: Designing control systems for induction motors and other three-phase systems benefits greatly from DQ modelling. It is possible to use control systems like field-oriented control (FOC) by converting the three-phase variables into DQ variables. Motor torque and flux may be precisely controlled thanks to FOC, which provides separate control of the direct and quadrature components. The design and execution of control algorithms are made simpler by the decoupling of the control variables, which enhances the effectiveness and responsiveness of the motor system.

3. Fault Analysis: In three-phase systems, fault analysis is facilitated by DQ modelling. Fault finding and diagnosis are made easier by translating the system variables into the DQ reference frames. It is possible to identify and analyse individually faults that primarily affect the D or Q axis, which helps with fault mitigation and system protection. For instance, a problem in the Q-axis, such as an imbalanced load, will predominantly influence the system's reactive power flow, whereas a fault in the D-axis, such as a shorted winding, will mostly affect the system's torque generation. It is possible to take the proper corrective measures by narrowing the source of the problem to one axis.

4. Harmonic Analysis: In three-phase systems, DQ modelling aids in the analysis and mitigation of harmonics. Unwanted voltage or current components called harmonics can skew the waveforms of a system and impair its functionality. It is simpler to comprehend the impacts of harmonics on the system's performance by separating the D and Q components. Harmonic distortion can be reduced and system quality increased by designing appropriate filters or control techniques based on the independent analysis of harmonics in the D and Q axes.

5. Power Flow Analysis: Power flow analysis in three-phase systems is made possible using DQ modelling. The active power and reactive power flow may be individually analysed by separating the D and Q components. As a result, it is possible to comprehend the system's power flow and how to regulate and optimise it. It makes it possible to analyse power flow management schemes more quickly and effectively. Examples include voltage regulation and power factor correction.

In conclusion, DQ modelling makes it easier to analyse and manage three-phase systems, including induction motors. It converts complicated three-phase variables into DQ variables so that system components may be analysed and controlled independently. Simplified analysis, control design, fault analysis, harmonic analysis, and power flow analysis are made possible by DQ modelling. Engineers may better understand system behaviour, create effective control strategies, properly identify problems, reduce harmonics, and enhance power flow in three-phase systems by using DQ modelling.

3.3 Dynamic Simulation of a Three-Phase Induction Motor using DQ Modelling in MATLAB

3.3.1 Equation Derivation

In a drive with variable speed, the transient behaviour of the induction motor must be taken into account. In addition, field-oriented or vector high performance drive controls. The induction motor's dynamic d-q model is the foundation for control. For the transient analysis of induction motors, especially for computer simulation studies in MATLAB/SIMULINK, the dynamic model in state space form is crucial. In order to dynamically simulate an induction motor, SIMULINK software is employed in this instance. Both a Rotating reference frame and a Stationary frame can be used to simulate the motor. Fluxes, currents, or a combination of both can be used as the electrical variables in the model. This work examines the flux linkages as the primary variables in the state space equations of the machine in rotating frame. Since MATLAB is a model operation programmer, it is simple to expand the MATLAB model by writing few additional lines of code to account for different control functions. The induction motor might be used as a sub model in a whole electric motor drive system.

A three-phase induction motor's design is seen in Figure 3.3.0 with the d,q axes overlaid. The q-axis is 90 degrees behind the d-axis. Stator phase A is exposed to a voltage while a current is flowing through it (ias).

In an effort to keep the graphic simple, Phases B and C are not depicted on it. The stator phase coils AS, BS, and CS are replaced by coils DS and QS in the d,q type, while the rotor phase coils AR, BR, and CR are replaced by coils DR and QR. The four coils DS, QS, DR, and QR have no relative speed to one another, despite the fact that the d,q axes can spin at any speed. The purpose of the D,Q coils in Figure 3.3.0 is to physically demonstrate how a new machine with four coils has effectively replaced the three-phase induction motor with its six coils. The original ABC variables must be translated into d,q variables in θ order to accurately forecast the mechanical and electrical behaviour of the original machine, but this transformation depends on the speed at which the D,Q coils rotate, thus each reference frame has a unique transformation. D, Q axes superimposed onto a three-phase induction motor which can be seen in the figure 3.3.0.

In general, for any arbitrary value of θ, the transformation of stator ABC phase variables [F_{ABC}] to d, q stator variables [F_{0dq}] is carried out through Park's transform as follows:

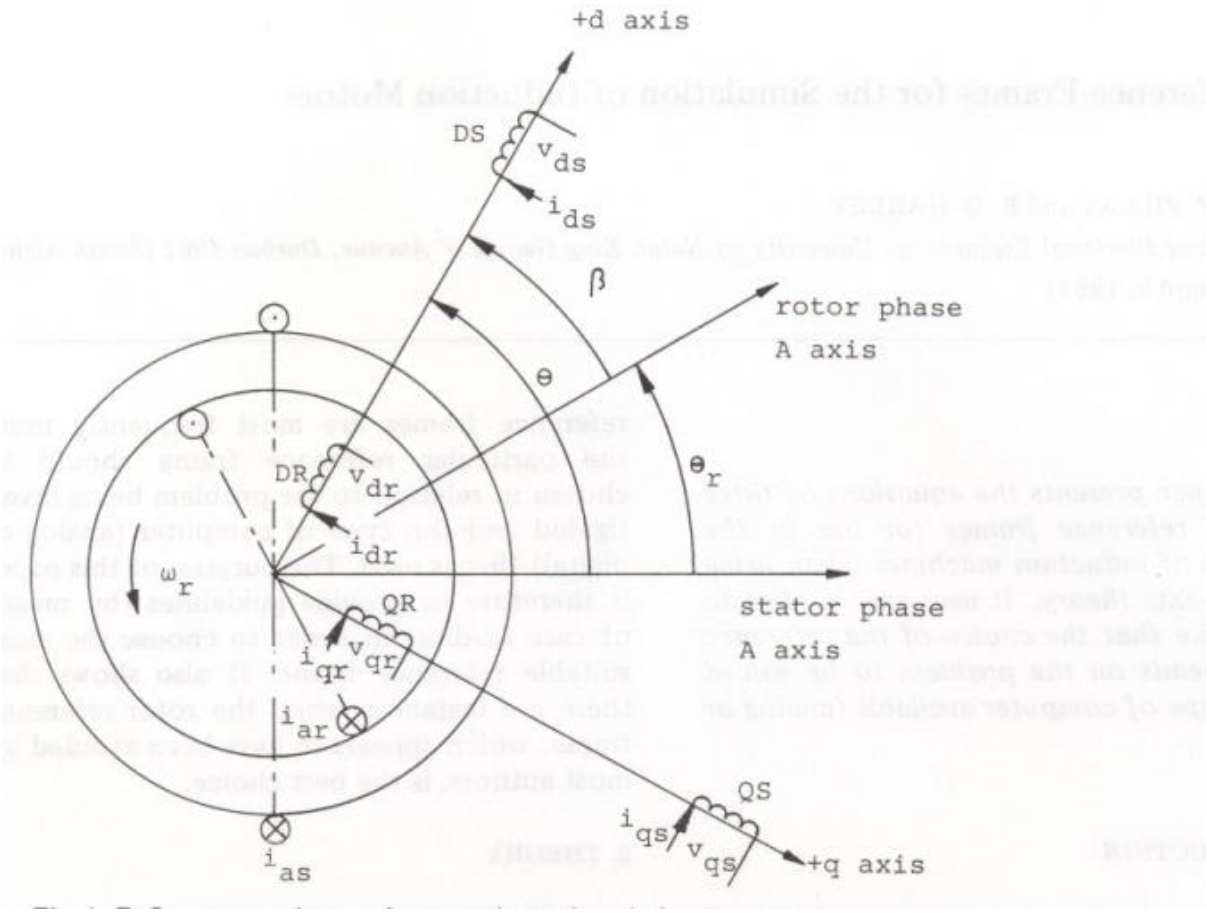

Figure 3.3.0
DQ axes imposed on a Three Phase Induction Motor

An induction motor's dynamic behaviour is described by time-varying voltage and torque equations. It involves some complexity but is successfully utilised to solve these differential equations. By removing any time-varying inductances caused by electric circuits in relative motion from the voltage equations [3.1, 3.2, 3.3, 3.4] of the device, it is possible to simplify these equations by changing the variables. By using this method, a poly-phase winding may be broken down into a group of two-phase windings (q-d) with quadrature-formed magnetic axes. In other words, an induction machine's reference frame, which may rotate at any angular velocity or stay fixed, receives the stator and rotor variables (voltages, currents, and flux couplings). In the context of generalized machine analysis, such a frame of reference is sometimes called an "arbitrary

reference frame." As we have shown in the figure 3.3.0 where DQ axes are imposed on a three phase induction motor. We have these depicted in the form of three equations [3.5, 3.6, 3.7].

In order to design any specific mode of operation, the dynamic analysis of the symmetrical induction machines in the arbitrary reference frame has been heavily utilized as a typical simulation technique. Comparing other machine simulators, Matlab/Simulink offers an advantage when modelling the induction machine utilizing dq0 axial transformations [3.8, 3.9]. It may be a potent method for putting the machine equations into practise after they have been converted to a specific frame of references [3.1, 3.6, 3.8, 3.10]. As a result, it is simple to construct each model equation in a single block and make all machine variables available for use in control and verification. This study simulates the dynamic performance of an induction motor model with stator and rotor variables referring to an arbitrary reference frame using MATLAB code. Since the given machine model provides full details about the Simulink structure of each of the model equations, it makes it simpler to follow and comprehend the implementation process. Figure 3.3.1 below depicts the induction machine's analogous circuit in the arbitrary reference frame [3.11, 3.12].

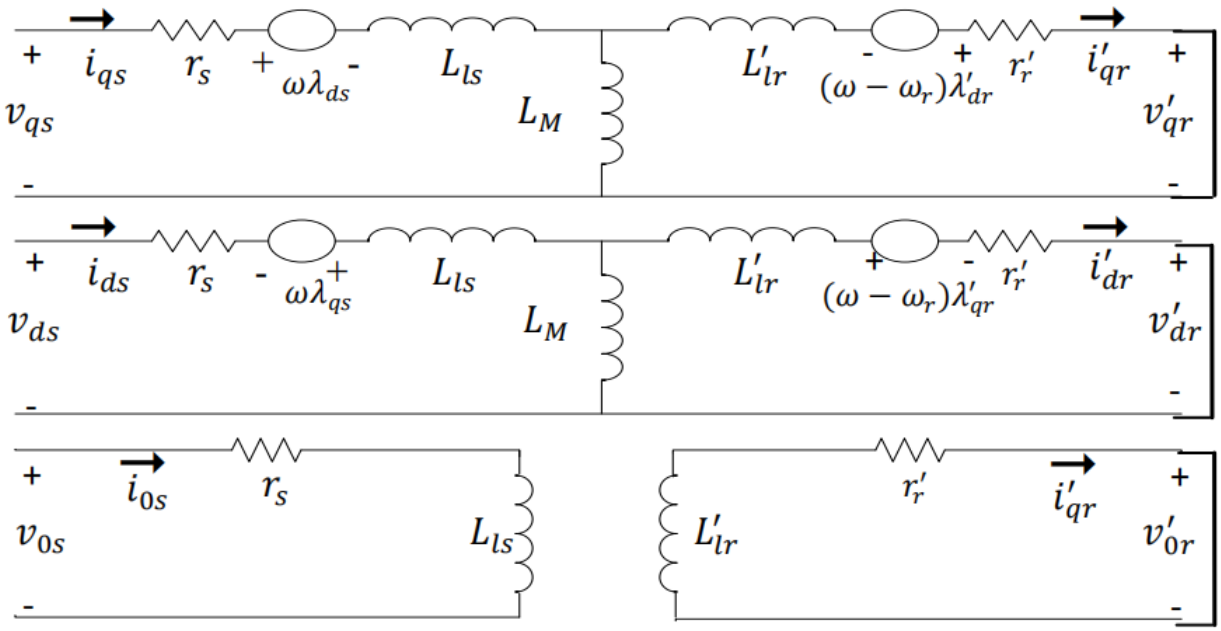

Figure 3.3.1

Dq0 equivalent circuit of Induction Motor

Now, the dq model of the induction motor can easily obtained using the circuit shown in figure 3.3.1. The flux linkages equations that are associated with the above circuit can be written as below.

$$\frac{d\varphi_{qs}}{dt} = \omega_b[V_{qs} - \frac{\omega_e}{\omega_b}\varphi_{ds} + \frac{R_s}{X_{ls}}(\varphi_{mq} - \varphi_{qs})] \quad \text{..... (3.1)}$$

$$\frac{d\varphi_{ds}}{dt} = \omega_b[V_{ds} + \frac{\omega_e}{\omega_b}\varphi_{qs} + \frac{R_s}{X_{ls}}(\varphi_{md} - \varphi_{ds})] \quad \text{..... (3.2)}$$

$$\frac{d\varphi_{qr}}{dt} = \omega_b[V_{qr} - \frac{\omega_e-\omega_r}{\omega_b}\varphi_{dr} + \frac{R_s}{X_{ls}}(\varphi_{mq} - \varphi_{qr})] \quad \text{..... (3.3)}$$

$$\frac{d\varphi_{dr}}{dt} = \omega_b[V_{dr} - \frac{\omega_e-\omega_r}{\omega_b}\varphi_{qr} + \frac{R_s}{X_{ls}}(\varphi_{md} - \varphi_{dr})] \quad \text{..... (3.4)}$$

Where,

$$\varphi_{mq} = X_{ml}[\frac{\varphi_{qs}}{X_{ls}} - \frac{\varphi_{qr}}{X_{lr}}] \quad \text{..... (3.5)}$$

$$\varphi_{md} = X_{ml}[\frac{\varphi_{ds}}{X_{ls}} - \frac{\varphi_{dr}}{X_{lr}}] \quad \text{..... (3.6)}$$

$$X_{ml} = {}^{1}\Big/{(\frac{1}{X_m} + \frac{1}{X_{ls}} + \frac{1}{X_{lr}})} \quad \text{..... (3.7)}$$

Then we can obtain the value of current by substituting the value of flux linkages.

$$i_{qs} = \frac{1}{X_{ls}}(\varphi_{qs} - \varphi_{mq}) \quad \text{..... (3.8)}$$

$$i_{ds} = \frac{1}{X_{ls}}(\varphi_{ds} - \varphi_{md}) \quad \text{..... (3.9)}$$

$$i_{qr} = \frac{1}{X_{lr}}(\varphi_{qr} - \varphi_{mq}) \quad \text{..... (3.10)}$$

$$i_{dr} = \frac{1}{X_{lr}}(\varphi_{dr} - \varphi_{md}) \quad \text{..... (3.11)}$$

Now based on the above equations torque and speed can be determined as follows:

$$T_e = \frac{3}{2}(\frac{P}{2})\frac{1}{\omega_b}(\varphi_{ds}i_{qs} - \varphi_{qs}i_{ds}) \quad \text{.....(3.12)}$$

$$\omega_r = \int \frac{P}{2J}(T_e - T_l) \quad \text{.....(3.13)}$$

Here, P: Number of Poles, J: Moment of Inertia (Kg/m^2). Now since the rotor bars are shorted, for a squirrel cage induction rotor voltages V_{qr} and V_{dr} are set to zero in the flux equations.

Applying the d-q axis transformation to the machine input (stator) voltages follows driving the torque and speed equations in terms of d-q flux linkages and stator currents in equations [3.1, 3.13, 3.14]. Under balanced circumstances, the three-phase stator voltages of an induction machine may be represented as:

$$V_a = \sqrt{2}\, V_{rms} \sin(\omega t) \qquad \text{…….... (3.14)}$$

$$V_b = \sqrt{2}\, V_{rms} \sin(\omega t - \tfrac{2\pi}{3}) \qquad \text{……. (3.15)}$$

$$V_c = \sqrt{2}\, V_{rms} \sin(\omega t + \tfrac{2\pi}{3}) \qquad \text{…….... (3.16)}$$

These three-phase voltages are transformed (d-q axis transformation) into a synchronously rotating reference frame in just two phases. Using the following two equations, this may be accomplished.

$$\begin{bmatrix} V_\alpha \\ V_\beta \end{bmatrix} = \tfrac{2}{3} \begin{bmatrix} 1 & \frac{1}{2} & -\frac{1}{2} \\ 0 & \frac{\sqrt{3}}{2} & -\frac{\sqrt{3}}{2} \end{bmatrix} \begin{bmatrix} V_a \\ V_b \\ V_c \end{bmatrix} \qquad \text{…….. (3.17)}$$

Now, the direct quadrature voltages are,

$$\begin{bmatrix} V_d \\ V_q \end{bmatrix} = \begin{bmatrix} \cos\theta & \sin\theta \\ -\sin\theta & \cos\theta \end{bmatrix} \begin{bmatrix} V_\alpha \\ V_\beta \end{bmatrix} \qquad \text{……. (3.18)}$$

In order to determine the instantaneous values of the stator and rotor currents in a three-phase system, the following transformation is used:

$$\begin{bmatrix} i_\alpha \\ i_\beta \end{bmatrix} = \begin{bmatrix} \cos\theta & -\sin\theta \\ \sin\theta & \cos\theta \end{bmatrix} \begin{bmatrix} i_d \\ i_q \end{bmatrix} \qquad \text{…….. (3.19)}$$

$$\begin{bmatrix} i_a \\ i_b \\ i_c \end{bmatrix} = \tfrac{2}{3} \begin{bmatrix} 1 & 0 \\ -\frac{1}{2} & -\frac{\sqrt{3}}{2} \\ -\frac{1}{2} & \frac{\sqrt{3}}{2} \end{bmatrix} \begin{bmatrix} i_\alpha \\ i_\beta \end{bmatrix} \qquad \text{…….. (3.20)}$$

Now, that we have done all mathematical derivation of DQ modelling of the Induction Motor we will simulate it using MATLAB. Syntax are written in script file of MATLAB 2023a and all the code of MATLAB are well commented so that anyone who uses the code will able to understand it.

3.3.2 MATLAB Implementation of Induction Motor DQ Modelling

The below written MATLAB code simulates the performance of a three-phase induction motor. Here's a step-by-step explanation of the code:

1. Motor Parameters: The code begins by defining various motor parameters such as voltage (V), stator resistance (rs), stator leakage reactance (Xls), rotor leakage reactance (Xlr), rotor resistance (rr), moment of inertia (J), and load torque (TL).

2. Electrical System Parameters: The base angular frequency (Wb) and the number of pole pairs (P) are specified.

3. Calculating Inductances: The code calculates various inductances based on the given reactances and angular frequency.

4. Simulation Parameters: The code sets the simulation time step (h) and the duration of the simulation (Tfinal). It also calculates the number of iterations (n) based on the time step and duration.

5. Pre-allocating Arrays: Arrays are preallocated to store the calculated values during the simulation.

6. DQ Transformation Matrix: A transformation matrix (B) is defined for converting voltages between the abc and dq frames.

7. Numerical Integration: The code performs numerical integration to simulate the motor behaviour over time. It iterates from i=3 to n, incrementing the time and iteration count.

8. Input Voltages in abc Frame: The input voltages in the abc frame (va, vb, vc) are calculated based on the time.

9. Convert Input Voltages to dq Frame: The input voltages (v_qs, v_ds) are transformed from the abc frame to the dq frame using the transformation matrix.

10. Numerical Integration of Flux Linkages: The code performs numerical integration to calculate the flux linkages (psi_ds, psi_qs, psi_dr, psi_qr) over time based on the input voltages and previous values.

11. Calculate Currents in dq Frame: The currents (i_ds, i_qs, i_dr, i_qr) in the dq frame are calculated based on the flux linkages and inductances.

12. Calculate Electromagnetic Torque: The electromagnetic torque (Tem) is computed based on the current components in the dq frame.

13. Calculate Mechanical Speed: The mechanical speed (Wrm) is calculated based on the electromagnetic torque, load torque, and moment of inertia.

14. Convert Currents to abc Frame: The currents (i_as, i_bs, i_cs) are transformed from the dq frame to the abc frame using the transformation matrix.

15. Plotting: Finally, the code plots the stator current (i_as), rotor current (i_dr), mechanical speed (Wr), and electromagnetic torque (Tem) as functions of time.

The resulting plots provide insights into the motor's behaviour, including stator and rotor current in figure 3.3.2.a and figure 3.3.2.b waveforms and the speed and torque characteristics in figure 3.3.2.c and 3.3.2.d respectively over time.

MATLAB Code

```
% Clear the workspace and command window
clear
clc;

% Motor Parameters
V=220;              % Voltage
rs=0.435;           % Stator resistance
Xls=0.754;          % Stator leakage reactance
XM=26.13;           % Magnetizing reactance
Xlr=0.754;          % Rotor leakage reactance
rr=0.816;           % Rotor resistance
J=0.089;            % Moment of inertia
TL=0;               % Load torque

% Electrical System Parameters
Wb=2*pi*50;         % Base angular frequency (rad/s)
P=4;                % Number of pole pairs

% Calculating Inductances
Lls=Xls/Wb;         % Stator leakage inductance
Llr=Xlr/Wb;         % Rotor leakage inductance
M=XM/Wb;            % Magnetizing inductance
Lss=Lls+M;          % Stator self-inductance
Lrr=Llr+M;          % Rotor self-inductance
D=Lss*Lrr-M^2;      % Determinant for calculating currents

% Simulation Parameters
h=1e-5;             % Time step
Tfinal=2;           % Simulation duration
n=round(Tfinal/h)+1; % Number of iterations

% Pre-allocate arrays for storing calculated values
psi_qs = zeros(1,n);
psi_ds = zeros(1,n);
psi_qr = zeros(1,n);
psi_dr = zeros(1,n);
Wrm = zeros(1,n);
Wrm = zeros(1,n);
i_qs = zeros(1,n);
i_ds = zeros(1,n);
```

```
i_qr = zeros(1,n);
i_dr = zeros(1,n);
Wr = zeros(1,n);
Tem = zeros(1,n);
i_as = zeros(1,n);
i_bs = zeros(1,n);
i_cs = zeros(1,n);
i_ar = zeros(1,n);
i_br = zeros(1,n);
i_cr = zeros(1,n);
v_qs = zeros(1,n);
v_ds = zeros(1,n);
v_qr = zeros(1,n);
v_dr = zeros(1,n);
TL = zeros(1,n);

% DQ Transformation Matrix
B = [1 0 1;
     -0.5 -sqrt(3)/2 1;
     -0.5  sqrt(3)/2 1];

% Numerical integration
time=0;
k(1)=0;
k(2)=0;
TL(1)=0;
TL(2)=0;
for i=3:n
    time=time+h;
    k(i)=k(i-1)+1;
    TL(i)=0;

    % Input voltages in abc frame
    va=V*sqrt(2/3)*sin(Wb*time);
    vb=V*sqrt(2/3)*sin(Wb*time-2*3.1415/3);
    vc=V*sqrt(2/3)*sin(Wb*time+2*3.1415/3);

    % Convert input voltages to dq frame
    v_qs(i)=2/3*(va-((vb+vc)/2));
    v_ds(i)=2/3*((-vb+vc)*sqrt(3)/2);

    % Numerical integration of flux linkages
    psi_ds(i) = psi_ds(i-1)+(h*(v_ds(i-1)-rs*i_ds(i-1)));
    psi_qs(i) = psi_qs(i-1)+(h*(v_qs(i-1)-rs*i_qs(i-1)));
    psi_dr(i) = psi_dr(i-1)+(h*(v_dr(i-1)-rr*i_dr(i-1)-Wr(i-1)*psi_qr(i-1)));
    psi_qr(i) = psi_qr(i-1)+(h*(v_qr(i-1)-rr*i_qr(i-1)+Wr(i-1)*psi_dr(i-1)));

    % Calculate currents in dq frame
    i_ds(i)=(Lrr*psi_ds(i)-(M*psi_dr(i)))/D;
    i_qs(i)=(Lrr*psi_qs(i)-(M*psi_qr(i)))/D;
    i_dr(i)=(Lss*psi_dr(i)-(M*psi_ds(i)))/D;
    i_qr(i)=(Lss*psi_qr(i)-(M*psi_qs(i)))/D;

    % Calculate electromagnetic torque
    Tem(i)= (P/2)*(psi_qr(i)*i_dr(i)-psi_dr(i)*i_qr(i));

    % Calculate mechanical speed
    Wrm(i) = Wrm(i-1)+(h*((Tem(i-1)-TL(i-1))/J));
    Wr(i) = (P/2)*Wrm(i);
```

```
    % Convert currents to abc frame
    i_as(i)=i_qs(i);
    i_bs(i)=-i_qs(i)/2+(i_ds(i)*(-sqrt(3)/2));
    i_cs(i)=-i_qs(i)/2+(i_ds(i)*(sqrt(3)/2));
end

t=0:h:Tfinal;

% Plotting

%Plot of stator current
figure();
plot(t,i_as,'b')
xlabel('Time (s)')
ylabel('Current (A)')
title('Phase Current i_a_s')
grid on

%Plot of rotor current
figure();
plot(t,i_dr,'r')
xlabel('Time (s)')
ylabel('Current (A)')
title('Phase Current i_d_r')
grid on

%plot of Mechanical speed
figure();
plot(t,Wr, 'm')
xlabel('Time (s)')
ylabel('Mechanical Speed (rad/s)')
title('Mechanical Speed (W_r)')
grid on

%plot of electromagnetic torque
figure();
plot(t,Tem, 'c')
xlabel('Time (s)')
ylabel('Torque (Nm)')
title('Electromagnetic Torque (T_em)')
grid on
```

We will now show all the plots in respective figures as mentioned above.

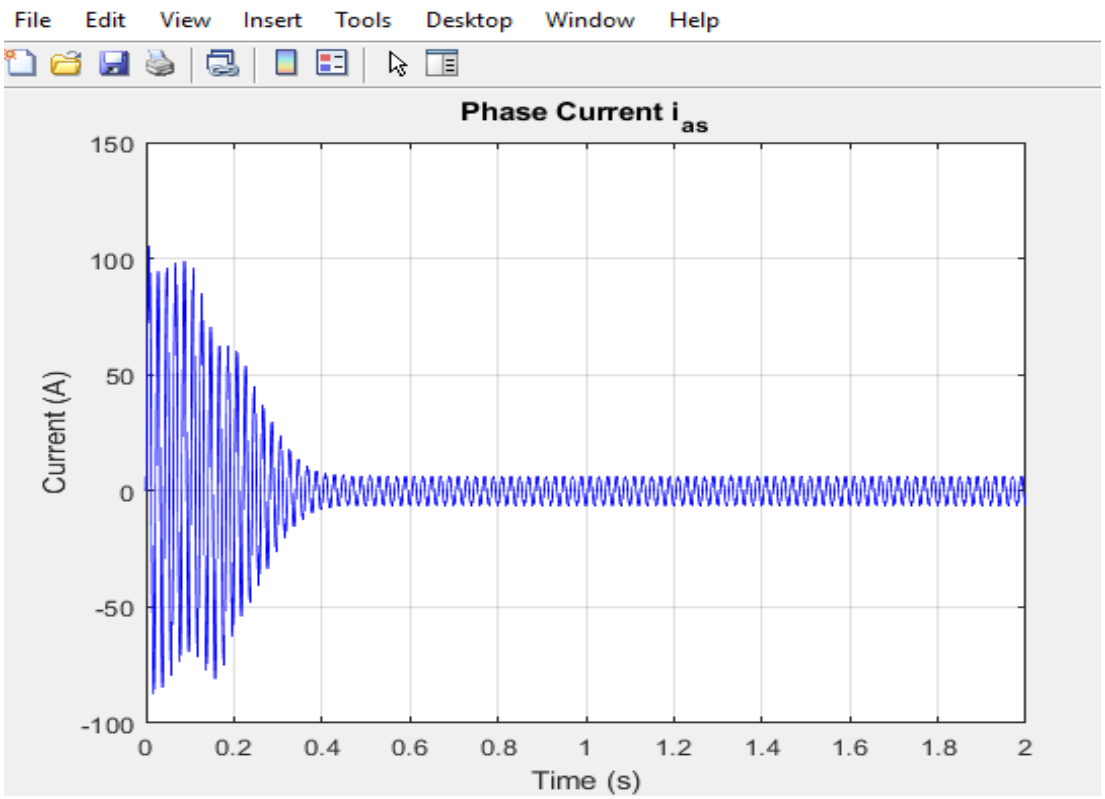

Figure 3.3.2.a

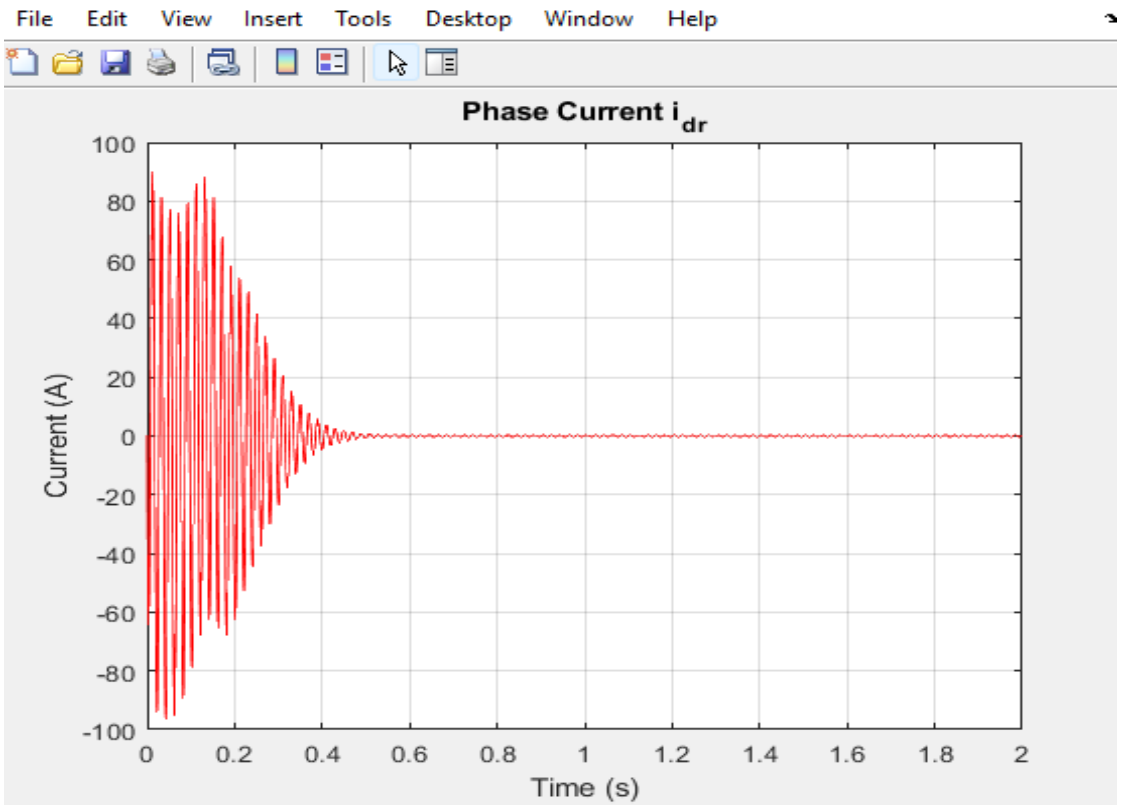

Figure 3.3.2.b

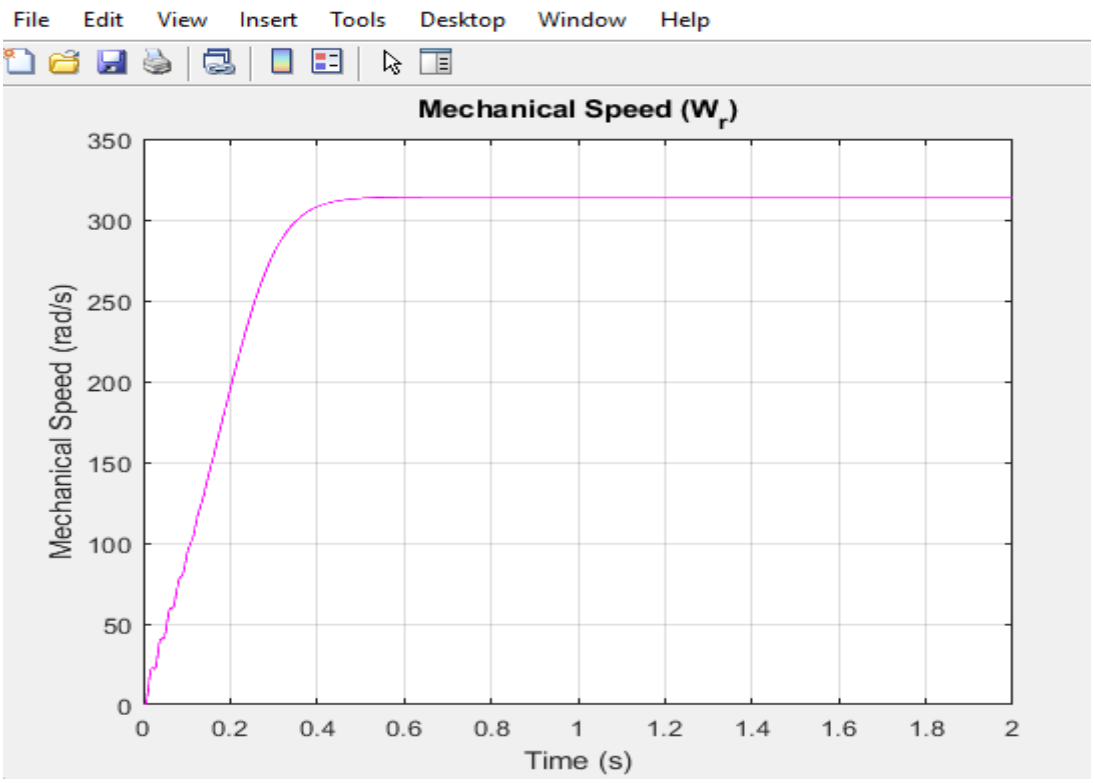

Figure 3.3.2.c

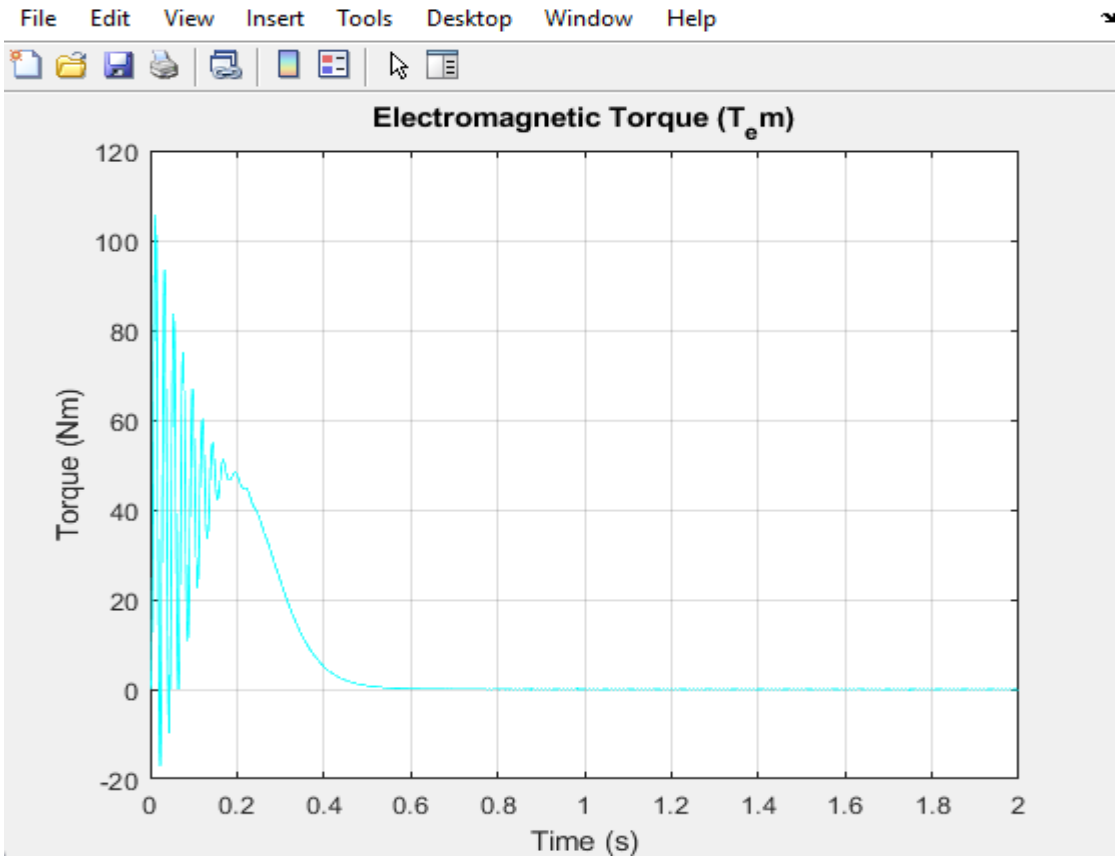

Figure 3.3.2.d

3.3.3 Induction Motor steady state model at no load

In previous chapter that is at chapter 3.3.1 we discussed about DQ model methodology which is used to simplify complex electrical system. That methodology was used to derive dynamic simulation of an induction motor in transient state in chapter 3.3.2. In this chapter we will derive the dynamic simulation of induction again from scratch but we will take it to next level by drawing its Thevenin's equivalent under steady state and then then we will plot Electromagnetic Torque and Angular velocity under steady state at no load condition using MATLAB 2023a by writing MATLAB code. The expression from angular velocity and electromagnetic torque would also be derived under steady state at no load. The parameters are taken considering a 1.5 KW 1Induction Motor. It is assumed that in the derived induction motor models, the rotor bars are short circuited and that there is no load. The D & Q axis models of the induction machine in Figures 3.3.3.1 and Figure 3.3.3.2 which are basically the circuit diagram of the Induction Motor respectively. It should be noted that the stator is used to refer to all variables on the figure and throughout this derivation.

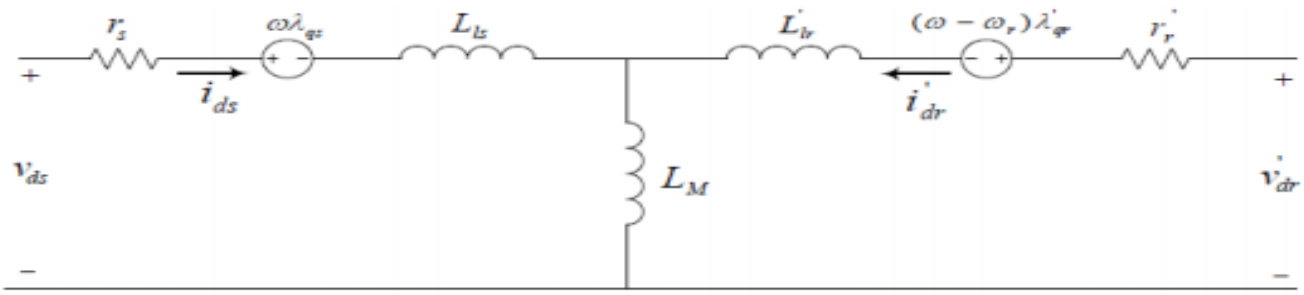

Figure 3.3.3.1

The D-axis of the Induction Motor

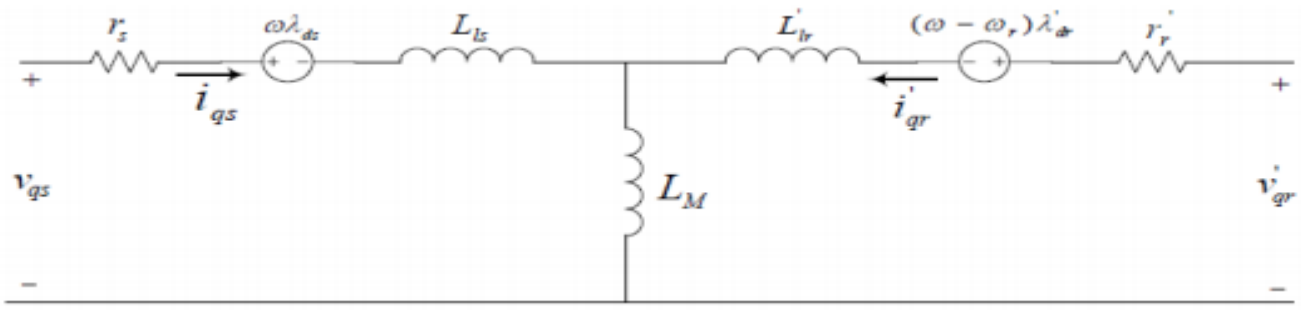

Figure 3.3.3.2

The Q-axis of the Induction Motor

Beginning with the Park Transformation of abc stator variables to d,q stator variables as stated in Equation (3.3.2), the d,q model is derived.

$$[V_{dq0}] = [K_s][V_{abc}] \tag{3.3.1}$$

Where,

$$K_s = \frac{2}{3}\begin{bmatrix} \cos\theta & \cos(\theta-\gamma) & \cos(\theta+\gamma) \\ \sin\theta & \sin(\theta-\gamma) & \sin(\theta+\gamma) \\ \frac{1}{2} & \frac{1}{2} & \frac{1}{2} \end{bmatrix} \tag{3.3.2}$$

The d, q variables of the stators are computed using simulation with a three-phase input power supply. After the circuit analysis, derivation of d, q model is obtained.

$$V_{qd0s} = r_s i_{qd0s} + \omega\lambda_{dq0s} + p\lambda_{dq0s} \tag{3.3.3}$$

$$V_{qd0r}\lambda_{qd0r} = r_r i_{qd0r} + (\omega-\omega_r)\lambda_{qd0r} + p\lambda_{qd0r} \tag{3.3.4}$$

The d, q flux linkages used in the stator variables are such as:

$$\begin{bmatrix}\lambda_{qd0s} \\ \lambda_{qd0r}\end{bmatrix} = \begin{bmatrix} K_s L_s {K_s}^{-1} & K_s L_{sr} {K_r}^{-1} \\ K_r (L_{sr)T} {K_s}^{-1} & K_r L_r {K_r}^{-1} \end{bmatrix}\begin{bmatrix} i_{qd0s} \\ i_{qd0r}\end{bmatrix} \tag{3.3.5}$$

$$K_s L_s {K_s}^{-1} = \begin{bmatrix} L_{ls}+L_M & 0 & 0 \\ 0 & L_{ls}+L_M & 0 \\ 0 & 0 & L_{ls}\end{bmatrix}, \; L_M = L_{ms}\frac{3}{4} \tag{3.3.6}$$

$$K_r L_r {K_r}^{-1} = \begin{bmatrix} L_{lsr}+L_M & 0 & 0 \\ 0 & L_{lr}+L_M & 0 \\ 0 & 0 & L_{lr}\end{bmatrix} \tag{3.3.7}$$

And,

$$K_r (L_{sr)T} {K_s}^{-1} = \; K_s L_{sr} {K_r}^{-1} \; = \begin{bmatrix} L_M & 0 & 0 \\ 0 & L_M & 0 \\ 0 & 0 & 0\end{bmatrix} \tag{3.3.8}$$

Therefore, we can express the d, q fluxes as following matrix:

$$\begin{bmatrix}\lambda_{qs} \\ \lambda_{qr}\end{bmatrix} = \begin{bmatrix} L_{ss} & L_M \\ L_M & L_{rr}\end{bmatrix}\begin{bmatrix} i_{qs} \\ i_{qr}\end{bmatrix} \tag{3.3.9.1}$$

$$\begin{bmatrix}\lambda_{ds} \\ \lambda_{dr}\end{bmatrix} = \begin{bmatrix} L_{ss} & L_M \\ L_M & L_{rr}\end{bmatrix}\begin{bmatrix} i_{ds} \\ i_{dr}\end{bmatrix} \tag{3.3.9.2}$$

The d, q flux variables of the induction machine may be found by performing the basic mathematical procedure. We extract the d, q stator and rotor voltages

from the D-axis and Q-axis circuits using the equivalent circuit analysis approach. Furthermore, the induction machine's rotor bars are short-circuited according to the presumptions, thus the rotor voltages are zero. Equations (3.3.10) and (3.3.11), which represent the stator d, q voltages, and Equations (3.3.13), which represent the rotor d, q voltages, are both found using circuit analysis.

$$V_{qs} = r_s i_{qs} + \omega\lambda_{ds} + p\lambda_{ds} \quad (3.3.10)$$

$$V_{ds} = r_s i_{ds} - \omega\lambda_{qs} + \lambda_{ds} \quad (3.3.11)$$

$$V_{qr} = r_r i_{qr} + (\omega - \omega_r)\lambda_{dr} + p\lambda_{qr} \quad (3.3.12)$$

$$V_{dr} = r_r i_{dr} - (\omega - \omega_r)\lambda_{qr} + p\lambda_{dr} \quad (3.3.13)$$

The stator and rotor resistances are given as r_s and r_r. The d, q flux linkages in terms of stator and rotor current and inductances can be expressed as,

$$\lambda_{qs} = L_{ls} i_{qs} + L_m(i_{qs} + i_{qr}) \quad (3.3.14)$$

$$\lambda_{ds} = L_{ls} i_{ds} + L_m(i_{ds} + i_{dr}) \quad (3.3.15)$$

$$\lambda_{qr} = L_{lr} i_{qr} + L_m(i_{qs} + i_{qr}) \quad (3.3.16)$$

$$\lambda_{dr} = L_{lr} i_{dr} + L_m(i_{ds} + i_{dr}) \quad (3.3.17)$$

In order to calculate for the currents and flux linkages, it is essential that we convert the reluctance of the stator, rotor, and mutual winding to inductance. Equations (3.3.18), (3.3.19) and (3.3.20) are used to accomplish this transition.

$L_{ls} = \frac{X_s}{2\pi f}$ (3.3.18), $L_{lr} = \frac{X_r}{2\pi f}$ (3.3.19) and $L_m = \frac{X_s\frac{2}{3}}{2\pi f}$ (3.3.20)

The self-inductances of stator and rotor can be represented respectively as,

$L_s = L_m + L_{ls}$ (3.3.21) and $L_r = L_m + L_{lr}$ (3.3.22)

We will calculate a parameter D to simplify our calculation. This is D is given as the difference of stator and rotor self-inductances product and square of mutual inductance, D = $L_s L_r - {L_m}^2$

We can now express rotor and stator current in terms of d, q flux linkages and stator and rotor self and mutual inductances as,

$$i_{ds} = \lambda_{ds}\frac{L_r}{D} - \lambda_{dr}\frac{L_r}{D} \quad (3.3.23)$$

$$i_{qs} = \lambda_{qs}\frac{L_r}{D} - \lambda_{qr}\frac{L_r}{D} \quad (3.3.24)$$

$$i_{qr} = \lambda_{qr}\frac{L_r}{D} - \lambda_{qs}\frac{L_r}{D} \quad (3.3.25)$$

$$i_{dr} = \lambda_{dr}\frac{L_r}{D} - \lambda_{ds}\frac{L_r}{D} \quad (3.3.26)$$

Thus the derivative of flux linkages with respect to time can equation be expressed as,

$$\frac{d\lambda_{ds}}{dt} = v_{ds} - \lambda_{ds}\frac{r_s L_r}{D} + \lambda_{dr}\frac{r_s L_m}{D} + \omega_e \lambda_{qs} \quad (3.3.27)$$

$$\frac{d\lambda_{qs}}{dt} = v_{qs} - \lambda_{qs}\frac{r_s L_r}{D} + \lambda_{qr}\frac{r_s L_m}{D} + \omega_e \lambda_{ds} \quad (3.3.28)$$

$$\frac{d\lambda_{qr}}{dt} = 0 - \lambda_{qr}\frac{r_r L_s}{D} + \lambda_{qs}\frac{r_r L_m}{D} - (\omega_e - \omega_r)\lambda_{dr} \quad (3.3.29)$$

$$\frac{d\lambda_{dr}}{dt} = 0 - \lambda_{dr}\frac{r_r L_s}{D} + \lambda_{ds}\frac{r_r L_m}{D} - (\omega_e - \omega_r)\lambda_{qr} \quad (3.3.30)$$

We can calculate the expression of torque as in N.m as,

$$T_e = \frac{3L_m P}{4}(i_{qs} i_{dr} - i_{ds} i_{qr}) \quad (3.3.31)$$

As the load torque under consideration is 0, we can calculate the rotor speed using the Electromagnetic torque and friction co-efficient B as,

$$\frac{d\omega_r}{dt} = \frac{T_e - B\omega_r}{J} \quad (3.3.32)$$

We explore the steady state equivalent model of the DQ Model of the Induction Motor after its DQ Model development. The goal of researching the steady state model is to determine the link between the induction machine's torque and angular speed. The IEEE equivalent induction motor circuit diagram shown in Figure 3.3.3.3 served as the foundation for the steady state model's development.

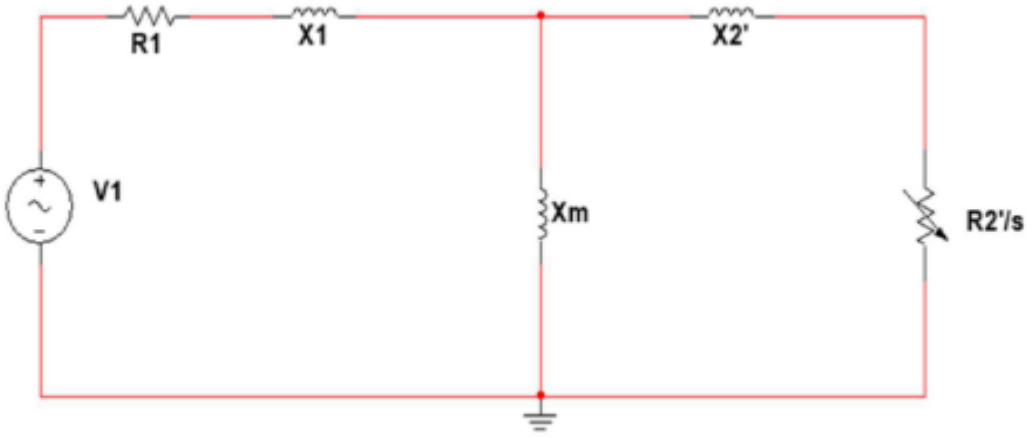

Figure 3.3.3.3

The same parameters will be used for analysis of the steady state equivalent circuit. We will do Circuit analysis to reduce the given circuit to its Thevenin's Equivalent which is shown below in figure 3.3.3.4.

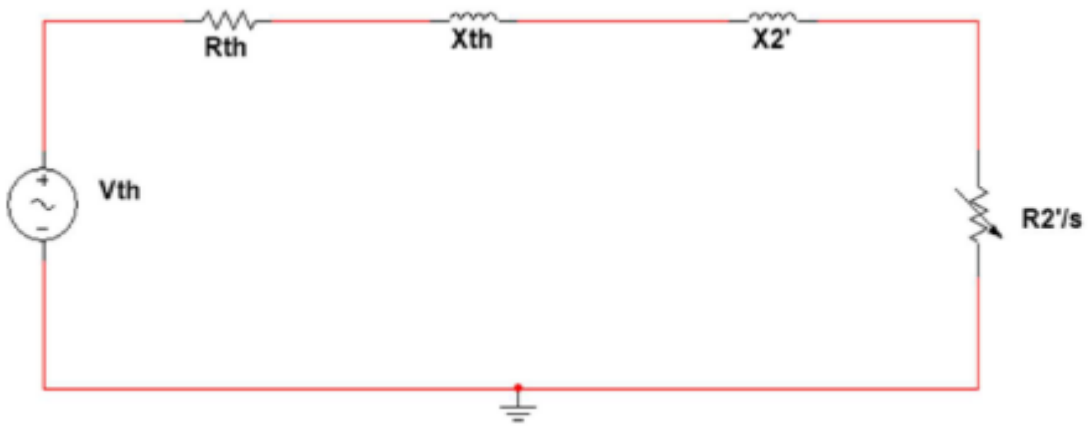

Figure 3.3.3.4

This will reduce all kind of complexity to obtain steady state value of torque and angular speed.

The angular synchronous speed can be written as, here Ns is synchronous speed.

$$\omega_s = \frac{2\pi N_s f}{60P} \qquad (3.3.33)$$

When determining the mechanical torque of an induction motor, the computation of the synchronous speed is crucial. A single Thevenin voltage source (Vth) and resistance (Zth) are also computed from the analogous circuit using Equations (3.3.36) and (3.3.35), respectively. The stator impedance, Zs, provided by Equation (34), is necessary for the derivation of the Thevenin resistance. The stator impedance can be written as,

$$Z_s = R_s + jX_s \qquad (3.3.34)$$

Since Rth and Xth are the real and imaginary components of Zth, respectively, we compute the Thevenin resistance Zth as,

$$Z_{th} = \frac{Z_s + jX_{th}}{Z_s + jX_m} \qquad (3.3.35)$$

$$V_{th} = \frac{V_s X_m}{\sqrt{({R_{th}}^2 + (X_m + X_{th})^2)}} \qquad (3.3.36)$$

So, the final expression of Electromagnetic Torque would be,

$$T_e = \frac{3{V_{th}}^2 \frac{R_r}{s}}{\omega_s\left(\left(R_{th} + \frac{R_r}{s}\right)^2 + (X_{th} + X_r)^2\right)} \qquad (3.3.37)$$

3.3.4 MATLAB implementation of Induction Motor under steady state model at no load

Here's a step-by-step explanation of the code:

1. Variable Initialization:

- The code begins by initializing the input variables such as resistance, reactance, moment of inertia, damping constant, number of pole pairs, frequency, and phase voltage.

- It also calculates the stator and rotor leakage inductances and the magnetizing inductance based on the given reactance values.

- Additionally, it initializes the load torque, time duration, and time step for the simulation.

2. Synchronous Speed and Angular Speed Initialization:

- The synchronous speed (Ns) of the motor is calculated based on the frequency and the number of pole pairs.

- The synchronous angular speed (ws) is then calculated using the synchronous speed.

- The initial rotor speed (wr) is set to zero.

3. Thevenin Equivalent Circuit Parameters:

- The code calculates the Thevenin equivalent circuit parameters, including the Thevenin impedance (Zth), Thevenin resistance (Rth), Thevenin reactance (Xth), and Thevenin voltage magnitude (Vth).

- The equivalent voltage magnitude (Veq) is also calculated.

4. Electromechanical Torque and Speed Calculation:

- The code enters a loop to calculate the electromechanical torque (Tem) and angular mechanical speed (wr) at each time step.

- Within each iteration, the slip (s) is calculated as the difference between the synchronous angular speed (ws) and the current angular speed (wr), divided by the synchronous angular speed.

- Using the slip, the electromechanical torque is calculated based on the Thevenin parameters and the slip value.

- The change in angular speed (delwr) is calculated based on the torque and the damping constant.

- The current angular speed (wr) is updated for the next iteration by adding the change in angular speed (delwr).

- The loop continues until the specified time duration is reached.

5. Plotting the Results:

- After the loop, the time array (t) is created using the linspace function to match the number of iterations.

- The code then plots the angular mechanical speed (wr) against time as shown in Figure 3.3.3.4(a), providing a visualization of how the speed changes over time.

- Similarly, it plots the electromechanical torque (Tem) against time as shown in figure 3.3.3.4(b), showing the torque characteristics during the simulation.

The code performs a numerical simulation for the analysis of behaviour of the induction motor under no-load conditions. It calculates the torque and speed characteristics and provides graphical representations of these variables over time.

MATLAB Code

```
clear;
clc;


% Initializing input variables
Rs = 1.5;                           % Stator resistance
Rr = 0.95;                          % Rotor resistance
Xs = 1.40;                          % Stator reactance
Xr = 1.40;                          % Rotor reactance
Xm = 38.71;                         % Magnetizing reactance
Lls = Xs / (2 * pi * 60);           % Stator leakage inductance
Llr = Xr / (2 * pi * 60);           % Rotor leakage inductance
Lm = (Xm * (2/3)) / (2 * pi * 60);  % Magnetizing inductance
J = 0.0138;                         % Moment of inertia
B = 0.0031;                         % Damping constant
TL = 0;                             % Load torque
P = 4;                              % Number of pole pairs
f = 60;                             % Frequency
Vs = 230;                           % Phase voltage
Vph = Vs / sqrt(3);                 % Phase voltage magnitude
```

```
%%% Express self inductances %%%%
Ls = Lls + Lm;                          % Stator self-inductance
Lr = Llr + Lm;                          % Rotor self-inductance


% Calculations of Synchronous Speed
Ns = 120 * f / P;                       % Synchronous speed
ws = (2 * pi * Ns) / 60;                % Synchronous angular speed
wr(1) = 0;                              % Initial speed of the machine


% Calculation of Thevenin equivalent circuit parameters
z1 = Rs + 1i * Xs;                      % Impedance of the stator
Zth = z1 * 1i * Xm / (z1 + 1i * Xm);    % Thevenin impedance
Rth = real(Zth);                        % Thevenin resistance
Xth = imag(Zth);                        % Thevenin reactance
Vth = Vph * Xm / sqrt(Rs^2 + (Xm + Xm)^2); % Thevenin voltage magnitude
Veq = abs(Vph * 1i * Xm / (Rs + 1i * (Xs + Xm))); % Equivalent voltage
magnitude


time = 2; % Number of seconds for the solution to run
tstep = 0.0001; % Step response time for numerical differential equations


% Calculations for Electromechanical Torque and Speed
for i = 1:1:time / tstep
    s = (ws - wr(i)) / ws; % Calculation of slip
    Tem(i) = (3 * (Vth^2) * (Rr^2 / s)) / ((ws * ((Rth + Rr / s)^2 + (Xth +
Xr)^2))); % Electromechanical torque
    if (i == time / tstep)
        break; % Break the loop when reaching the end time
    end


    delwr = tstep * (Tem(i) - B * wr(i)) / J; % Change in speed
    wr(i + 1) = wr(i) + delwr; % Update the speed for the next iteration
end


t = linspace(0, time - tstep, i); % Time array for plotting
```

```
% Plotting the graphs
plot(t, wr, 'm');
title('Angular Mechanical Speed Vs Time Plot at No Load');
xlabel('Time (s)');
ylabel('Angular Mechanical Speed of Motor (rad/s)');
grid;


figure;
plot(t, Tem, 'c');
title('Electromechanical Torque Vs Time Plot at No Load');
xlabel('Time (s)');
ylabel('Electromechanical Torque (Nm)');
grid;
```

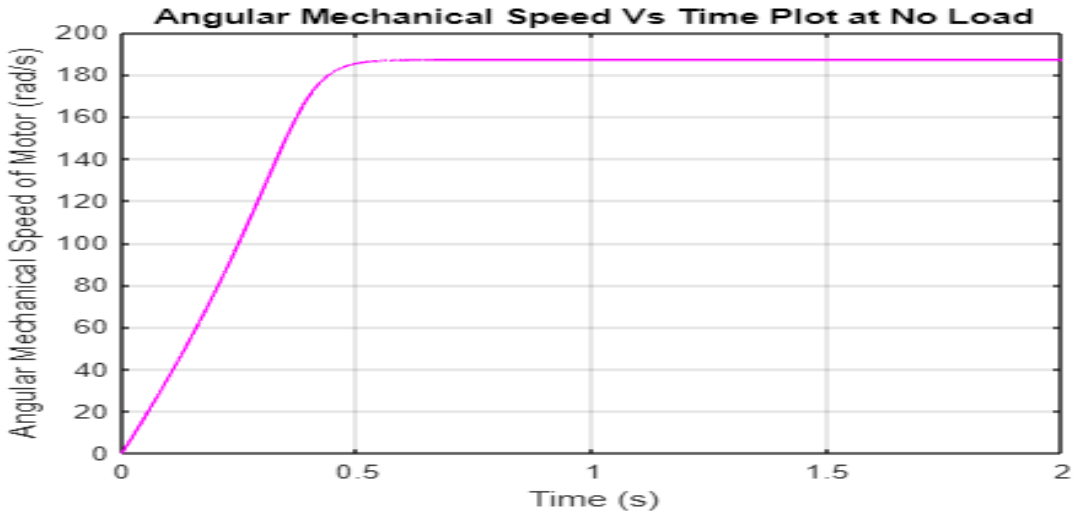

Figure 3.3.3.4(a)

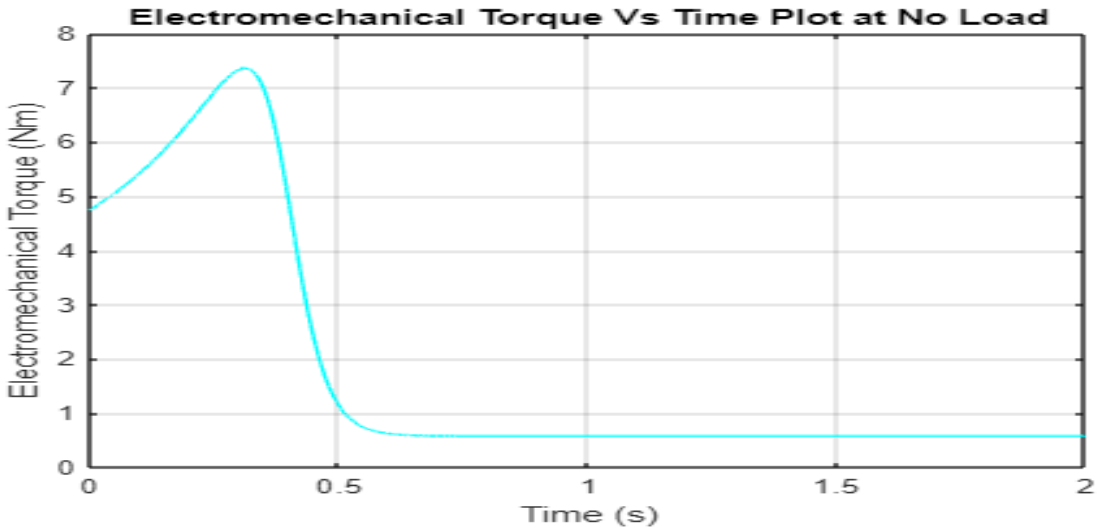

Figure 3.3.3.4(b)

Chapter 4

Air Gap Eccentricity

When the distance between the stator and the rotor is not uniform, it is said to have an air gap eccentricity. The front perspective of the stator and rotor positioning is shown in figure 4.1 below. The rotor axis and rotation point under air-gap eccentricity, as well as the stator axis and ideal rotation point, are also easily discernible. The distance between rotational points is denoted by the symbol dr.

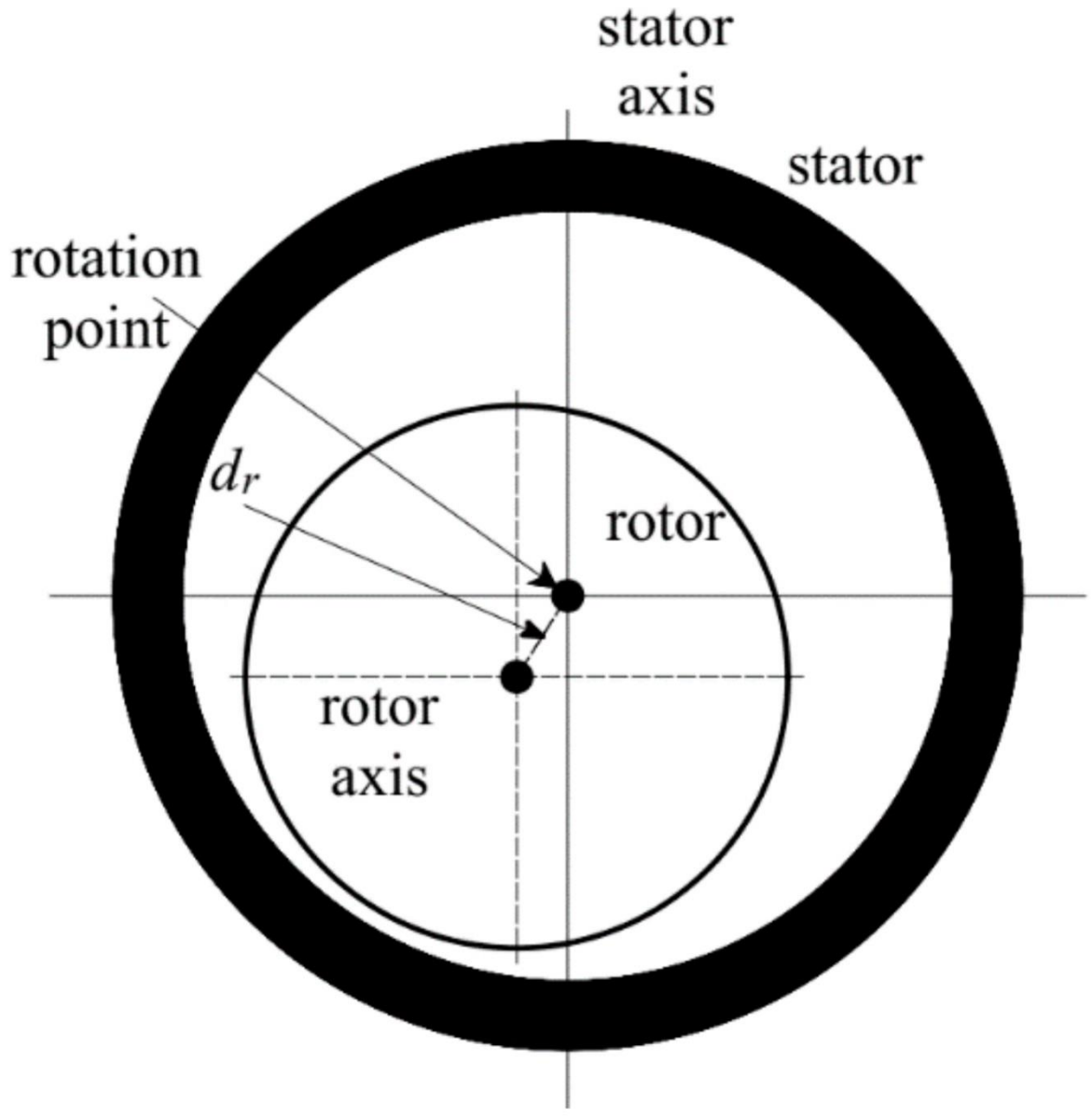

Figure 4.0

4.1 Types of Air Gap Eccentricity

There are three different types of eccentricity.

- **Static Air-gap Eccentricity.** The stator core's ovality, the stator core and bearing's inadvertent location, or both are to blame for this. This kind of eccentricity fixes the minimal air gap.
- **Dynamic Air-gap eccentricity.** When the shaft is not positioned in the Rotor's centre, eccentricity occurs. Because of this, their centres are not aligned when viewed from the front. High levels of static air-gap eccentricity frequently result in dynamic air-gap eccentricity, in which the rotor's centre of rotation is off-center and the minimum air-gap location rotates with the rotor. Figure below shows several types of eccentricity in comparison to typical concentricity. Actually, the intensity of static eccentricity might cause this eccentricity as well.
- **Mixed Air-gap eccentricity.** This eccentricity is the type of eccentricity which is the combination of both.

The Figure 4.1.1 below displays the top view of a motor when it is positioned vertically under various conditions. The Concentric diagram depicts a motor operating normally. Both the static and dynamic eccentricities are depicted. In a static eccentricity, the shaft is at the centre of the rotor, but the rotor and stator's axes of rotation are spaced apart, whereas in a dynamic eccentricity, the shaft is not in the centre of the rotor and the line connecting the two rotates continuously.

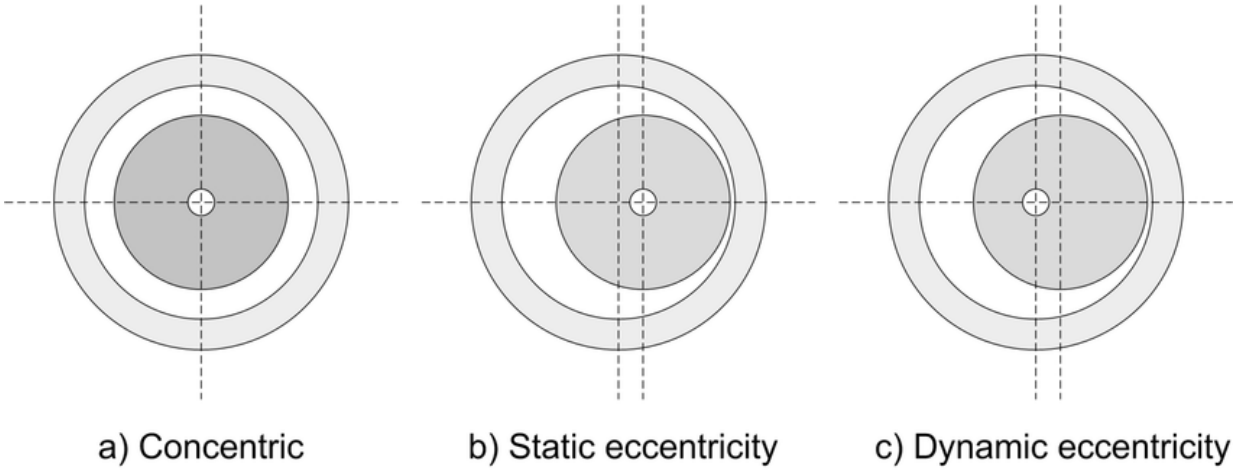

Figure 4.1.1

4.2 Causes of Air Gap eccentricity

The Eccentricity of the air gap as a whole is a mechanical problem. Variations in the distance between the rotor and the stator can have a variety of causes. They often consist of two factors: Rotor dimensions that are oblong in relation to the axis of rotation or stator bores that are eccentric, meaning that they are not entirely round and have some ovality to them. This may also be a result of the fact that the rotor and stator are circular in shape but have distinct rotational axes, or the rotor and shaft may also exhibit this phenomenon. The numerous causes of eccentricity production in an induction motor are explained below.

1. **Manufacturing Defects:** Uneven air gaps may result from errors or flaws that occurred during the construction of the motor. These defects may exist in the stator core, rotor core, mechanical assembly, or both of these components of the motor. Manufacturing errors can lead to uneven air gaps, which can eventually lead to eccentricity.
2. **Assembly Errors:** If the motor is built incorrectly, air gap eccentricity may be seen. For example, improper stator and rotor alignment or poor rotor attachment may result in eccentricity. Even minor errors committed during the assembly process have the potential to alter the air gap.
3. **Thermal Effects**: When an induction motor is operating, heat is produced. When there is thermal cycling or an unequal distribution of temperatures, the stator and rotor of a motor may expand and contract at different rates. Changes in the air gap brought on by this thermal stress may result in eccentricity. Heat generation is still necessary despite the fact that an induction motor has fans installed at one end of the shaft to keep it cool while it operates.
4. **Mechanical Vibrations:** Excessive mechanical vibrations might also contribute to the eccentricity of the air gap. Vibrations can be brought on by a variety of things, such as misaligned coupling components, unbalanced loads, and improper motor installation. These vibrations have the force to move the rotor and alter the air gap's eccentricity.
5. **Rotor Deformation:** The rotor may eventually mechanically bend due to mechanical stress, faults in the rotor bar, or even laminations in the rotor core. Any irregularity in the rotor's structure might lead to eccentricity and throw off the alignment with the stator's air gap.
6. **Wear and Tear:** Prolonged use and motor ageing can cause component wear and tear, especially on the rotor and stator. As a motor ages, the bearings may begin to fail, leading to shaft misalignment and eventually

eccentricity. Similar to this, the air gap eccentricity may also be influenced by deteriorating laminations.

7. **Shaft bent or Warped:** The motor shaft can stretch or flex, which can lead to eccentric air gaps. This can be caused by mechanical stress, improper handling, or external factors like accidents or large loads. A bent shaft will result in an uneven air gap, which will affect the motor's performance.
8. **Rotor imbalance:** The mass distribution of the rotor may be unbalanced, which would lead to air gap eccentricity. A buildup of dirt or debris on the rotor surface, rotor winding wear, or faults committed during manufacture can all result in imbalance. Due of the uneven mass distribution, the rotor departs from the ideal concentric position.
9. **Uneven Magnetic Field**: The magnetic field of the stator winding should be symmetrical and constant to sustain efficient motor operation. However, variations in the magnetic field caused by issues like unequal winding currents or winding faults might result in air gap eccentricity.
10. **External Forces:** Induction motors are susceptible to external forces like vibrations, shocks, or mechanical impacts. Eccentric air gaps will develop from the misalignment of the rotor and stator caused by these external forces.
11. **Rotor shaft displacement**: By moving the rotor shaft either axially or radially, air gap eccentricity may be created. High axial or radial loads, bearing degeneration, or improper installation might all cause this displacement. The rotor shaft's displacement will cause the rotor to move away from its center, which will cause eccentricity.
12. **Rotor Core Faults:** The rotor core of an induction motor is constructed of laminations that may deteriorate over time. Some of these flaws include localized short circuits, degraded insulation, and the presence of foreign objects between the laminations. These defects may result in an unequal distribution of magnetic flux and raise the air gap's eccentricity.
13. **Environmental Conditions**: Unfavorable climatic conditions like extreme temperatures, high humidity, or exposure to contaminants can have an effect on the dimensional stability of motor components. Thermal expansion or contraction, moisture entry, or the presence of corrosive compounds can all lead to air gap eccentricity.
14. **Electrical Faults:** Eccentric air gap Unbalanced voltages, phase asymmetry, or harmonics in the power supply can cause uneven magnetic fields, which can ultimately lead to eccentricity in the air gap.

4.3 Significance of Air Gap eccentricity

Three-phase power is used in induction motors to create spinning electromagnetic fields. This revolving electromagnetic field causes the rotor to conduct electricity. Different levels of voltage are induced on the rotor when there is air-gap eccentricity because the magnet pull is non-uniform and out of balance. It may also cause the stator and rotor to rub against one another, which might seriously harm the stator and rotor core. There are various strains placed on a motor's essential parts when it is operating. These strains further rise because of the eccentricity of the air gap. Acoustic noise and mechanical vibration are also brought on by air-gap eccentricity. These are some changes that can occur due to air gap eccentricity:

1. Air Gap Length: The stator-to-rotor air gap length may vary as a result of eccentricity. This might lead to an uneven distribution of magnetic flux and have an impact on motor performance.

2. Magnetic Flux Density: The eccentricity modifies the air gap's magnetic flux distribution. This may result in an uneven distribution of magnetic flux density, producing torque and magnetic forces that are out of balance.

3. Air Gap Magnetic Field: The eccentricity causes the air gap magnetic field to be asymmetrical. It may result in higher-order spatial components and harmonics of the magnetic field, increasing losses and vibrations.

4. Magnetic Saturation: Localised areas of increased magnetic saturation may occur from the eccentricity's uneven air gap. The motor's overall performance and magnetic characteristics may be impacted by this saturation.

5. Torque Pulsations: Due to the fluctuating air gap length, air gap eccentricity causes torque pulsations. These pulsations can result in motor inefficiency, mechanical vibrations, and increased noise.

6. Increased Losses: The motor experiences more losses as a result of the non-uniform air gap, including copper losses, iron losses, and extra losses brought on by the higher harmonic components.

7. Unbalanced Magnetic Forces: Eccentricity causes imbalanced magnetic forces to act on the rotor, resulting in mechanical vibrations that compromise the mechanical integrity of the motor.

8. Efficiency Reduction: Reduced motor efficiency is the result of higher losses, torque pulsations, and uneven magnetic forces.

4.4 Detection of Air Gap eccentricity

There are several ways to find the air gap eccentricity in an induction motor. Here are some often employed methods:

1. Air Gap Measurement: Using a feeler gauge or other specialised air gap measurement equipment to directly measure the air gap is one of the easiest approaches. Multiple locations on the circumference of the motor are used to measure the air gap; any deviations show eccentricity. The below figure 4.4.1 shows a feeler gauge.

Figure 4.4.1

2. Current Signature Analysis: Air gap eccentricity-related irregularities can be found by looking at the stator current waveform. Eccentricity alters the magnetic field, resulting in asymmetrical rotor-stator interactions and distinctive frequency components in the current spectrum. Current sensing sensor that can be installed to measure stator current

Fig 4.4.2

3. Vibration Analysis: Eccentricity of the air gap can cause mechanical vibrations in the motor. You may find and examine the vibration patterns by employing vibration analysis tools, such as accelerometers or proximity probes. The vibration spectrum of eccentricity frequently has certain frequency components. Below figure 4.4.3(a) shows an accelerometer based on the piezo-electric effect. And a proximity probes 4.4.3(b).

Figure 4.4.3(a)

Figure 4.4.3(b)

4. Flux Probe Measurement: Specialized instruments called flux probes can directly measure the magnetic flux density in the air gap. By scanning the air gap with a flux probe, variations in the flux distribution caused by eccentricity can be detected. Figure 4.4.4 gives placement of a flux probes over stator.

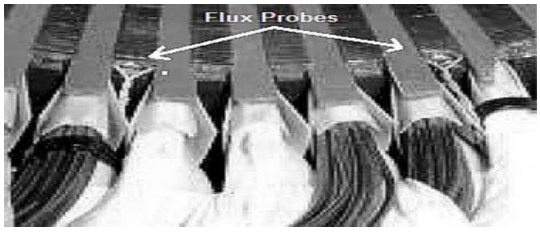

Figure 4.4.4

5. Motor Current Signature Analysis (MCSA): A diagnostic method called Motor Current Signature Analysis (MCSA) is used to evaluate the condition and effectiveness of induction motors. It entails inspecting the current waveform during steady-state operation or motor startup to look for anomalies or departures from a reference signature. MCSA is a useful method for detecting the presence of air gap eccentricity. The current waveform during typical motor operation follows a certain pattern that is consistent with the motor's construction and function. The optimum current signature, however, is deviated from when air gap eccentricity is present because it leads to unequal magnetic fields and mechanical stresses inside the motor. In order to identify the existence of eccentricity, MCSA focuses on recording these changes and comparing them to a reference signature.

6. Electrical Signature Analysis (ESA): An induction motor's electrical characteristics are examined as part of the diagnostic process known as Electrical Signature Analysis (ESA), which seeks to identify numerous defects, including air gap eccentricity. ESA entails looking at the harmonics, power factor, and voltage and current waveforms to spot any changes that would point to the existence of eccentricity. The voltage and current waveforms show particular patterns and correlations that relate to the motor's design and operating circumstances when it is running normally. However, when air gap eccentricity happens, it can influence the motor's electrical behaviour, leading to perceptible changes in these waveforms.

It is also possible to perform the study by simulating alternative air gap eccentricity profiles and then analysing the parameters, or more specifically, the current signature.

4.5 Air Gap eccentricity profiles

These are simplest illustrative example of air gap eccentricity profile which are used for modelling of air gap eccentricity in induction motor.

1.Elliptical Eccentricity Profile:

In cases of air gap eccentricity in induction motors, the deviation of the rotor axis from the center of the stator results in an elliptical-shaped air gap. This elliptical shape can be characterized by two parameters: the major axis and the minor axis of the ellipse. The major axis of the ellipse represents the maximum deviation of the rotor axis from the center of the stator. It indicates the largest distance between the rotor and the stator along a particular direction. In other words, it represents the maximum eccentricity of the air gap. The major axis determines the magnitude of the eccentricity and provides information about the severity of the deviation. On the other hand, the minor axis of the ellipse represents the minimum deviation of the rotor axis from the center of the stator. It represents the smallest distance between the rotor and the stator along a perpendicular direction to the major axis. The minor axis corresponds to the minimum eccentricity of the air gap. While the major axis indicates the maximum eccentricity, the minor axis provides information about the minimum deviation of the rotor. By characterizing the air gap eccentricity with these two parameters, the elliptical shape and the extent of the deviation can be described. The major and minor axes allow for a quantitative assessment of the eccentricity, providing valuable information about the size and orientation of the elliptical air gap. Understanding the major and minor axes of the elliptical air gap is crucial for diagnosing and addressing the eccentricity issue. It helps in determining the corrective measures required, such as rotor realignment, bearing replacement, or repairs to the stator or rotor components. By quantifying the eccentricity using these parameters, maintenance personnel can take appropriate actions to restore the motor's optimal performance and prevent further damage or efficiency losses. It's important to note that the major and minor axes of the air gap ellipse can vary depending on the specific motor and the characteristics of the eccentricity. Detailed measurements and analysis, such as using specialized equipment or techniques like laser-based measurements or magnetic flux probes, may be required to accurately determine the values of the major and minor axes and fully characterize the air gap eccentricity. We will write the code of Elliptical Eccentricity profile in MATLAB 2023a and simulate the result to have the better grasp of elliptical eccentricity profile. We will apply the Elliptical eccentricity on rotor side and plot the difference of stator and rotor current. The code written is dummy code on some arbitrary motor parameters.

```
% Induction Motor Air Gap Eccentricity Simulation for Elliptical Profile

% Parameters
R = 0.5;           % Stator resistance
L = 1;             % Stator inductance
J = 0.1;           % Moment of inertia
B = 0.01;          % Damping coefficient
P = 4;             % Number of poles
f = 50;            % Frequency
V = 1;             % Stator voltage
N = 1000;          % Number of time steps
T = 1/f;           % Time period
t = linspace(0, T, N);  % Time vector

% Air Gap Eccentricity Parameters
e_max_major = 0.1;       % Maximum eccentricity (major axis)
e_max_minor = 0.05;      % Maximum eccentricity (minor axis)
e_major = e_max_major * cos(2*pi*f*t);  % Eccentricity profile (major axis)
e_minor = e_max_minor * sin(2*pi*f*t);  % Eccentricity profile (minor axis)

% Simulation Loop
theta = 0;         % Initial rotor angle
theta_dot = 2*pi*f;  % Initial rotor speed
i_s = zeros(1, N);  % Stator current
i_r = zeros(1, N);  % Rotor current

for n = 1:N
    % Calculate air gap length
    e_major_n = e_major(n);
    e_minor_n = e_minor(n);
    d = 2*(1 + e_major_n + e_minor_n);  % Air gap length (assume circular rotor
and stator)

    % Calculate stator and rotor currents
    i_s(n) = V/(R + 1i*2*pi*f*L) * exp(1i*2*pi*f*t(n));
    i_r(n) = V/(R + 1i*2*pi*f*L) * exp(1i*(2*pi*f*t(n) - theta));

    % Update rotor angle and speed
    theta = theta + theta_dot*T;
    theta_dot = (P/2) * (2*pi*f - theta_dot*(R/J) - B/J*theta_dot*T);
end

% Plotting
figure;
subplot(3, 1, 1);
plot(t, e_major);
hold on;
plot(t, e_minor);
title('Air Gap Eccentricity Profile');
xlabel('Time');
ylabel('Eccentricity');
legend('Major Axis', 'Minor Axis');

subplot(3, 1, 2);
plot(t, real(i_s), 'b', t, real(i_r), 'r');
title('Stator and Rotor Currents');
xlabel('Time');
ylabel('Current');
legend('Stator Current', 'Rotor Current');
```

```
subplot(3, 1, 3);
plot(t, abs(i_s - i_r));
title('Difference between Stator and Rotor Currents');
xlabel('Time');
ylabel('Current Difference');

% Air Gap Eccentricity Detection
threshold = 0.1;   % Detection threshold

% Calculate the magnitude of the difference between stator and rotor currents
current_diff = abs(i_s - i_r);

% Detect air gap eccentricity based on current difference exceeding the threshold
eccentricity_detected = current_diff > threshold;

% Print the time steps when eccentricity is detected
eccentricity_detected_indices = find(eccentricity_detected);
if ~isempty(eccentricity_detected_indices)
    disp('Eccentricity detected at the following time steps:');
    disp(eccentricity_detected_indices);
else
    disp('No eccentricity detected.');
end
```

We can see the plot of Elliptical Air Gap eccentricity profile.

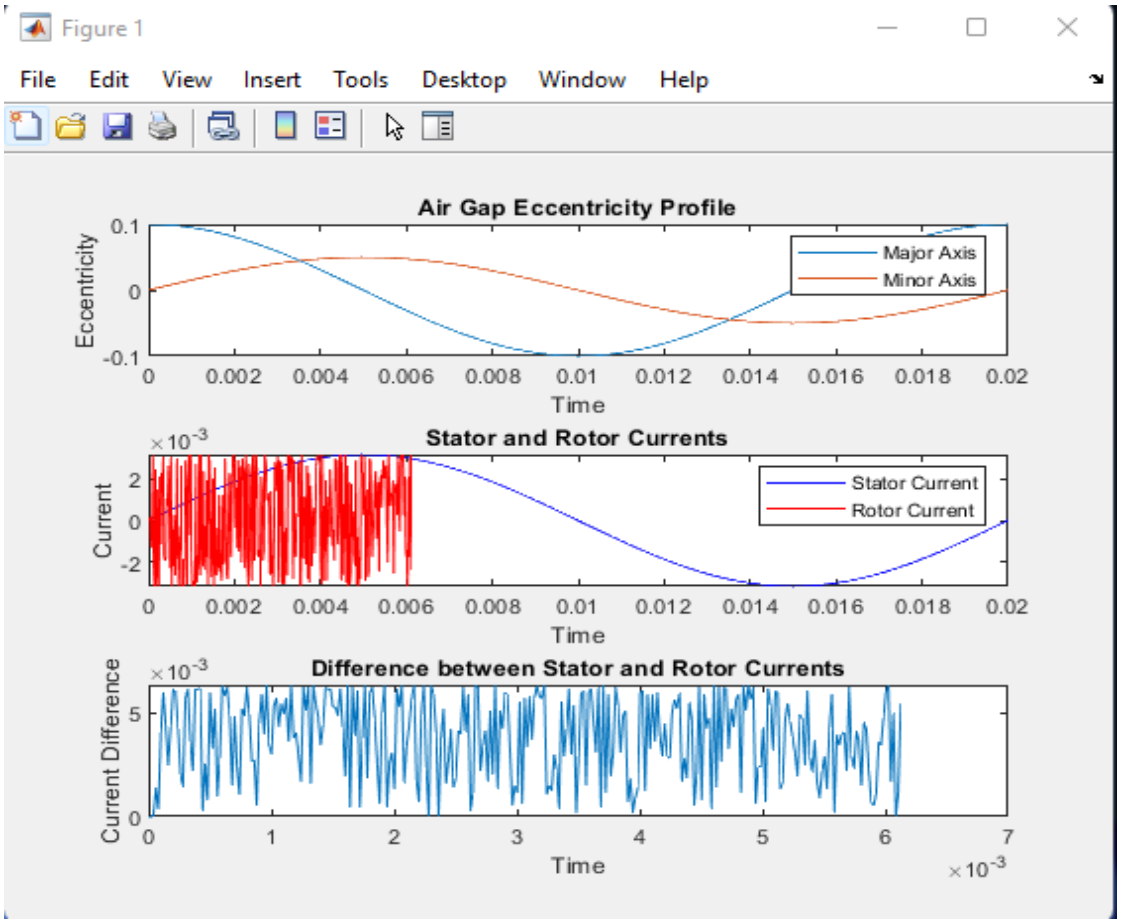

Figure 4.5.1

2. Sinusoidal Eccentricity Profile:

In certain cases of air gap eccentricity in induction motors, the deviation of the rotor axis from the center of the stator follows a sinusoidal pattern, resulting in a periodic variation of the air gap. This sinusoidal variation can be described by two parameters: the amplitude and the frequency of the sinusoidal waveform. The amplitude of the sinusoidal waveform represents the maximum deviation of the rotor axis from the center of the stator. It indicates the maximum distance between the rotor and the stator during each cycle of the sinusoidal pattern. The amplitude provides information about the magnitude of the eccentricity and its impact on the air gap. A larger amplitude indicates a greater deviation and can suggest a more significant eccentricity issue. On the other hand, the frequency of the sinusoidal waveform determines the number of sinusoidal cycles that occur within a given distance. It represents the rate at which the eccentricity pattern repeats itself along the circumference of the air gap. The frequency is usually measured in cycles per unit length (e.g., cycles per millimeter or cycles per inch). A higher frequency means that more sinusoidal cycles occur within a given distance, indicating a faster variation of the eccentricity. By characterizing the air gap eccentricity with these two parameters, the sinusoidal pattern and its characteristics can be described quantitatively. The amplitude and frequency provide valuable information about the magnitude and rate of the eccentricity variation, respectively. Understanding the amplitude and frequency of the sinusoidal air gap eccentricity helps in diagnosing and addressing the issue effectively. Maintenance personnel can determine the severity of the eccentricity and its impact on motor performance. By identifying the amplitude and frequency, suitable corrective actions can be taken, such as realigning the rotor, addressing bearing issues, or performing repairs on the affected components. This knowledge aids in restoring the motor's optimal performance and minimizing the risks associated with eccentricity. Again, it is important to note that the sinusoidal pattern of air gap eccentricity may not always be perfectly regular or uniform. Other factors or disturbances within the motor may introduce irregularities or variations in the sinusoidal waveform. In such cases, more sophisticated analysis techniques, including Fourier analysis or advanced signal processing methods, may be required to accurately extract the amplitude and frequency of the eccentricity pattern. We will write the code of Sinusoidal Eccentricity profile in MATLAB 2023a and simulate the result to have the better grasp of Sinusoidal eccentricity profile. We will apply the Sinusoidal eccentricity on rotor side and plot the difference of stator and rotor current.

```
% Induction Motor Air Gap Eccentricity Simulation for Sinusoidal Profile

% Parameters
R = 0.5;           % Stator resistance
L = 1;             % Stator inductance
J = 0.1;           % Moment of inertia
B = 0.01;          % Damping coefficient
P = 4;             % Number of poles
f = 50;            % Frequency
V = 1;             % Stator voltage
N = 1000;          % Number of time steps
T = 1/f;           % Time period
t = linspace(0, T, N);  % Time vector

% Air Gap Eccentricity Parameters
e_max = 0.1;       % Maximum eccentricity
e_profile = e_max * sin(2*pi*f*t);  % Eccentricity profile (sinusoidal)

% Simulation Loop
theta = 0;         % Initial rotor angle
theta_dot = 2*pi*f;  % Initial rotor speed
i_s = zeros(1, N);  % Stator current
i_r = zeros(1, N);  % Rotor current

for n = 1:N
    % Calculate air gap length
    e = e_profile(n);
    d = 2*(1 + e);  % Air gap length (assume circular rotor and stator)

    % Calculate stator and rotor currents
    i_s(n) = V/(R + 1i*2*pi*f*L) * exp(1i*2*pi*f*t(n));
    i_r(n) = V/(R + 1i*2*pi*f*L) * exp(1i*(2*pi*f*t(n) - theta));

    % Update rotor angle and speed
    theta = theta + theta_dot*T;
    theta_dot = (P/2) * (2*pi*f - theta_dot*(R/J) - B/J*theta_dot*T);
end

% Plotting
figure;
subplot(3, 1, 1);
plot(t, e_profile);
title('Air Gap Eccentricity Profile');
xlabel('Time');
ylabel('Eccentricity (e)');

subplot(3, 1, 2);
plot(t, real(i_s), 'b', t, real(i_r), 'r');
title('Stator and Rotor Currents');
xlabel('Time');
ylabel('Current');
legend('Stator Current', 'Rotor Current');

subplot(3, 1, 3);
plot(t, abs(i_s - i_r));
title('Difference between Stator and Rotor Currents');
xlabel('Time');
ylabel('Current Difference');
```

```
% Air Gap Eccentricity Detection
threshold = 0.1;   % Detection threshold

% Calculate the magnitude of the difference between stator and rotor currents
current_diff = abs(i_s - i_r);

% Detect air gap eccentricity based on current difference exceeding the threshold
eccentricity_detected = current_diff > threshold;

% Print the time steps when eccentricity is detected
eccentricity_detected_indices = find(eccentricity_detected);
if ~isempty(eccentricity_detected_indices)
    disp('Eccentricity detected at the following time steps:');
    disp(eccentricity_detected_indices);
else
    disp('No eccentricity detected.');
end
```

We can see the plot of Sinusoidal Air Gap eccentricity profile.

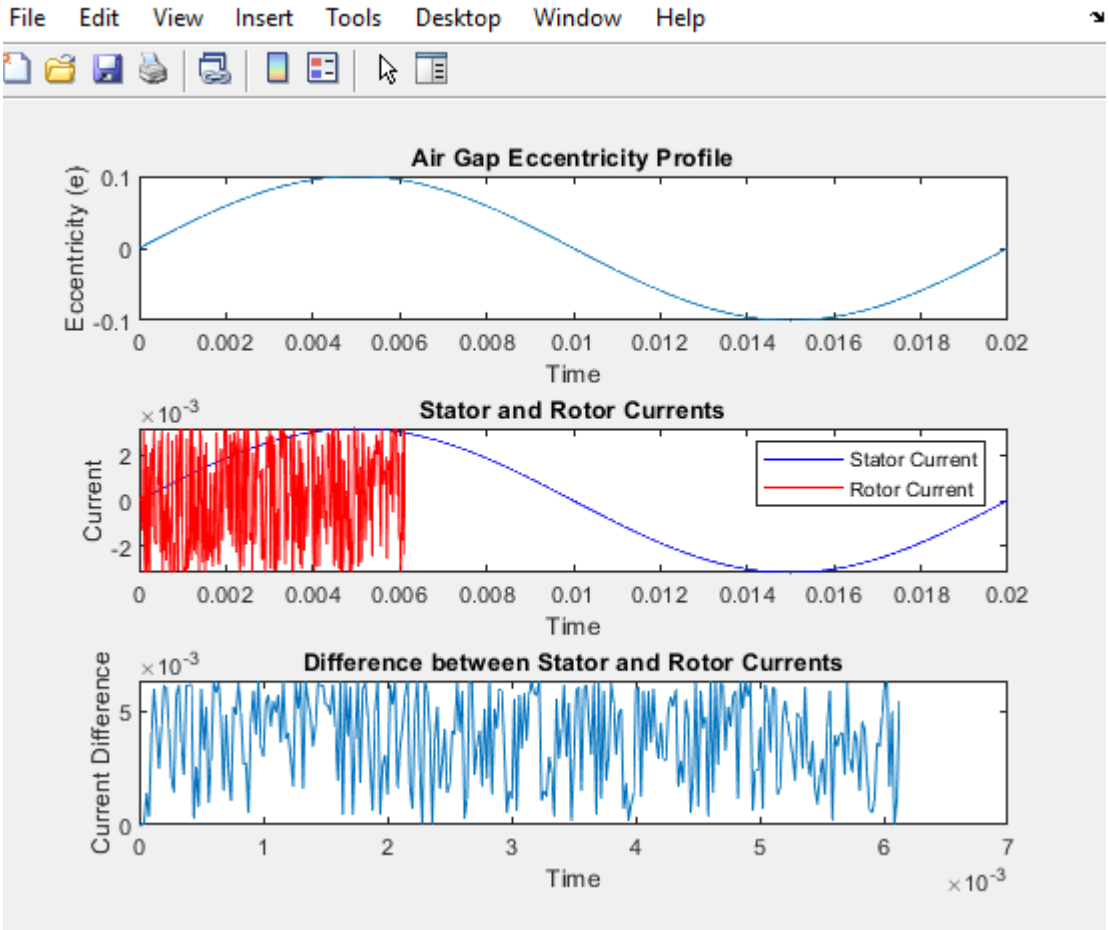

Figure 4.5.2

3. Stepped Eccentricity Profile:

In certain cases of air gap eccentricity in induction motors, the deviation of the rotor axis from the center of the stator exhibits a stepped or discontinuous pattern. This means that the rotor axis deviates from the center in discrete steps or increments, resulting in uneven variations in the air gap. The stepped or discontinuous pattern of eccentricity can be characterized by two main parameters: the step size and the magnitude of each discrete deviation. The step size represents the distance or increment between consecutive steps in the eccentricity pattern. It indicates the discrete change in the position of the rotor axis as it deviates from the center of the stator. The step size provides information about the scale or size of each deviation. A larger step size indicates a more significant change in the rotor position, while a smaller step size suggests smaller deviations. The magnitude of each discrete deviation represents the extent of each individual step in the eccentricity pattern. It signifies the maximum distance between the rotor and the stator during each step. The magnitude provides information about the amplitude of the eccentricity at each discrete position. It helps in understanding the impact of each deviation on the air gap and motor performance. By characterizing the air gap eccentricity with these parameters, the stepped or discontinuous pattern can be described quantitatively. The step size and magnitude provide valuable insights into the nature and magnitude of the deviations. Understanding the step size and magnitude of the eccentricity pattern helps in diagnosing and addressing the issue effectively. Maintenance personnel can determine the severity and distribution of the eccentricity and its potential impact on motor performance. By identifying the step size and magnitude, appropriate corrective actions can be taken, such as realigning the rotor, addressing mechanical issues, or performing repairs on the affected components. This knowledge aids in restoring the motor's optimal performance and minimizing the risks associated with eccentricity. As discussed previously, it is important to note that the stepped or discontinuous pattern of air gap eccentricity may arise from various causes, such as mechanical faults, misalignment, or improper assembly. Identifying the specific cause of the eccentricity is essential to determine the appropriate corrective measures. Detailed inspection and analysis may be required to accurately quantify the step size and magnitude of the eccentricity pattern and address the underlying issues effectively. We will write the code of Stepped Eccentricity profile in MATLAB 2023a and simulate the result to have the better grasp of stepped eccentricity profile. We will apply the Stepped eccentricity on rotor side and plot the difference of stator and rotor current.

```
% Induction Motor Air Gap Eccentricity Simulation for step profile
```

```
% Parameters
R = 0.5;           % Stator resistance
L = 1;             % Stator inductance
J = 0.1;           % Moment of inertia
B = 0.01;          % Damping coefficient
P = 4;             % Number of poles
f = 50;            % Frequency
V = 1;             % Stator voltage
N = 1000;          % Number of time steps
T = 1/f;           % Time period
t = linspace(0, T, N);  % Time vector
% Air Gap Eccentricity Parameters
e_step = 0.1;       % Step eccentricity
e_period = T/4;     % Eccentricity period

% Calculate the number of steps per eccentricity period
num_steps = floor(N * e_period / T);

% Initialize the eccentricity profile
e_profile = zeros(1, N);

% Generate the stepped eccentricity profile
step_size = e_step / num_steps;
for n = 1:num_steps
    start_index = floor((n - 1) * N / num_steps) + 1;
    end_index = floor(n * N / num_steps);
    e_profile(start_index:end_index) = (n - 1) * step_size;
end
% Simulation Loop
theta = 0;           % Initial rotor angle
theta_dot = 2*pi*f;  % Initial rotor speed
i_s = zeros(1, N);   % Stator current
i_r = zeros(1, N);   % Rotor current

for n = 1:N
    % Calculate air gap length
    e = e_profile(n);
    d = 2*(1 + e);  % Air gap length (assume circular rotor and stator)

    % Calculate stator and rotor currents
    i_s(n) = V/(R + 1i*2*pi*f*L) * exp(1i*2*pi*f*t(n));
    i_r(n) = V/(R + 1i*2*pi*f*L) * exp(1i*(2*pi*f*t(n) - theta));

    % Update rotor angle and speed
    theta = theta + theta_dot*T;
    theta_dot = (P/2) * (2*pi*f - theta_dot*(R/J) - B/J*theta_dot*T);
end

% Plotting
figure;
subplot(3, 1, 1);
plot(t, e_profile);
title('Air Gap Eccentricity Profile');
xlabel('Time');
ylabel('Eccentricity (e)');

subplot(3, 1, 2);
plot(t, real(i_s), 'b', t, real(i_r), 'r');
```

```
title('Stator and Rotor Currents');
xlabel('Time');
ylabel('Current');
legend('Stator Current', 'Rotor Current');

subplot(3, 1, 3);
plot(t, abs(i_s - i_r));
title('Difference between Stator and Rotor Currents');
xlabel('Time');
ylabel('Current Difference');

% Air Gap Eccentricity Detection
threshold = 0.1;   % Detection threshold

% Calculate the magnitude of the difference between stator and rotor currents
current_diff = abs(i_s - i_r);

% Detect air gap eccentricity based on current difference exceeding the threshold
eccentricity_detected = current_diff > threshold;

% Print the time steps when eccentricity is detected
eccentricity_detected_indices = find(eccentricity_detected);
if ~isempty(eccentricity_detected_indices)
    disp('Eccentricity detected at the following time steps:');
    disp(eccentricity_detected_indices);
else
    disp('No eccentricity detected.');
end;
```

We can see the plot of Stepped Air Gap eccentricity profile.

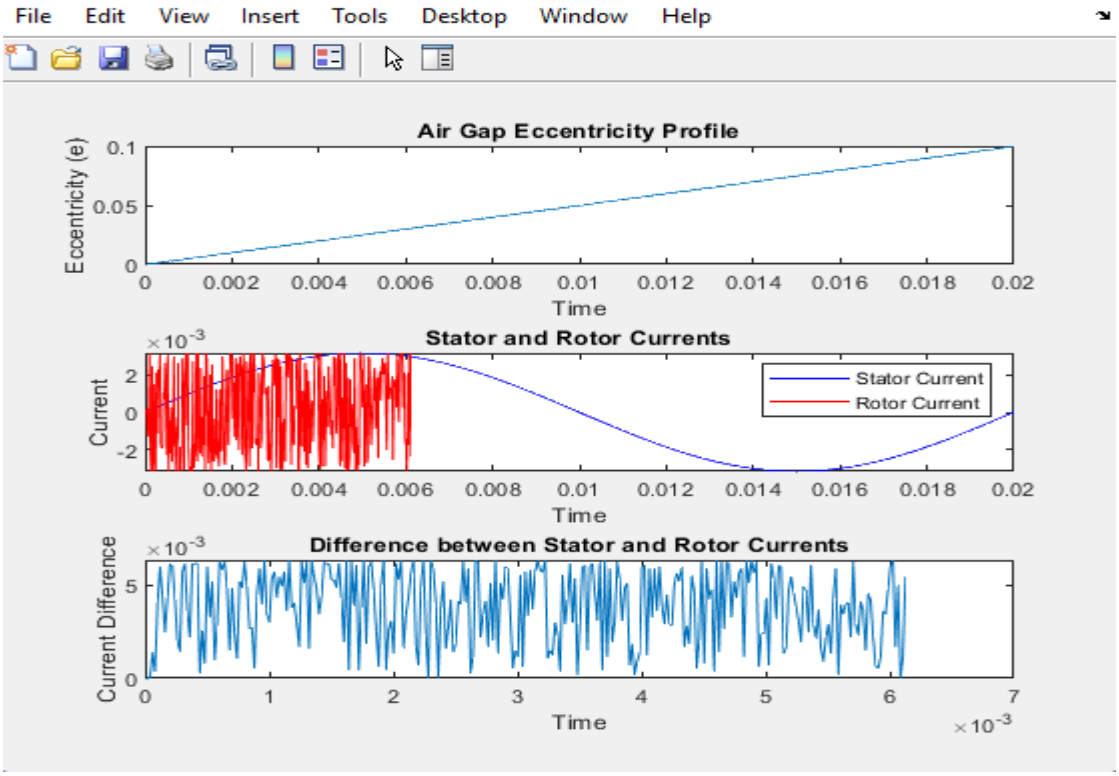

Figure 4.5.3

Indeed, the profiles mentioned earlier (elliptical, sinusoidal, and stepped) are simplified representations of air gap eccentricity for illustrative purposes. In reality, the eccentricity profile can be much more complex and diverse, depending on various factors such as motor design, manufacturing tolerances, operating conditions, and external influences.

In practice, air gap eccentricity rarely conforms strictly to a single profile. Instead, it can involve a combination of different profiles or exhibit variations across different sections of the air gap. The actual eccentricity profile may be influenced by factors such as rotor deformations, manufacturing imperfections, bearing wear, thermal effects, and external mechanical forces.

For example, a motor may exhibit a combination of elliptical and sinusoidal components in its eccentricity profile. This can occur if there are both static and dynamic factors contributing to the eccentricity, such as rotor misalignment and mechanical vibrations. The eccentricity profile may show varying amplitudes and frequencies at different angular positions around the air gap.

Additionally, the eccentricity profile can change over time due to factors such as temperature variations, aging of motor components, or changes in operating conditions. For instance, as the motor heats up during operation, thermal expansion can lead to alterations in the eccentricity pattern.

Furthermore, external influences such as external magnetic fields, mechanical stresses, or uneven loading can introduce additional complexities to the eccentricity profile. These factors can cause localized variations or irregularities in the eccentricity pattern, making it even more challenging to characterize accurately.

To accurately analyze and diagnose eccentricity in practical scenarios, it may be necessary to employ advanced diagnostic techniques, such as high-resolution measurements, advanced signal processing algorithms, or even finite element analysis (FEA) simulations. These techniques can provide a more comprehensive understanding of the eccentricity profile and its effects on motor performance.

Overall, it's crucial to acknowledge that real-world eccentricity profiles are diverse and multifaceted, often involving a combination of different profiles and variations. Understanding and effectively addressing these complex profiles require expertise, advanced diagnostic tools, and a comprehensive approach to motor condition monitoring and maintenance.

Chapter 5

Modelling of Air Gap Eccentricity in Induction Motor

In Chapter 3 we learnt how to simulate Induction Motor after transforming its equation in DQ frame. We learn to derive the equations for both dynamic simulation as well as steady state simulation of Induction Motor. With MATLAB code written on live script, we were able to see the plots of Stator and Rotor Current, Electromagnetic Torque and Angular velocity of the motor in transient state as well as in steady state under no load condition so the load torque was considered 0 throughout the calculation for the sake of simplicity. The expression for Electromagnetic Torque is obtained in both the state and equivalent electrical circuit is drawn.

In Chapter 4 we learnt about Air gap eccentricity in induction motor. We learned about the various kind simplest air gap eccentricity profiles that can be mathematically expressed to represent stator and rotor eccentricity. While in real life scenarios there are more complex eccentricity profiles, than the ones mentioned earlier, which can be combination of simple one or may even involve more complex profile like tangential, radial etc. We will limit our modelling to Elliptical, Sinusoidal and Stepped Eccentricity profiles only for the sake of lucidity. Few more Modelling however can be made by the combination of these profiles.

In this chapter we will apply air gap eccentricity profiles in the DQ model of Induction Motor and observe the nature of plots both in transient condition as well as under normal condition.

The general theory for induction motor Air gap eccentricity is that if eccentricity is present there the inductance of the motor changes because of unbalanced magnetic pull. Now we can add this eccentrcity profile as mathematical expression in inductance equation of Induction motor transient model. This way we can observe the changes in plot. The magnitude of eccentricity are taken in such a way that we get similar kind of plot in all the air gap eccentricity modelling. We will write the code using live script of MATLAB and will use MATLAB 2023a for plot analysis under these various eccentricity profile.

5.1 Air Gap Eccentricity Modelling in DQ transient profile

In this chapter we will just modify the code written for dynamic DQ modelling of Induction Motor by adding Air gap eccentricity profiles. The plot of stator current, rotor current, Electromagnetic Torque and Angular velocity is obtained.

5.1.1 Air Gap Eccentricity Modelling in DQ transient profile using Elliptical Eccentricity

1. Elliptical eccentricity profile:

- The geometry of the air gap variation is elliptical..

- As the rotor revolves, the distance between the surfaces of the rotor and stator changes Sinusoidally.

- The degree of eccentricity is determined by the eccentricity ratio, which compares the lengths of the major and minor axes of an elliptical form..

- It may be brought on by things like mechanical misalignments, heat expansion, or manufacturing flaws.

- It results in imbalanced magnetic forces, increased vibration and noise, decreased efficiency, and the possibility of the motor being damaged.

The following MATLAB codes are written and the eccentricity addition as well simulation loop are well explained using comments.

MATLAB Code

```
clear;
clc;

V = 220;
rs = 0.435;
Xls = 0.754;
XM = 26.13;
Xlr = 0.754;
rr = 0.816;
J = 0.089;
TL = 0;
Wb = 2*pi*50;
P = 4;
Lls = Xls/Wb;
Llr = Xlr/Wb;
M = XM/Wb;

% Define eccentricity parameters
eccentricity_amplitude_major = 0.01;   % Eccentricity amplitude (major axis)
```

```
eccentricity_amplitude_minor = 0.005;  % Eccentricity amplitude (minor axis)
eccentricity_angle = pi/4;              % Eccentricity angle (in radians)

% Calculate eccentricity-induced changes in inductances
delta_Lls = eccentricity_amplitude_major * cos(eccentricity_angle);
delta_Llr = eccentricity_amplitude_minor * sin(eccentricity_angle);

Lss = Lls + M + delta_Lls;
Lrr = Llr + M + delta_Llr;

Lms = M + delta_Lls/2;
Lmr = M + delta_Llr/2;

D = Lss*Lrr - Lms*Lmr;

h = 1e-5;
Tfinal = 1;
n = round(Tfinal/h) + 1;

psi_qs = zeros(1,n);
psi_ds = zeros(1,n);
psi_qr = zeros(1,n);
psi_dr = zeros(1,n);
Wrm = zeros(1,n);
Wrm = zeros(1,n);

i_qs = zeros(1,n);
i_ds = zeros(1,n);
i_qr = zeros(1,n);
i_dr = zeros(1,n);
Wr = zeros(1,n);
Tem = zeros(1,n);

i_as = zeros(1,n);
i_bs = zeros(1,n);
i_cs = zeros(1,n);

i_ar = zeros(1,n);
i_br = zeros(1,n);
i_cr = zeros(1,n);

v_qs = zeros(1,n);
v_ds = zeros(1,n);
v_qr = zeros(1,n);
v_dr = zeros(1,n);
TL = zeros(1,n);

B = [1 0 1;
     -0.5 -sqrt(3)/2 1;
     -0.5 sqrt(3)/2 1];

% Stepped eccentricity parameters
eccentricity_step_value = 0.002;      % Eccentricity step value
eccentricity_step_duration = 0.2;     % Eccentricity step duration (in seconds)

% Numerical integration
time = 0;
k(1) = 0;
k(2) = 0;
```

```
TL(1) = 0;
TL(2) = 0;
for i = 3:n
    time = time + h;
    k(i) = k(i-1) + 1;
    TL(i) = 0;

    va = V*sqrt(2/3)*sin(Wb*time);
    vb = V*sqrt(2/3)*sin(Wb*time - 2*pi/3);
    vc = V*sqrt(2/3)*sin(Wb*time + 2*pi/3);
    v_qs(i) = 2/3*(va - ((vb + vc)/2));
    v_ds(i) = 2/3*((-vb + vc)*sqrt(3)/2);

    psi_ds(i) = psi_ds(i-1) + h*(v_ds(i-1) - rs*i_ds(i-1));
    psi_qs(i) = psi_qs(i-1) + h*(v_qs(i-1) - rs*i_qs(i-1));
    psi_dr(i) = psi_dr(i-1) + h*(v_dr(i-1) - rr*i_dr(i-1) - Wr(i-1)*psi_qr(i-1));
    psi_qr(i) = psi_qr(i-1) + h*(v_qr(i-1) - rr*i_qr(i-1) + Wr(i-1)*psi_dr(i-1));
    Wrm(i) = Wrm(i-1) + h*(Tem(i-1) - TL(i-1))/J;

    % Apply stepped eccentricity
    step_time = mod(time, eccentricity_step_duration);
    if step_time <= eccentricity_step_duration/2
        delta_Lls = eccentricity_step_value;
        delta_Llr = eccentricity_step_value;
    else
        delta_Lls = 0;
        delta_Llr = 0;
    end

    Lss = Lls + M + delta_Lls;
    Lrr = Llr + M + delta_Llr;

    Lms = M + delta_Lls/2;
    Lmr = M + delta_Llr/2;

    D = Lss*Lrr - Lms*Lmr;

    i_ds(i) = (Lrr*psi_ds(i) - M*psi_dr(i))/D;
    i_qs(i) = (Lrr*psi_qs(i) - M*psi_qr(i))/D;
    i_dr(i) = (Lss*psi_dr(i) - M*psi_ds(i))/D;
    i_qr(i) = (Lss*psi_qr(i) - M*psi_qs(i))/D;

    Tem(i) = (P/2)*(psi_qr(i)*i_dr(i) - psi_dr(i)*i_qr(i));
    Wr(i) = (P/2)*Wrm(i);

    i_as(i) = i_qs(i);
    i_bs(i) = -i_qs(i)/2 + i_ds(i)*(-sqrt(3)/2);
    i_cs(i) = -i_qs(i)/2 + i_ds(i)*(sqrt(3)/2);
end

t = 0:h:Tfinal;
figure();
plot(t, i_as, 'b');
figure();
plot(t, i_dr, 'r');
figure();
plot(t, Wr, 'm');
figure();
plot(t, Tem, 'c');
```

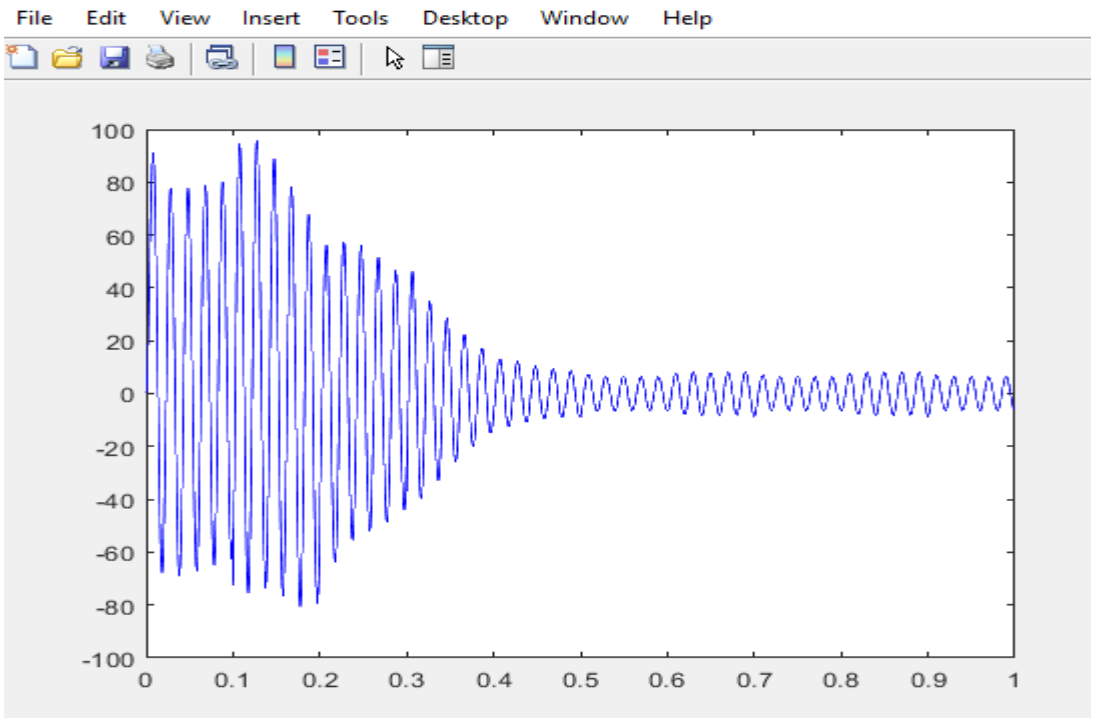

Figure 5.1.1(a)

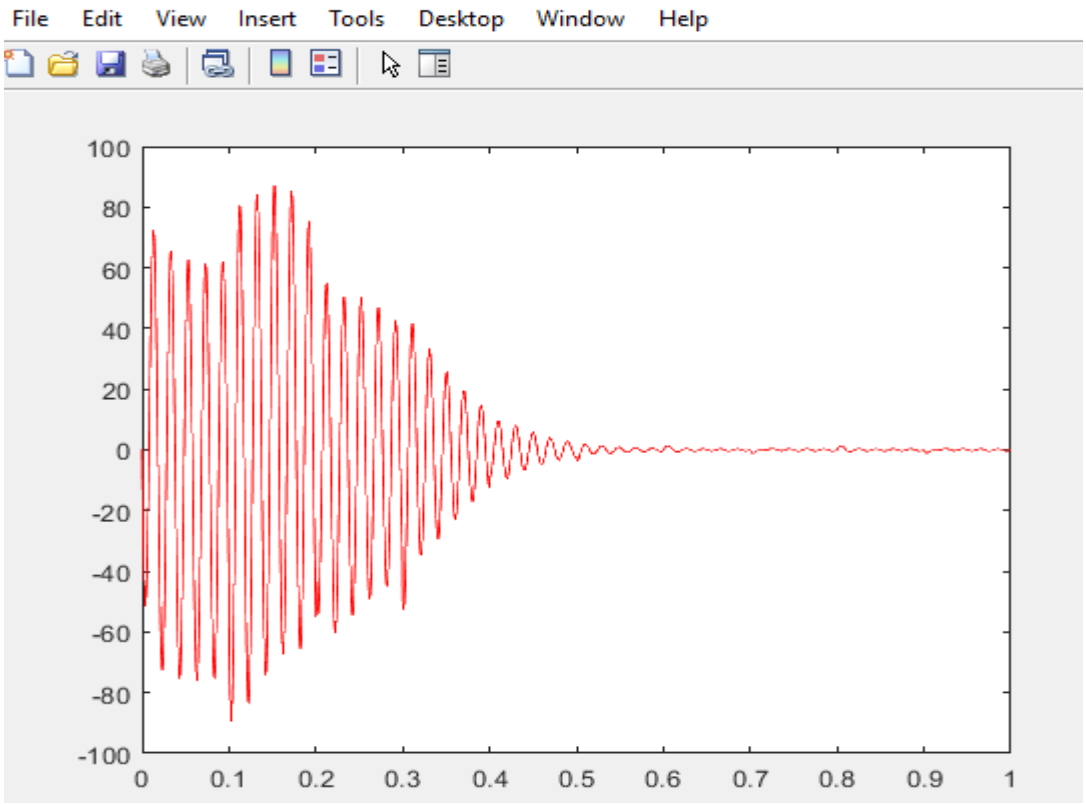

Figure 5.1.1(b)

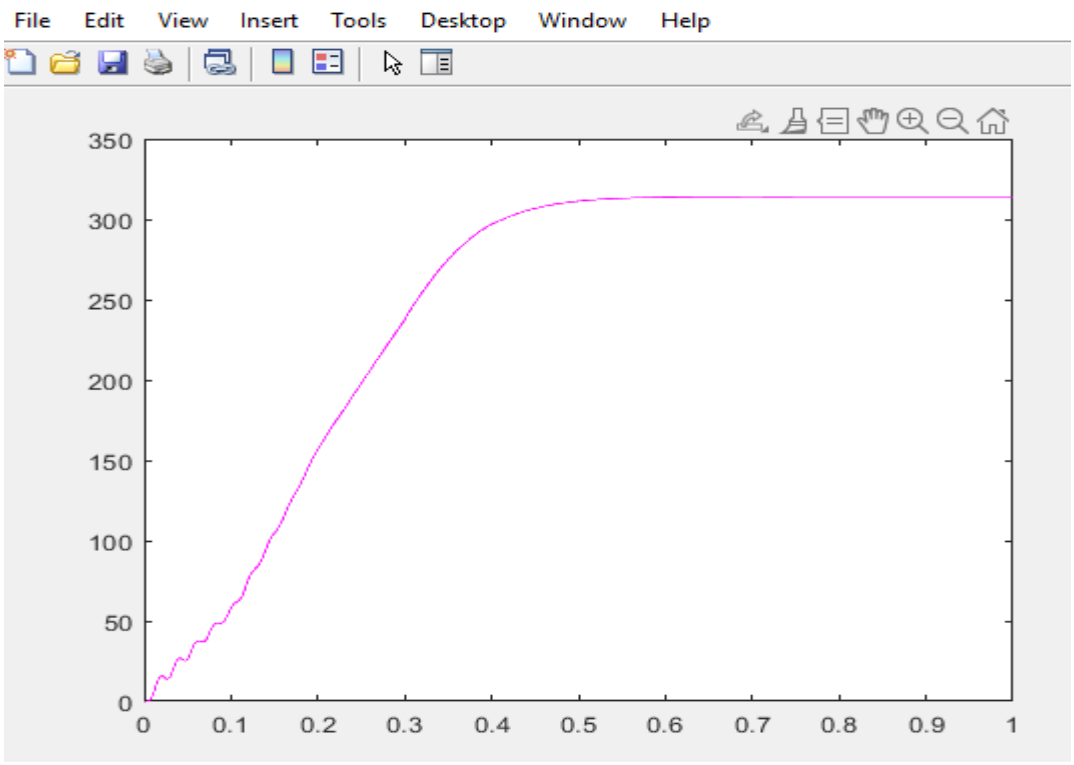

Figure 5.1.1(c)

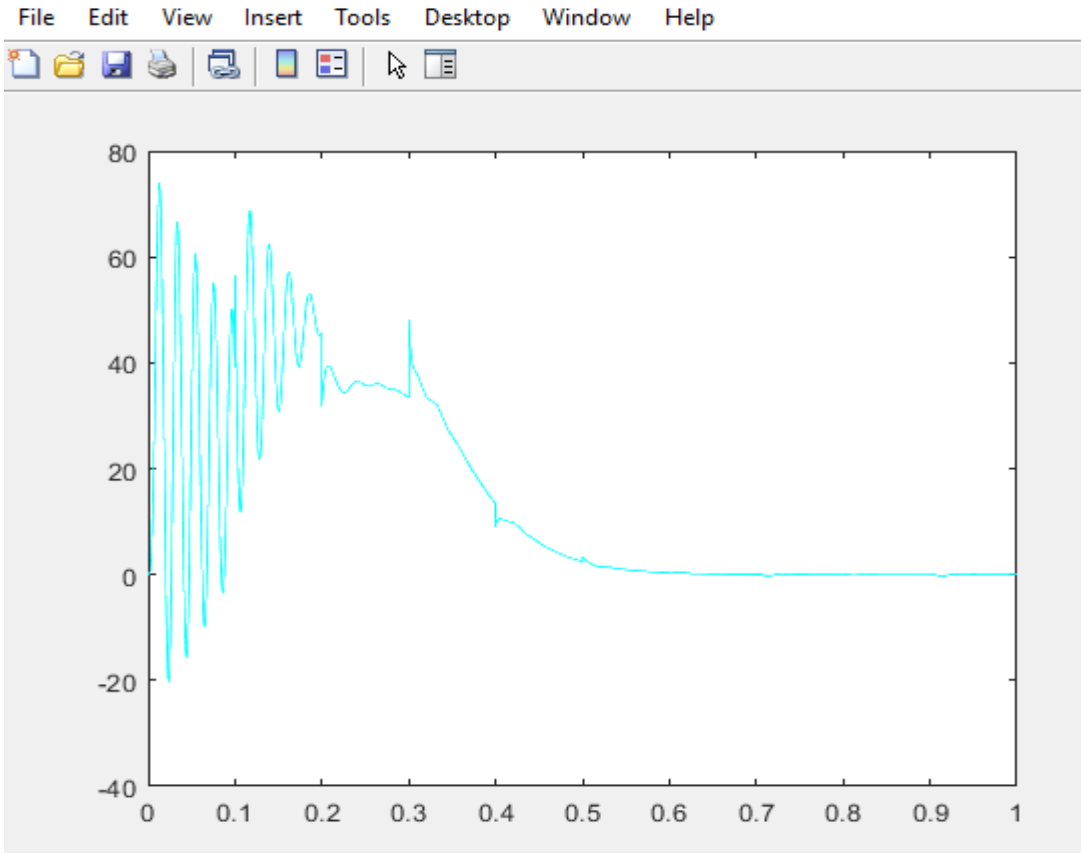

Figure 5.1.1(d)

5.1.2 Air Gap Eccentricity Modelling in DQ Transient profile using Sinusoidal Eccentricity

2. Sinusoidal eccentricity profile:

- The fluctuation in the air gap has a sinusoidal structure.

- As the rotor revolves, the distance between the surfaces of the rotor and stator changes sinusoidally.

- Mechanical misalignments or flaws in the production process may be to blame.

- The sinusoidal variation's magnitude and frequency define how severe the eccentricity is.

- It leads to unbalanced magnetic forces, increased vibration, noise, reduced efficiency, and potential motor damage, similar to elliptical eccentricity.

MATLAB Code

```
clear;
clc;
V = 220;
rs = 0.435;
Xls = 0.754;
XM = 26.13;
Xlr = 0.754;
rr = 0.816;
J = 0.089;
TL = 0;
Wb = 2*pi*50;
P = 4;
Lls = Xls/Wb;
Llr = Xlr/Wb;
M = XM/Wb;

% Define eccentricity parameters
eccentricity_amplitude = 0.001;   % Eccentricity amplitude
eccentricity_frequency = 2*pi*5;  % Eccentricity frequency (adjust as needed)
eccentricity_phase = pi/4;        % Eccentricity phase (in radians)

h = 1e-5;
Tfinal = 1;
n = round(Tfinal/h) + 1;

psi_qs = zeros(1,n);
psi_ds = zeros(1,n);
psi_qr = zeros(1,n);
psi_dr = zeros(1,n);
Wrm = zeros(1,n);
Wrm = zeros(1,n);
```

```
i_qs = zeros(1,n);
i_ds = zeros(1,n);
i_qr = zeros(1,n);
i_dr = zeros(1,n);
Wr = zeros(1,n);
Tem = zeros(1,n);

i_as = zeros(1,n);
i_bs = zeros(1,n);
i_cs = zeros(1,n);

i_ar = zeros(1,n);
i_br = zeros(1,n);
i_cr = zeros(1,n);

v_qs = zeros(1,n);
v_ds = zeros(1,n);
v_qr = zeros(1,n);
v_dr = zeros(1,n);
TL = zeros(1,n);

B = [1 0 1;
     -0.5 -sqrt(3)/2 1;
     -0.5  sqrt(3)/2 1];

% Numerical integration
time = 0;
k(1) = 0;
k(2) = 0;
TL(1) = 0;
TL(2) = 0;
for i = 3:n
    time = time + h;
    k(i) = k(i-1) + 1;
    TL(i) = 0;

    va = V*sqrt(2/3)*sin(Wb*time);
    vb = V*sqrt(2/3)*sin(Wb*time-2*pi/3);
    vc = V*sqrt(2/3)*sin(Wb*time+2*pi/3);
    v_qs(i) = 2/3*(va-((vb+vc)/2));
    v_ds(i) = 2/3*((-vb+vc)*sqrt(3)/2);

    psi_ds(i) = psi_ds(i-1) + h*(v_ds(i-1) - rs*i_ds(i-1));
    psi_qs(i) = psi_qs(i-1) + h*(v_qs(i-1) - rs*i_qs(i-1));
    psi_dr(i) = psi_dr(i-1) + h*(v_dr(i-1) - rr*i_dr(i-1) - Wr(i-1)*psi_qr(i-1));
    psi_qr(i) = psi_qr(i-1) + h*(v_qr(i-1) - rr*i_qr(i-1) + Wr(i-1)*psi_dr(i-1));
    Wrm(i) = Wrm(i-1) + h*(Tem(i-1) - TL(i-1))/J;

    eccentricity = eccentricity_amplitude * sin(eccentricity_frequency*time +
eccentricity_phase);
    delta_Lls = eccentricity;
    delta_Llr = eccentricity;

    Lss = Lls + M + delta_Lls;
    Lrr = Llr + M + delta_Llr;

    Lms = M + delta_Lls/2;
    Lmr = M + delta_Llr/2;
```

```
    D = Lss*Lrr - Lms*Lmr;

    i_ds(i) = (Lrr*psi_ds(i) - M*psi_dr(i))/D;
    i_qs(i) = (Lrr*psi_qs(i) - M*psi_qr(i))/D;
    i_dr(i) = (Lss*psi_dr(i) - M*psi_ds(i))/D;
    i_qr(i) = (Lss*psi_qr(i) - M*psi_qs(i))/D;

    Tem(i) = (P/2)*(psi_qr(i)*i_dr(i) - psi_dr(i)*i_qr(i));
    Wr(i) = (P/2)*Wrm(i);

    i_as(i) = i_qs(i);
    i_bs(i) = -i_qs(i)/2 + i_ds(i)*(-sqrt(3)/2);
    i_cs(i) = -i_qs(i)/2 + i_ds(i)*(sqrt(3)/2);
end

t = 0:h:Tfinal;
figure();
plot(t, i_as, 'b');
figure();
plot(t, i_dr, 'r');
figure();
plot(t, Wr, 'm');
figure();
plot(t, Tem, 'c');
```

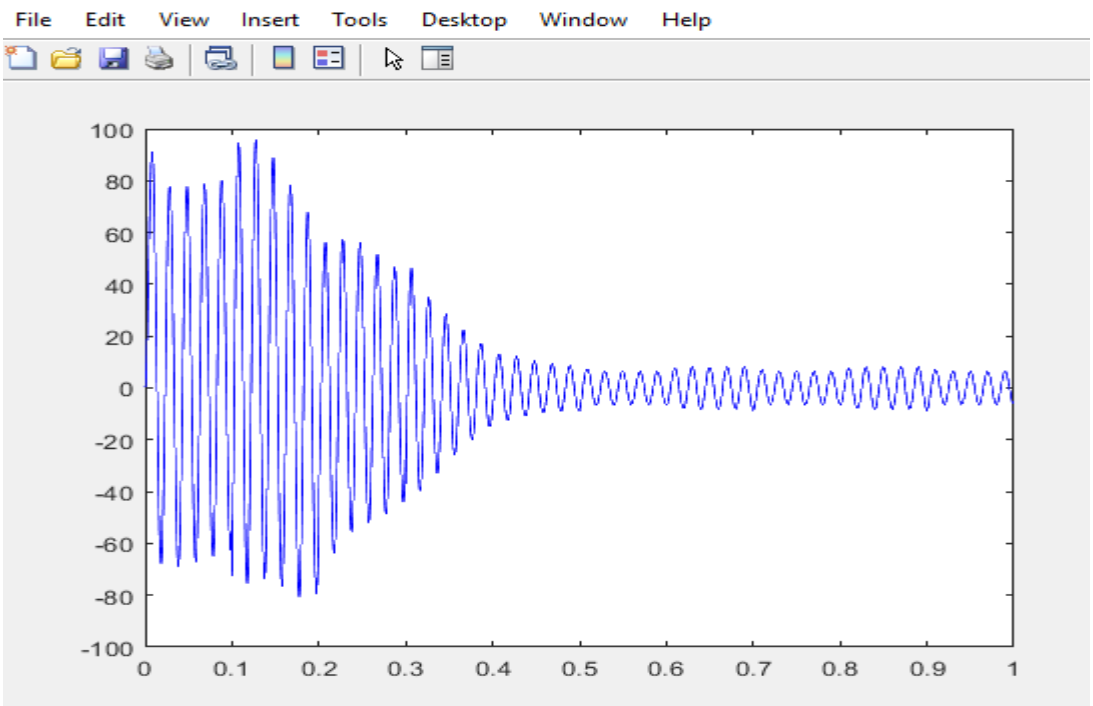

Figure 5.1.2(a)

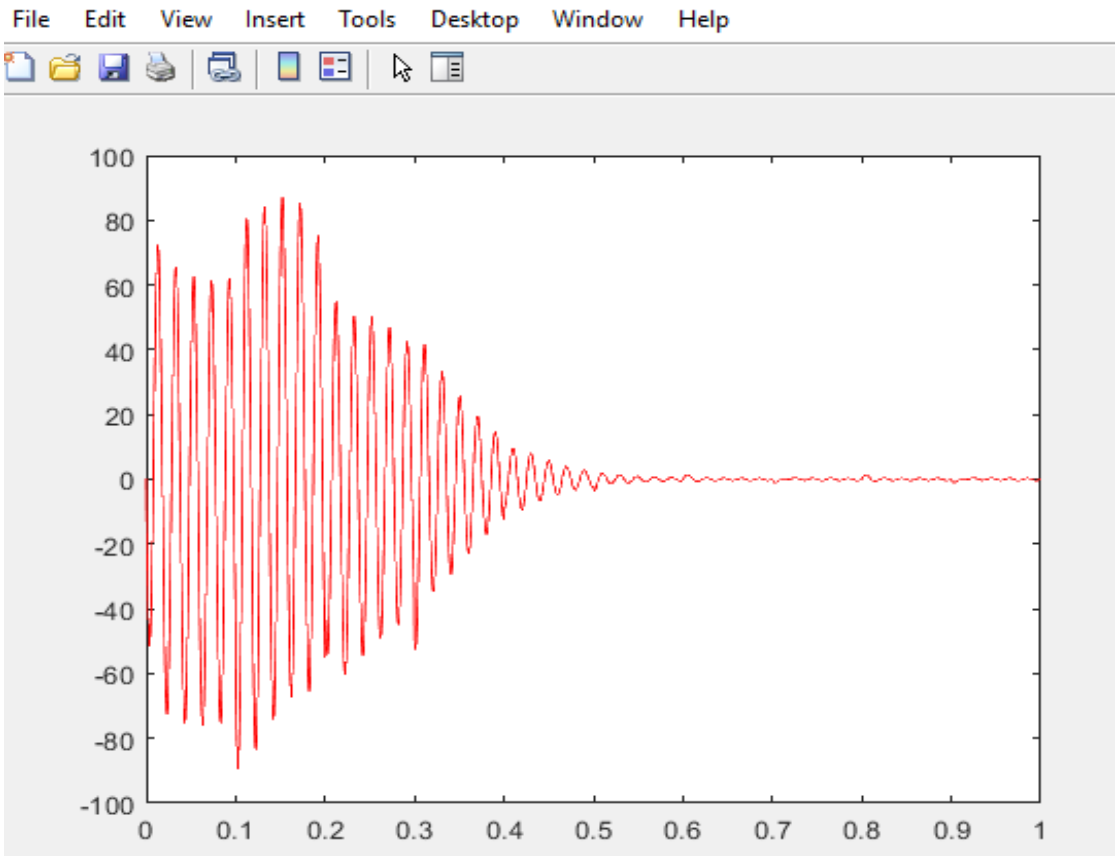

Figure 5.1.2(b)

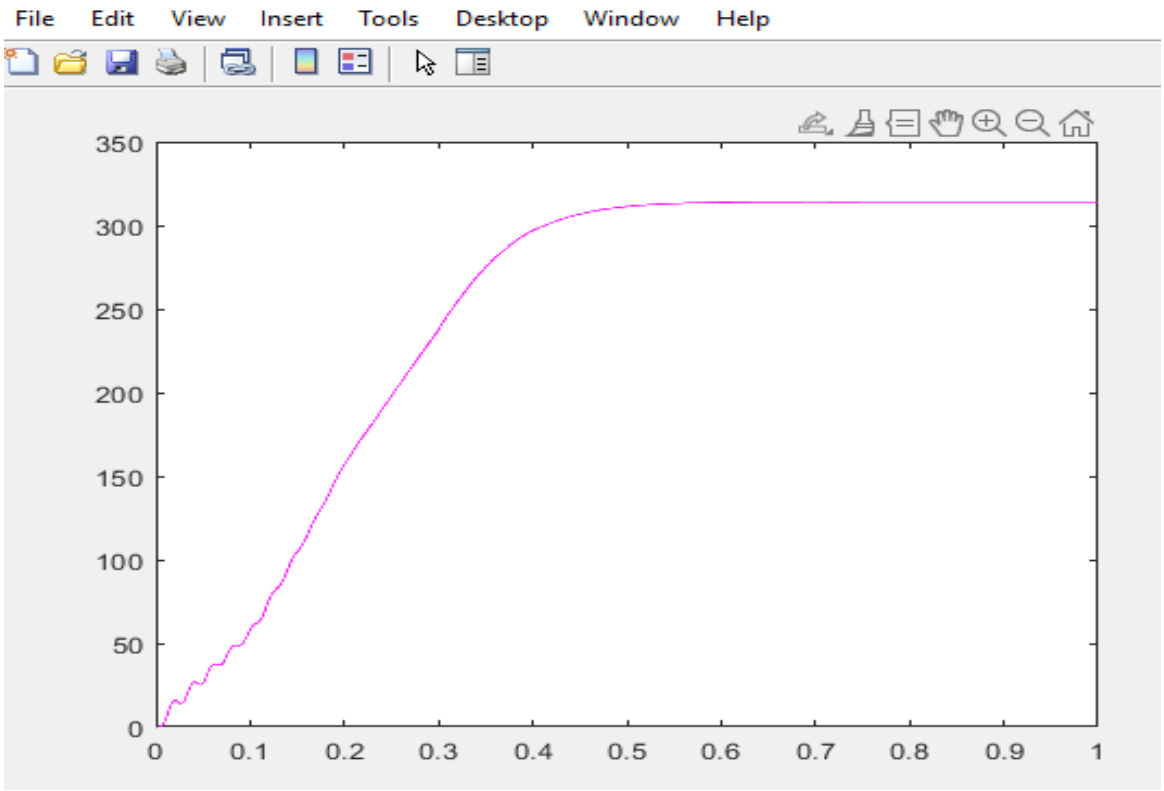

Figure 5.1.2(c)

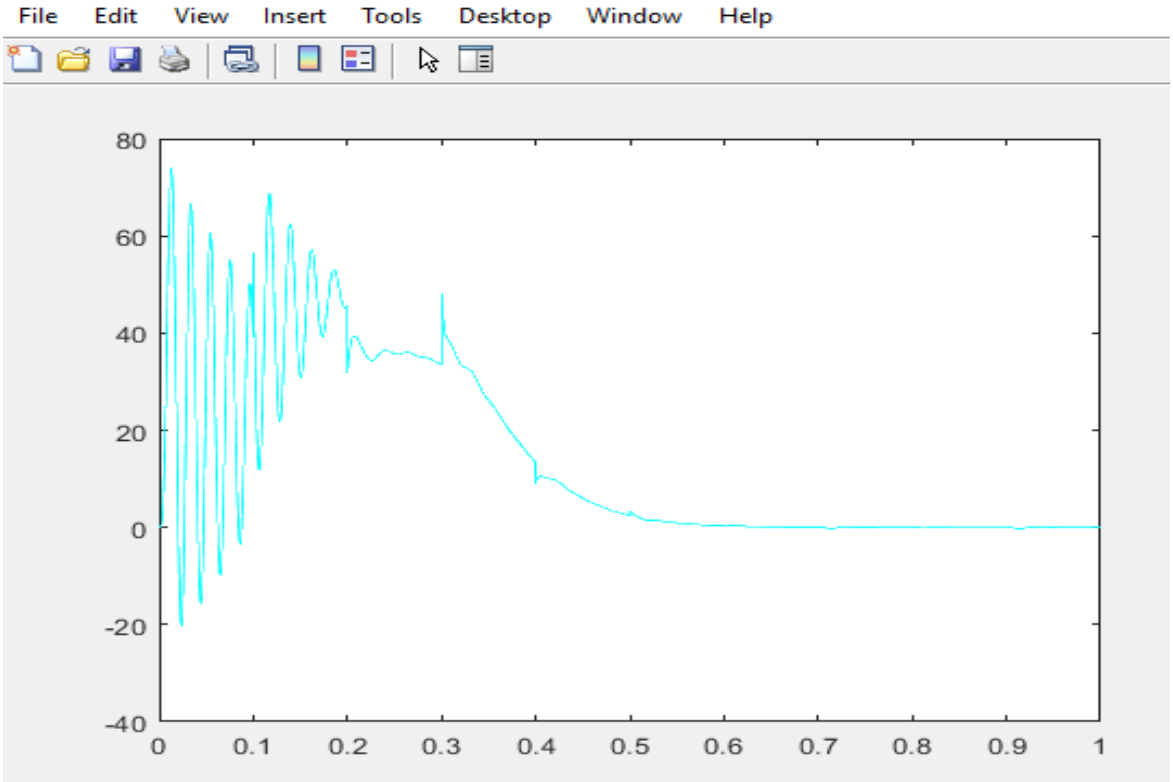

Figure 5.1.2(d)

5.1.3 Air Gap Eccentricity Modelling in DQ transient profile using Stepped Eccentricity

3. Stepped eccentricity profile:

- The air gap varies in distinct levels or increments.

- At precise points throughout the circle, the distance between the surfaces of the rotor and stator abruptly changes.

- It may be the consequence of mechanical damage, poor assembly, or manufacturing flaws.

- Localised magnetic disturbances and an irregular magnetic flux density distribution are brought on by stepped eccentricity.

In summary, elliptical eccentricity has an elliptical-shaped air gap variation, sinusoidal eccentricity has a sinusoidal-shaped variation, and stepped eccentricity has a stepped or discrete level variation. All three profiles result

non-uniform air gaps and can negatively impact motor performance and reliability.

MATLAB Code

```
clear;
clc;

V = 220;
rs = 0.435;
Xls = 0.754;
XM = 26.13;
Xlr = 0.754;
rr = 0.816;
J = 0.089;
TL = 0;
Wb = 2*pi*50;
P = 4;
Lls = Xls/Wb;
Llr = Xlr/Wb;
M = XM/Wb;

% Define eccentricity parameters
eccentricity_amplitude = 0.001;    % Eccentricity amplitude
eccentricity_step_duration = 0.1;  % Duration of each step (adjust as needed)
eccentricity_step_value = 0.002;   % Eccentricity step value (adjust as needed)

h = 1e-5;
Tfinal = 1;
n = round(Tfinal/h) + 1;

psi_qs = zeros(1,n);
psi_ds = zeros(1,n);
psi_qr = zeros(1,n);
psi_dr = zeros(1,n);
Wrm = zeros(1,n);
Wrm = zeros(1,n);

i_qs = zeros(1,n);
i_ds = zeros(1,n);
i_qr = zeros(1,n);
i_dr = zeros(1,n);
Wr = zeros(1,n);
Tem = zeros(1,n);

i_as = zeros(1,n);
i_bs = zeros(1,n);
i_cs = zeros(1,n);

i_ar = zeros(1,n);
i_br = zeros(1,n);
i_cr = zeros(1,n);

v_qs = zeros(1,n);
v_ds = zeros(1,n);
v_qr = zeros(1,n);
v_dr = zeros(1,n);
TL = zeros(1,n);
```

```
B = [1 0 1;
     -0.5 -sqrt(3)/2 1;
     -0.5  sqrt(3)/2 1];

% Numerical integration
time = 0;
k(1) = 0;
k(2) = 0;
TL(1) = 0;
TL(2) = 0;
for i = 3:n
    time = time + h;
    k(i) = k(i-1) + 1;
    TL(i) = 0;

    va = V*sqrt(2/3)*sin(Wb*time);
    vb = V*sqrt(2/3)*sin(Wb*time-2*pi/3);
    vc = V*sqrt(2/3)*sin(Wb*time+2*pi/3);
    v_qs(i) = 2/3*(va-((vb+vc)/2));
    v_ds(i) = 2/3*((-vb+vc)*sqrt(3)/2);

    psi_ds(i) = psi_ds(i-1) + h*(v_ds(i-1) - rs*i_ds(i-1));
    psi_qs(i) = psi_qs(i-1) + h*(v_qs(i-1) - rs*i_qs(i-1));
    psi_dr(i) = psi_dr(i-1) + h*(v_dr(i-1) - rr*i_dr(i-1) - Wr(i-1)*psi_qr(i-1));
    psi_qr(i) = psi_qr(i-1) + h*(v_qr(i-1) - rr*i_qr(i-1) + Wr(i-1)*psi_dr(i-1));
    Wrm(i) = Wrm(i-1) + h*(Tem(i-1) - TL(i-1))/J;

    % Apply stepped eccentricity
    step_time = mod(time, eccentricity_step_duration);
    if step_time <= eccentricity_step_duration/2
        delta_Lls = eccentricity_step_value;
        delta_Llr = eccentricity_step_value;
    else
        delta_Lls = 0;
        delta_Llr = 0;
    end

    Lss = Lls + M + delta_Lls;
    Lrr = Llr + M + delta_Llr;

    Lms = M + delta_Lls/2;
    Lmr = M + delta_Llr/2;

    D = Lss*Lrr - Lms*Lmr;

    i_ds(i) = (Lrr*psi_ds(i) - M*psi_dr(i))/D;
    i_qs(i) = (Lrr*psi_qs(i) - M*psi_qr(i))/D;
    i_dr(i) = (Lss*psi_dr(i) - M*psi_ds(i))/D;
    i_qr(i) = (Lss*psi_qr(i) - M*psi_qs(i))/D;

    Tem(i) = (P/2)*(psi_qr(i)*i_dr(i) - psi_dr(i)*i_qr(i));
    Wr(i) = (P/2)*Wrm(i);

    i_as(i) = i_qs(i);
    i_bs(i) = -i_qs(i)/2 + i_ds(i)*(-sqrt(3)/2);
    i_cs(i) = -i_qs(i)/2 + i_ds(i)*(sqrt(3)/2);
end
```

```
t = 0:h:Tfinal;
figure();
plot(t, i_as, 'b');
figure();
plot(t, i_dr, 'r');
figure();
plot(t, Wr, 'm');
figure();
plot(t, Tem, 'c');
```

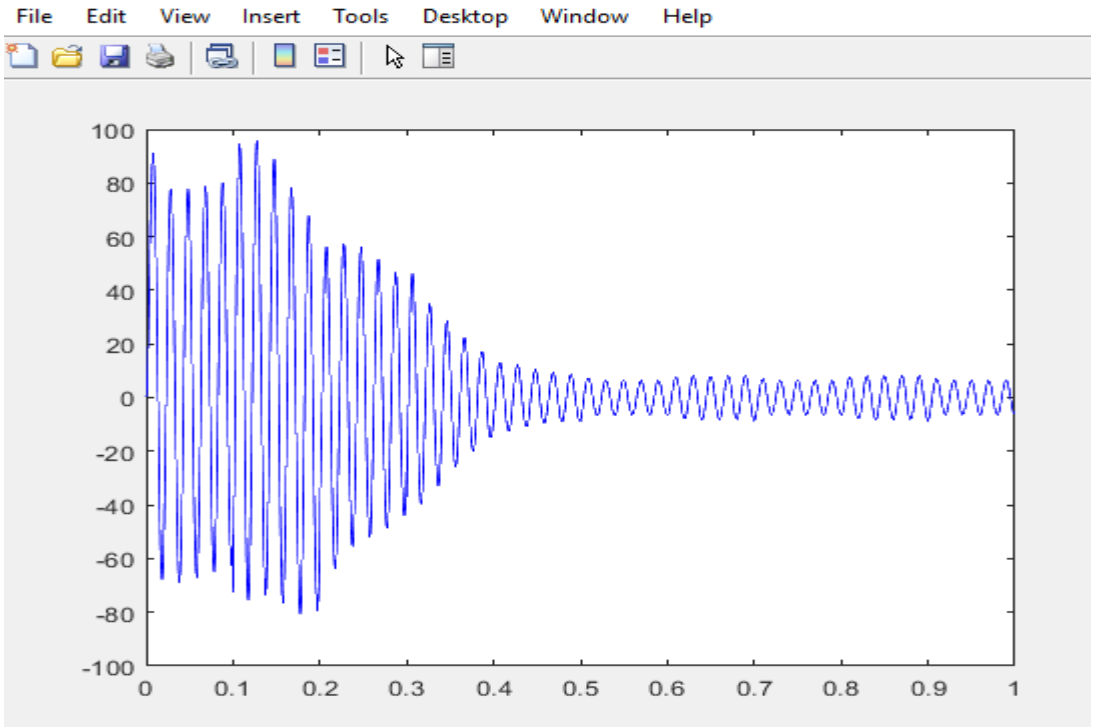

Figure 5.1.3(a)

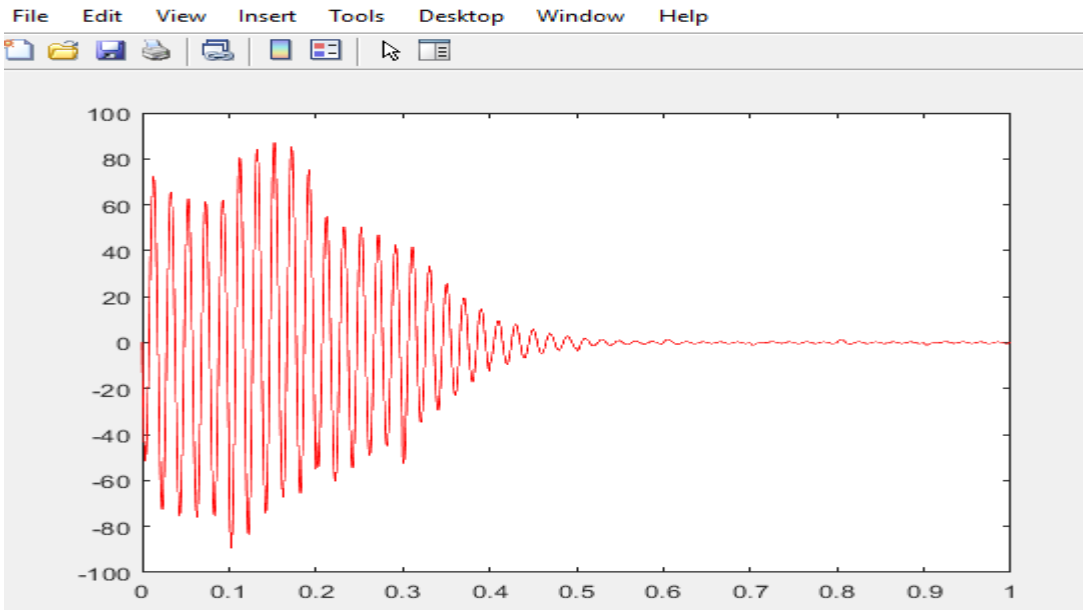

Figure 5.1.3(b)

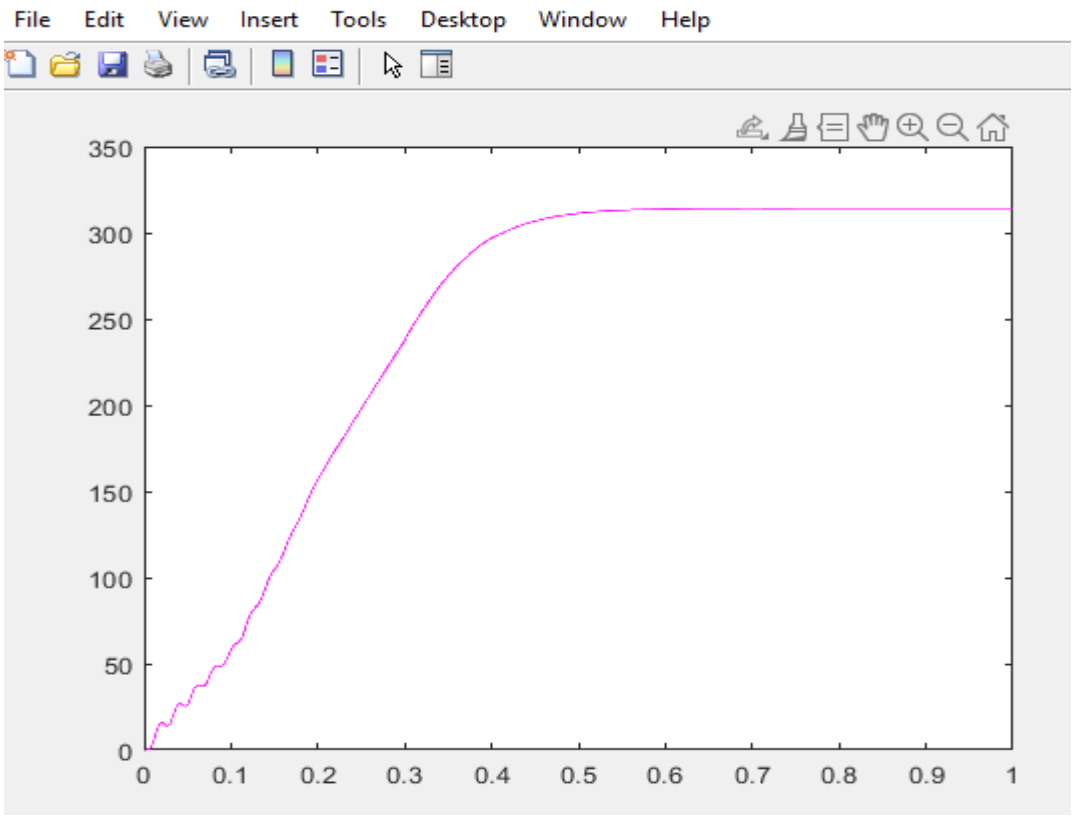

Figure 5.1.3(c)

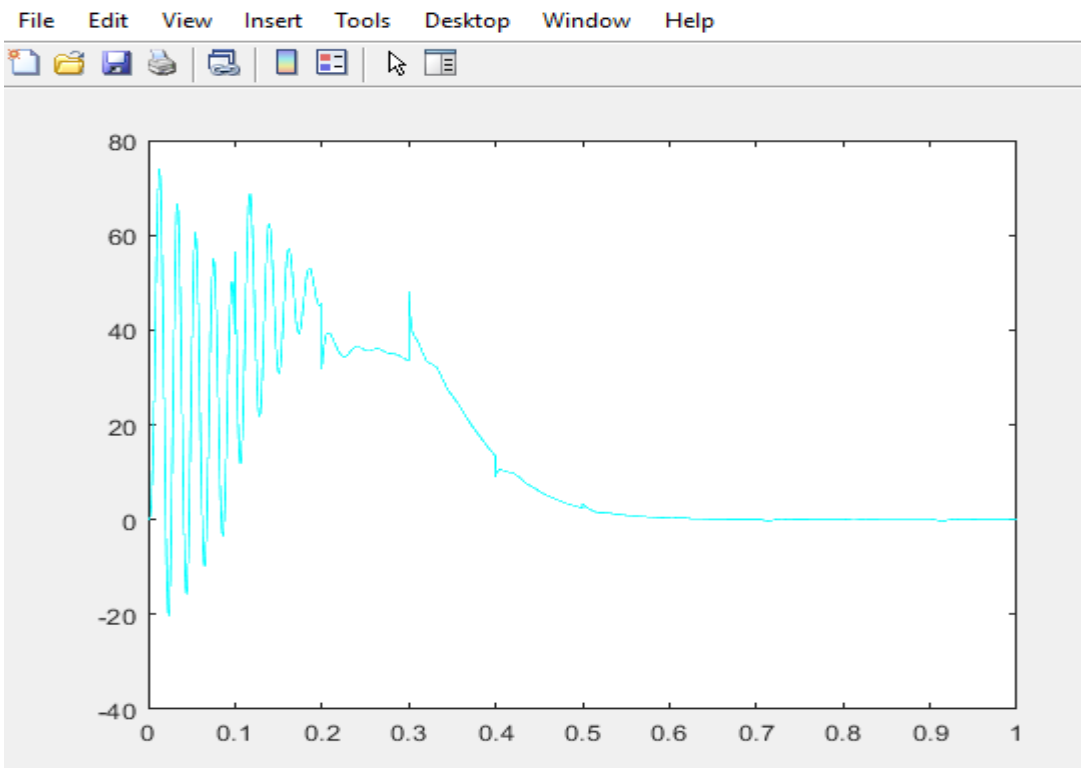

Figure 5.1.3(d)

5.2 Modelling of Induction Motor parameter variance with Air Gap Eccentricity profile

In this chapter we will again apply the three simplest eccentricity profile on induction DQ model. This induction Motor DQ model plots each real and imaginary component of current, it also plot angular velocity as well as electromagnetic torque. In these plots the variance of these Induction Motor parameters are shown along with variance in eccentricity curve.

These models are all self-explanatory. The provided codes are MATLAB simulation of an induction motor with air gap eccentricity using the DQ (d-axis and q-axis) model. Here is a short explanation of the codes:

1. Parameters: A number of parameters are defined at the beginning of the code, including the number of poles (P), frequency (f), stator voltage (V), stator resistance (R), stator inductance (Ls), rotor inductance (Lr), mutual inductance (Lm), moment of inertia (J), and damping coefficient (B).

2. Air Gap Eccentricity Parameters: According to the eccentricity profile used by the code, the parameters relating to air gap eccentricity are defined.

3. Time Settings: The programme constructs a simulation time vector (t_sim) for the duration of a cycle and sets the sampling time (Ts) depending on the frequency.

4. Calculate Eccentricity Profile: The programme determines the eccentricity profile (e_profile) as a function of time using the eccentricity parameters and the simulation time vector. Combining the x-axis and y-axis eccentricities while taking into account the elliptical form yields the eccentricity profile.

5. Simulation Variables: Stator current (i_s), rotor current (i_r), rotor angle (theta_r), electromagnetic torque (Te), and rotor speed (omega_r) are only a few of the variables that the code initialises before the simulation begins.

6. Simulation Loop: Every time step in the simulation time vector is iterated through by the main simulation loop. Based on the mechanical system feedback, the algorithm determines the rotor angle and speed inside the loop. Following that, it uses the DQ model equations to estimate the eccentricity at the current time step, compute the stator current in the dq reference frame, and compute the rotor current in the dq reference frame.

7. Electromagnetic Torque: Based on the computed rotor current and stator current in the d, q reference frame, the code determines the electromagnetic torque.

8. Plotting: Plotting instructions are included in the code to display the outcomes. In the first image, it creates two subplots: one shows the evolution of the air gap eccentricity profile, while the other displays the stator and rotor currents along the d-axis.

9. Another Figure: Another figure with three subplots is produced by the code. The air gap eccentricity profile is displayed in the first subplot, electromagnetic torque is shown in the second, and rotor speed is shown in the third.

The simulation shows how the induction motor's current, torque, and speed characteristics are impacted by air gap eccentricity. To see how eccentricity affects motor performance over time, the eccentricity profile, electromagnetic torque, and rotor speed are displayed.

An important point to note is that,

“The dotted component in the plots are imaginary component of the currents whereas the real component of currents are shown by bold line on the plot.”

5.2.1 Elliptical Eccentricity Profile

```
% Induction Motor Air Gap Eccentricity Simulation using DQ Model

% Parameters
P = 4;               % Number of poles
f = 50;              % Frequency (Hz)
V = 220;             % Stator voltage (V)
R = 0.1;             % Stator resistance (ohm)
Ls = 0.01;           % Stator inductance (H)
Lr = 0.02;           % Rotor inductance (H)
Lm = 0.003;          % Mutual inductance (H)
J = 0.01;            % Moment of inertia (kg.m^2)
B = 0.1;             % Damping coefficient (N.m.s)

% Air Gap Eccentricity Parameters
e_max = 0.01;        % Maximum eccentricity (m)
e_x = 0.008;         % Eccentricity in x-axis (m)
e_y = 0.006;         % Eccentricity in y-axis (m)
e_freq = 4;          % Eccentricity frequency (Hz)
```

```
% Time settings
Ts = 1/(10*f);       % Sampling time
t_sim = 0:Ts:1/f;    % Simulation time vector

% Calculate eccentricity profile
e_profile = e_max * sqrt((e_x^2 * sin(2*pi*e_freq*t_sim)).^2 + (e_y^2 *
cos(2*pi*e_freq*t_sim)).^2);

% Simulation variables
N = length(t_sim);
i_s = zeros(2, N);     % Stator current (d-axis and q-axis components)
i_r = zeros(2, N);     % Rotor current (d-axis and q-axis components)
theta_r = zeros(1, N); % Rotor angle
Te = zeros(1, N);      % Electromagnetic torque
omega_r = zeros(1, N); % Rotor speed (angular velocity)

% Simulation loop
for k = 2:N
    % Calculate rotor angle and speed
    omega_r(k) = (P/2) * (2*pi*f - theta_r(k-1)*(R/J) - B/J*theta_r(k-1)*Ts);
%Mechanical system Feedback for Angular Velocity
    theta_r(k) = theta_r(k-1) + omega_r(k)*Ts;

    % Calculate eccentricity at current time step
    e = e_profile(k);

    % Calculate stator current in dq reference frame
    i_s(1, k) = V/(R + 1i*2*pi*f*Ls) * exp(1i*2*pi*f*t_sim(k));
    i_s(2, k) = 0; % Assuming no q-axis current

    % Calculate rotor current in dq reference frame
    i_rds = (1/Lr) * (Lm * i_s(:, k) - e);
    i_r(:, k) = i_rds;

    % Calculate electromagnetic torque
    Te(k) = real(3/2 * P * Lm * (conj(i_rds(1)) * i_s(1, k) - i_rds(2) *
conj(i_s(1, k))));
end
% Plotting
figure;
subplot(2, 1, 1);
plot(t_sim, e_profile, 'k');
title('Air Gap Eccentricity Profile');
xlabel('Time');
ylabel('Eccentricity (m)');

subplot(2, 1, 2);
plot(t_sim, real(i_s(1, :)), 'b', t_sim, real(i_r(1, :)), 'r');
hold on;
plot(t_sim, imag(i_s(1, :)), 'b--', t_sim, imag(i_r(1, :)), 'r--');
hold off;
title('Stator and Rotor Currents (d-axis)');
xlabel('Time');
ylabel('Current (A)');
legend('Stator (d-axis)', 'Rotor (d-axis)');


% Plotting
figure;
```

```
subplot(3, 1, 1);
plot(t_sim, e_profile);
title('Air Gap Eccentricity Profile (Elliptical)');
xlabel('Time');
ylabel('Eccentricity (m)');


subplot(3, 1, 2);
plot(t_sim, Te);
title('Electromagnetic Torque', 'c');
xlabel('Time');
ylabel('Torque (N.m)');

subplot(3, 1, 3);
plot(t_sim, omega_r);
title('Rotor Speed', 'm');
xlabel('Time');
ylabel('Angular Velocity (rad/s)');
```

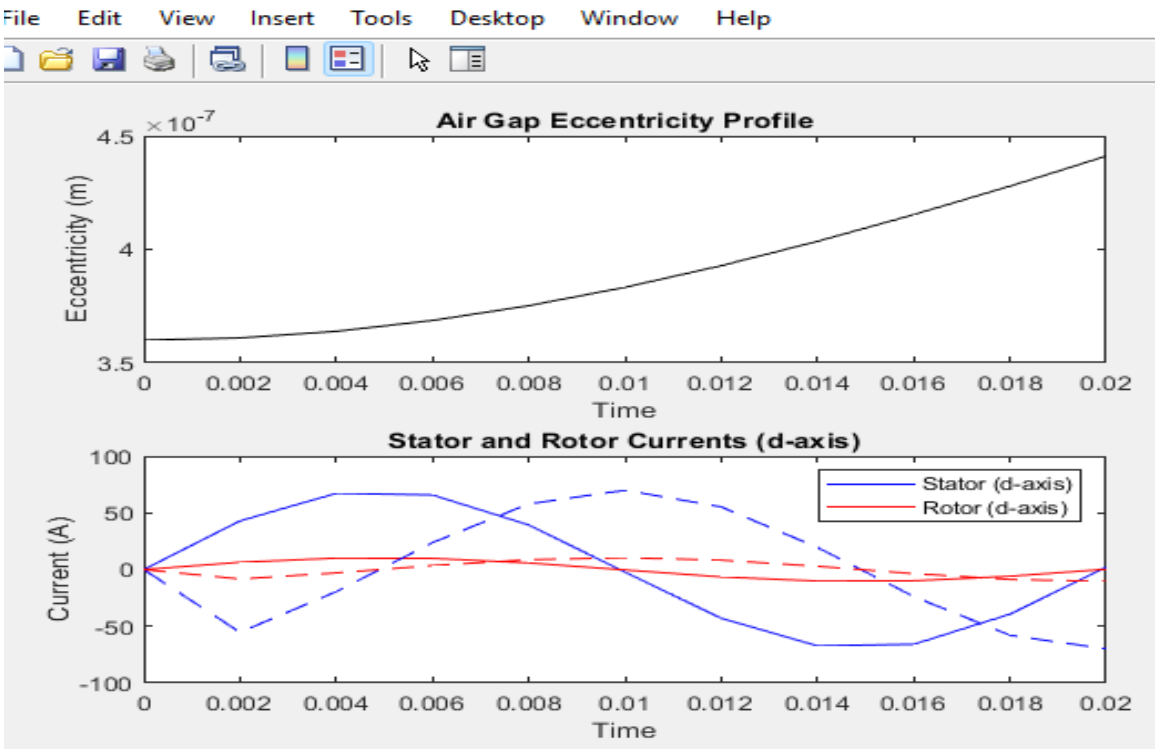

Figure 5.2.1(a)

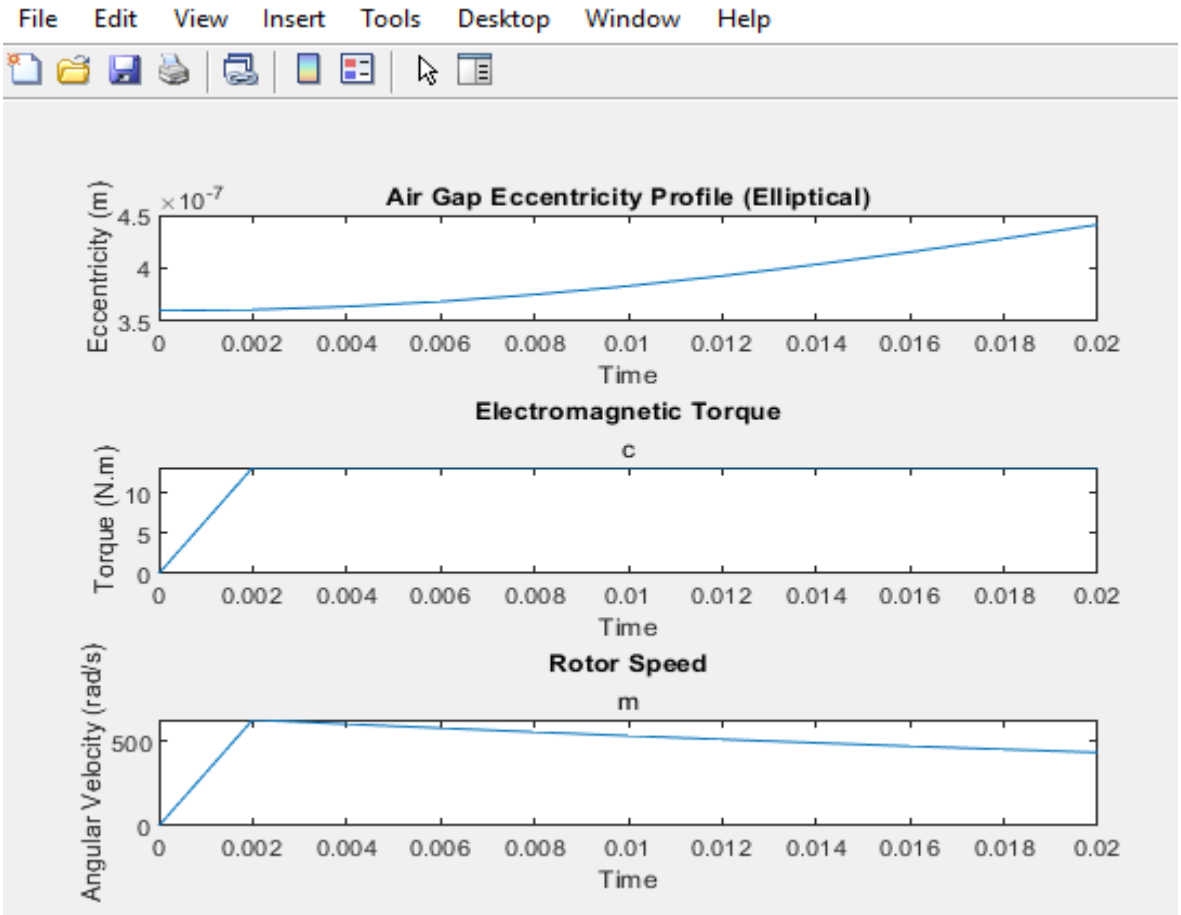

Figure 5.2.1(b)

5.2.2 Sinusoidal Eccentricity Profile

```
% Induction Motor Air Gap Eccentricity Simulation using DQ Model

% Parameters
P = 4;                  % Number of poles
f = 50;                 % Frequency (Hz)
V = 220;                % Stator voltage (V)
R = 0.1;                % Stator resistance (ohm)
Ls = 0.01;              % Stator inductance (H)
Lr = 0.02;              % Rotor inductance (H)
Lm = 0.003;             % Mutual inductance (H)
J = 0.01;               % Moment of inertia (kg.m^2)
B = 0.1;                % Damping coefficient (N.m.s)

% Air Gap Eccentricity Parameters
e_max = 0.01;           % Maximum eccentricity (m)
e_freq = 4;             % Eccentricity frequency (Hz)

% Time settings
Ts = 1/(10*f);          % Sampling time
t_sim = 0:Ts:1/f;       % Simulation time vector

% Calculate eccentricity profile
e_profile = e_max * sin(2*pi*e_freq*t_sim);
```

```
% Simulation variables
N = length(t_sim);
i_s = zeros(2, N);     % Stator current (d-axis and q-axis components)
i_r = zeros(2, N);     % Rotor current (d-axis and q-axis components)
theta_r = zeros(1, N); % Rotor angle
Te = zeros(1, N);      % Electromagnetic torque
omega_r = zeros(1, N); % Rotor speed (angular velocity)

% Simulation loop
for k = 2:N
    % Calculate rotor angle and speed
    omega_r(k) = (P/2) * (2*pi*f - theta_r(k-1)*(R/J) - B/J*theta_r(k-1)*Ts); %
Mechanical system Feedback for Angular Velocity
    theta_r(k) = theta_r(k-1) + omega_r(k)*Ts;

    % Calculate eccentricity at current time step
    e = e_profile(k);

    % Calculate stator current in dq reference frame
    i_s(1, k) = V/(R + 1i*2*pi*f*Ls) * exp(1i*2*pi*f*t_sim(k));
    i_s(2, k) = 0; % Assuming no q-axis current

    % Calculate rotor current in dq reference frame
    i_rds = (1/Lr) * (Lm * i_s(:, k) - e);
    i_r(:, k) = i_rds;

    % Calculate electromagnetic torque
    Te(k) = real(3/2 * P * Lm * (conj(i_rds(1)) * i_s(1, k) - i_rds(2) *
conj(i_s(1, k))));
end

% Plotting
figure;
subplot(2, 1, 1);
plot(t_sim, e_profile, 'k');
title('Air Gap Eccentricity Profile');
xlabel('Time');
ylabel('Eccentricity (m)');

subplot(2, 1, 2);
plot(t_sim, real(i_s(1, :)), 'b', t_sim, real(i_r(1, :)), 'r');
hold on;
plot(t_sim, imag(i_s(1, :)), 'b--', t_sim, imag(i_r(1, :)), 'r--');
hold off;
title('Stator and Rotor Currents (d-axis)');
xlabel('Time');
ylabel('Current (A)');
legend('Stator (d-axis)', 'Rotor (d-axis)');

% Plotting
figure;
subplot(3, 1, 1);
plot(t_sim, e_profile);
title('Air Gap Eccentricity Profile (Sinusoidal)');
xlabel('Time');
ylabel('Eccentricity (m)');

subplot(3, 1, 2);
plot(t_sim, Te);
```

```
title('Electromagnetic Torque');
xlabel('Time');
ylabel('Torque (N.m)');

subplot(3, 1, 3);
plot(t_sim, omega_r);
title('Rotor Speed');
xlabel('Time');
ylabel('Angular Velocity (rad/s)');
```

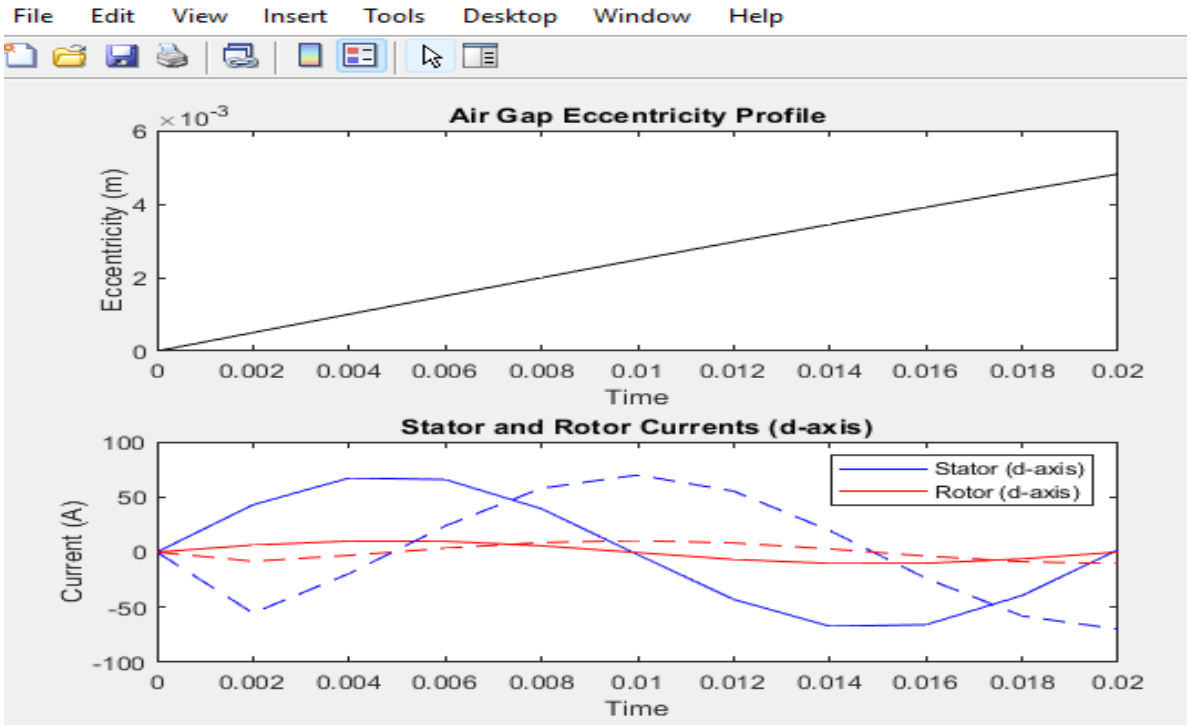

Figure 5.2.2(a)

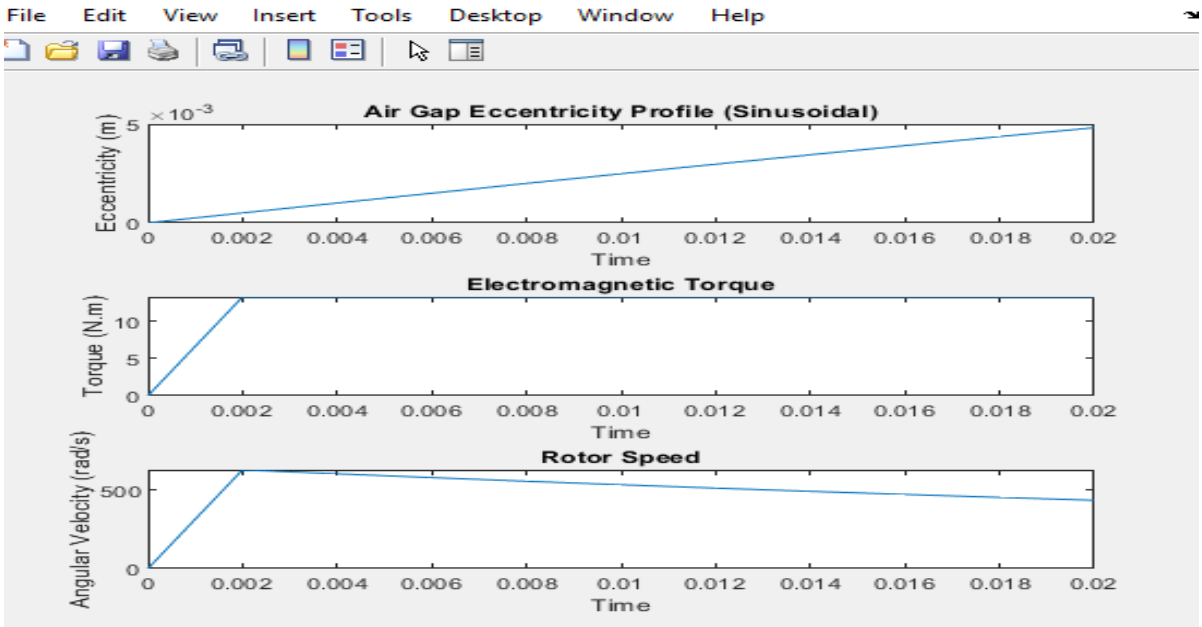

Figure 5.2.2(b)

5.2.3 Stepped Eccentricity Profile

```
% Induction Motor Air Gap Eccentricity Simulation using DQ Model

% Parameters
P = 4;                % Number of poles
f = 50;               % Frequency (Hz)
V = 220;              % Stator voltage (V)
R = 0.1;              % Stator resistance (ohm)
Ls = 0.01;            % Stator inductance (H)
Lr = 0.02;            % Rotor inductance (H)
Lm = 0.003;           % Mutual inductance (H)
J = 0.01;             % Moment of inertia (kg.m^2)
B = 0.1;              % Damping coefficient (N.m.s)

% Air Gap Eccentricity Parameters
e_max = 0.01;         % Maximum eccentricity (m)
e_step = 0.004;       % Step size of eccentricity (m)
e_duration = 0.02;    % Duration of each step (s)

% Time settings
Ts = 1/(10*f);        % Sampling time
t_sim = 0:Ts:1/f;     % Simulation time vector

% Calculate eccentricity profile
e_profile = zeros(size(t_sim));
step_start = 0;
while step_start < t_sim(end)
    step_end = step_start + e_duration;
    e_profile(step_start < t_sim & t_sim <= step_end) = e_max;
    step_start = step_end;
end

% Simulation variables
N = length(t_sim);
i_s = zeros(2, N);     % Stator current (d-axis and q-axis components)
i_r = zeros(2, N);     % Rotor current (d-axis and q-axis components)
theta_r = zeros(1, N); % Rotor angle
Te = zeros(1, N);      % Electromagnetic torque
omega_r = zeros(1, N); % Rotor speed (angular velocity)

% Simulation loop
for k = 2:N
    % Calculate rotor angle and speed
    omega_r(k) = (P/2) * (2*pi*f - theta_r(k-1)*(R/J) - B/J*theta_r(k-1)*Ts); %
Mechanical system Feedback for Angular Velocity
    theta_r(k) = theta_r(k-1) + omega_r(k)*Ts;

    % Calculate eccentricity at current time step
    e = e_profile(k);

    % Calculate stator current in dq reference frame
    i_s(1, k) = V/(R + 1i*2*pi*f*Ls) * exp(1i*2*pi*f*t_sim(k));
    i_s(2, k) = 0; % Assuming no q-axis current

    % Calculate rotor current in dq reference frame
    i_rds = (1/Lr) * (Lm * i_s(:, k) - e);
    i_r(:, k) = i_rds;
```

```
    % Calculate electromagnetic torque
    Te(k) = real(3/2 * P * Lm * (conj(i_rds(1)) * i_s(1, k) - i_rds(2) *
conj(i_s(1, k))));
end

% Plotting
figure;
subplot(2, 1, 1);
plot(t_sim, e_profile, 'k');
title('Air Gap Eccentricity Profile');
xlabel('Time');
ylabel('Eccentricity (m)');

subplot(2, 1, 2);
plot(t_sim, real(i_s(1, :)), 'b', t_sim, real(i_r(1, :)), 'r');
hold on;
plot(t_sim, imag(i_s(1, :)), 'b--', t_sim, imag(i_r(1, :)), 'r--');
hold off;
title('Stator and Rotor Currents (d-axis)');
xlabel('Time');
ylabel('Current (A)');
legend('Stator (d-axis)', 'Rotor (d-axis)');

% Plotting
figure;
subplot(3, 1, 1);
plot(t_sim, e_profile);
title('Air Gap Eccentricity Profile (Stepped)');
xlabel('Time');
ylabel('Eccentricity (m)');

subplot(3, 1, 2);
plot(t_sim, Te);
title('Electromagnetic Torque');
xlabel('Time');
ylabel('Torque (N.m)');

subplot(3, 1, 3);
plot(t_sim, omega_r);
title('Rotor Speed');
xlabel('Time');
ylabel('Angular Velocity (rad/s)');
```

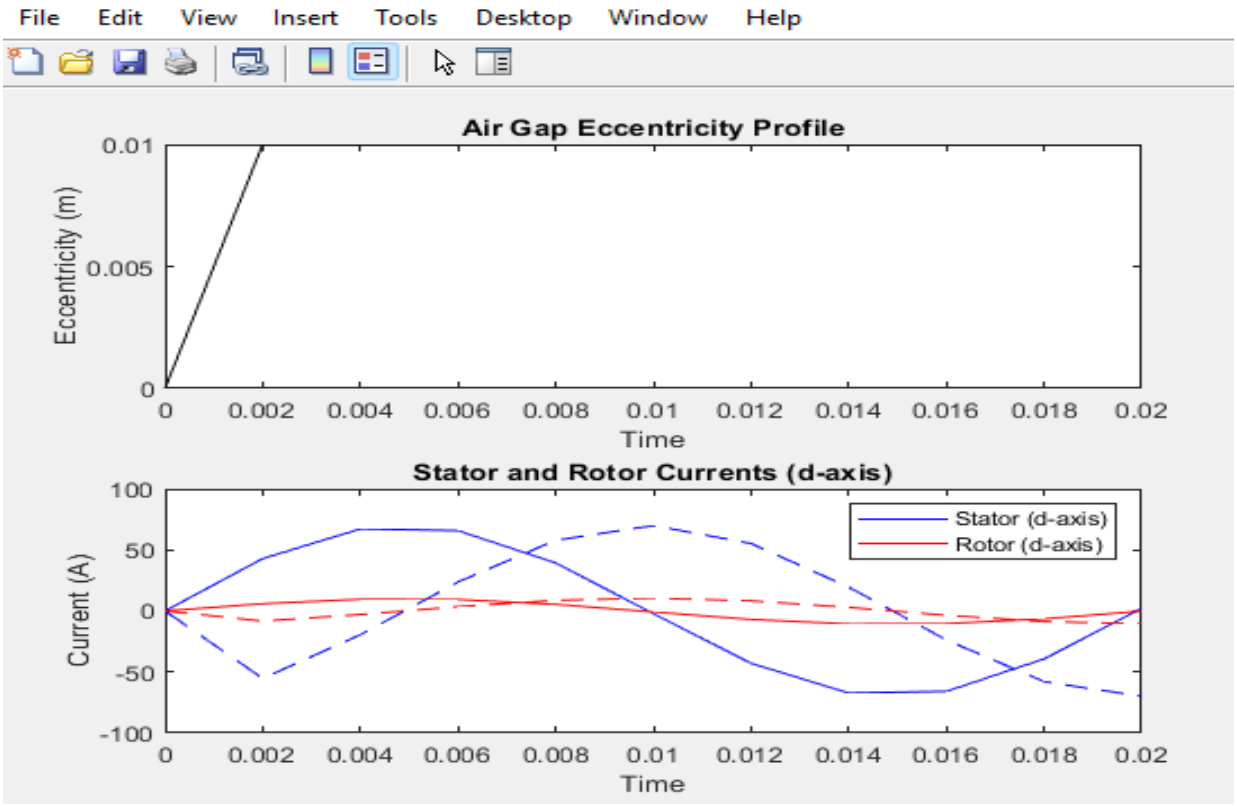

Figure 5.2.3(a)

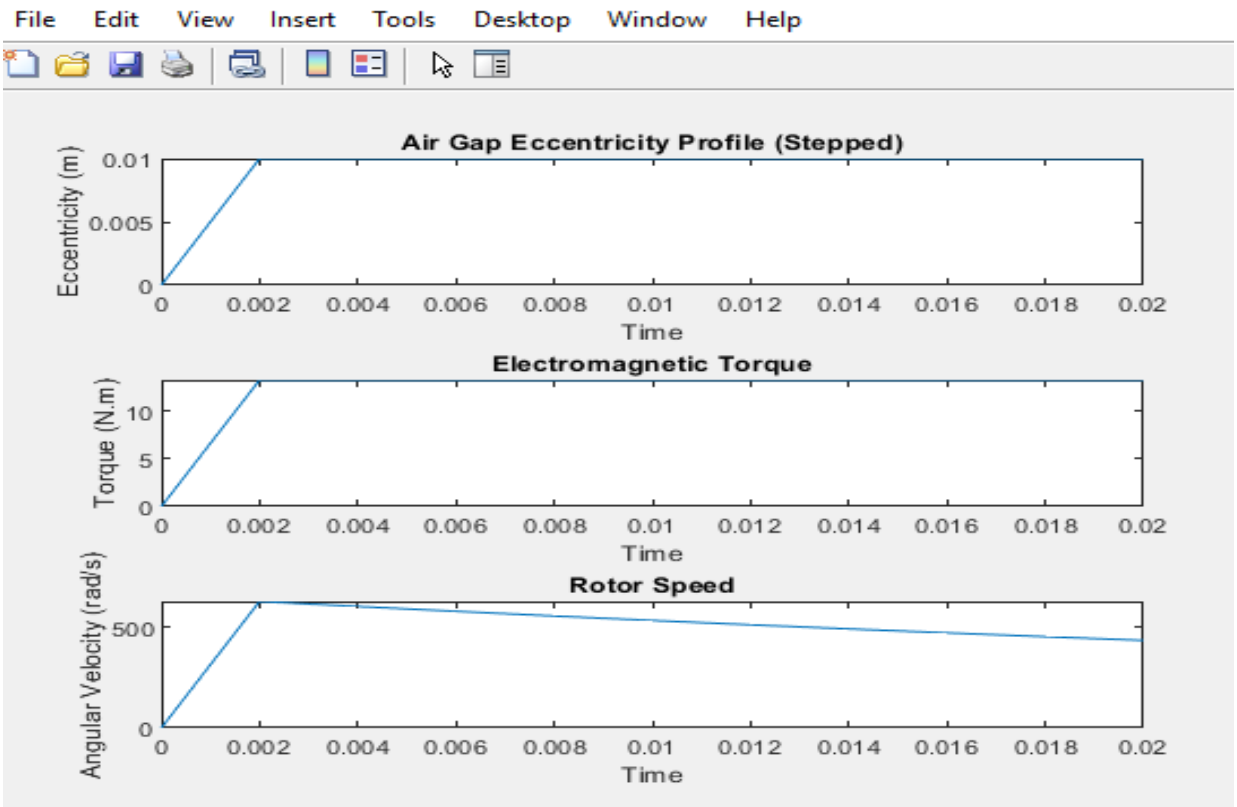

Figure 5.2.3(b)

Chapter 6

Conclusion

6.1 Contribution to the work

First of all a literature review is done after doing a literature survey related to the research area that is air gap eccentricity.

Induction motors are by far the most used Electrical Machine in industry. And of all the motors, induction motors are most commonly deployed in industry wherever mechanical power is required as around in 95% of such scenarios Induction Motor is used and they consume approximately 40% of all the electrical energy generated. Induction motors, like other types of motors, may malfunction despite their high reliability, low failure rates, and ease of maintenance. Unexpected motor failures result in unacceptably high levels of output loss. These malfunctions are unacceptably unacceptable when applied to induction motors, which are essential in every sector.

Air Gap Eccentricity is one of the main reason of failure of an Induction Motor as the motor with eccentricity causes different level of voltage induction, mechanical rub, productions of acoustic noises and mechanical air gaps. Despite them being indispensable, there are no lucid modelling of Air gap eccentricity available.

In this thesis the modelling of Air Gap eccentricity of Induction motor under simple eccentricity profiles is done so as to analyze Motor Currents, Angular Speed and Electromagnetic Torque under these profiles. Although in reality the eccentricity profiles are more complex and may involve combination of these or other eccentricity profiles such as Cycloidal, Harmonic, Parabolic, Tangential, Radial, Bezier, Catmul-rom, B spline and Fillet profiles.

First of all DQ model of an Induction motor is driven using equations in MATLAB code then Eccentricity profiles are deployed and the overall code is modified by introducing change in the inductance value. The plot of motor parameters are obtained. Another DQ model of Induction motor is derived and by modifying IEEE induction motor under steady state to its Thevenin equivalent circuit Electromagnetic Torque and Angular Speed are plotted under No load condition. We then plotted both real and imaginary part of the induction motor current alongside these eccentricity profiles.

6.2 Future Scope of the work

While in this thesis only elliptical, stepped and sinusoidal profiles are studied and deployed in induction motor dynamic simulation. There are several other profiles such as Cycloidal, Harmonic, Parabolic, Tangential, Radial, Bezier, Catmul-rom, B spline and Fillet profiles that are used in mathematics to express the eccentricity. More and more Air Gap Eccentricity Modelling can be done by using these profiles or combination of them.

References

[1] J. R. Cameron, W. T. Thomson, and A. B. Dow, “Vibration and cunent monitoring for detecting airgap eccentricity in large induction motors,” Proc. Inst. Elect. Eng.,, vol. 133, pt. B, no. 3, pp. 155-163, May 1986.

[2] W. T. Thomson, “On-line current monitoring to diagnose shaft misalignment in three-phase induction motor drive systems,” in Proc. ICEM’94, Paris, France, 1994

[3] D. G. Dorrell, “The sources and characteristics of unbalanced magnetic pull in cage induction motors with either static or dynamic rotor eccentricity,” in Stockholm Power Tech. Con$, Stockholm, Sweden, June 18-22, 1995, pp. 229-234.

[4] J. Penman, M. N. Dey, A. J. Tait and W. E. Bryau, “Condition Monitoring of Electrical Drives,” Proceedings IEE, Pt B, Vol. 133, No 3, pp 142-148, May, 1981

[5] EPRI, “Improved motors for utility applications and improved motors for utility applications industry assessment study”, Vol. 1, EPRI EL-2678, 1763-1, final report, and Vol. 2, 1763-1 final report, October 1982

[6] D. G. Dorrell, W. T. Thomson, and S. Roach, “Analysis of airgap flux, current, and vibration signals as a function of the combination fo static and dynamic airgap eccentricity in 3-phase induction motors,” IEEE Transactions on Industry Applications, Vol. 33, No. 1, Jan./Feb. 1997, pp24-34.

[7] W. T. Thomson and A. Barbour, “On-line current monitoring and application of a finite method to predict the level of static airgap eccentricity in three-phase induction motors,” IEEE Transactions on Energy Conversion, Vol. 13, No. 4, Dec. 1998, pp347-357.

[8] W. T. Thomson, D. Rankin, and D. G. Dorrell, “On-line current monitoring to diagnose airgap eccentricity in large three-phase induction motors-industrial case histories verify the predictions,” IEEE Transactions on Energy Conversion, Vol. 14, No. 4, Dec. 1999, pp1372-1378.

[9] W. T. Thomson, D. Rankin, and D. G. Dorrell, “On-line current monitoring to diagnose airgap eccentricity-an industrial case history of a large high-voltage three-phase induction motors,” Electric Machines and Drives Conference Record, 1997, ppMA2/4.1-MA2/4.3.

[10] W. T. Thomson and A. Barbour, “The on-line prediction of airgap eccentricity levels in large (MW range) 3-phase induction motors,” IEEE International Electric Machines and Drives Conference, 1999, pp383-385.

[11] R. Schoen and T. G. Habetler, “Effects of time-varying loads on rotor fault detection in induction machines,” IEEE Transactions on Industry Applications, Vol. 31, No. 4, July/Aug. 19995, pp900-906.

[12] R. Schoen and T. G. Habetler, “Effects of time-varying loads on rotor fault detection in induction machines,” IEEE Industry Applications Society Annual Meeting, 1993, pp324-330.

[13] R. Schoen, B. K. Lin, T. G. Habetler, Jay H. Schlag, and Samir Farag, “An unsupervised, on-line system for induction motor fault detection using stator current monitoring,” IEEE Transactions on Industry Applications, Vol. 31, No. 6, Nov./Dec. 1995, pp1280-1286.

[14] R. Schoen and T. G. Habetler, “Evaluation and implementation of a system to eliminate arbitrary load effects in current based monitoring of induction machines,” IEEE Transactions on Industry Applications, Vol. 33, No. 6, Nov./Dec. 1997, pp1571-1577.

[15] B. Yazici and G. B. Kliman, “An adaptive statistical time-frequency method for detection of broken bars and bearing faults in motors using stator current,” IEEE Transactions on Industry Applications, Vol. 35, No. 2, Mar./Apr. 1999, pp442- 452.

[16] A. Bellini, F. Filippetti, G. Franceschini, and C. Tassoni, “Closed-loop control impact on the diagnosis of induction motors faults,” IEEE Transactions on Industry Applications, Vol. 36, No. 5, Sept./Oct. 2000, 1318-1329.

[17] R. M. Tallam, T. G. Habetler, and Ronald G. Harley, “Stator winding turn-fault detection for closed-loop induction motor drives,” IEEE Industry Applications Society Annual Meeting, 2002, pp1553-1557.

[18] R. R. Obaid and T. G. Habetler, “Current-based algorithm for mechanical fault detection in induction motors with arbitrary load conditions,” IEEE Industry Applications Society Annual Meeting, 2003, pp. 1347-1351.

[19] R. R. Obaid, T. G. Habetler, and D. J. Gritter, “A simplified technique for detecting mechanical faults using stator current in small induction motors,” IEEE Industry Applications Society Annual Meeting, 2000, pp479-483.

[20] J. S. Hsu, “Monitoring of defects in induction motors through air-gap torque observation,” IEEE Transactions on Industry Applications, Vol. 31, No. 5, Sept./Oct. 1995, pp1016-1021.

[21] J. S. Hsu, H. H. Woodson, W. F. Weldon, “Possible errors in measurement of airgap torque pulsations of induction motors,” IEEE Transactions on Energy Conversion, Vol. 7, No. 1, Mar. 1992, pp202-208.

[22] S. Nandi, S. Ahmed, and H. A. Toliyat, “Detection of rotor slot and other eccentricity related harmonics in a three phase induction motor with different rotor cages,” IEEE Transactions on Energy Conversion, Vol. 16, No. 3, Sept. 2001, pp253-260.

[23] S. Nandi, R. Mohan Bharadwaj, and H. A. Toliyat, “Mixed eccentricity in three phase induction machines: analysis, simulation and experiments,” IEEE Industry Applications Society Annual Meeting, 2002, pp1525-1532.

[24] H. A. Toliyat, M. S. Arefeen, and A. G. Parlos, “A method for dynamic simulation of air-gap eccentricity in induction machines,” IEEE Transactions on Industry Applications, Vol. 32, No. 4, July/Aug. 1996, pp910-918.

[25] A. Bellini, et. al., “On-field experience with online diagnosis of large induction motors cage failure using MCSA,” IEEE Transactions on Industry Applications, Vol. 38, No. 4, July/Aug. 2002, pp1045-1053.

[26] W. T. Thomson and M. Fenger, “Industrial application of current signal analysis to diagnose faults in 3-phase squirrel cage induction motors,” Pulp and Paper Industry Technical Conference, 2000, pp205-211.

[27] M. E. H. Benbouzidi, M. Viera, and C. Theys, “Induction motors’ faults detection and localization using stator current advanced signal processing techniques,” IEEE Transactions on Power Electronics, Vol. 14, No. 1, Jan. 1999, pp14-22.

[28] M. E. H. Benbouzid, H. Nejjari, R. Beguenane, and M. Vieira, “Induction motor asymmetrical faults detection using advanced signal processing techniques,” IEEE Transactions on Energy Conversion, Vol. 14, No. 2, June 1999, pp147-152.

[29] A. Barbour and W. T. Thomson, “Finite element study of rotor slot designs with respect to current monitoring for detecting static airgap eccentricity in squirrelcage induction motors,” IEEE Industry Applications Society Annual Meeting, 1997, pp112-119.

[30] N. A. O. Demerdash and J. F. Bangura, “Characterization of induction motors in adjustable-speed drives using a time-stepping coupled finite-element state-space method including experimental validation,” IEEE Transactions on Industry Applications, Vol. 35, No. 4, July/Aug. 1999, pp790-802.

[31] W. N. Fu, P. Zhou, D. Lin, S. Stanton, and Z. J. Cendes, “Modeling of solid conductors in 2-D transient finite element analysis and its application to electric machines,” IEEE International Electric Machines and Drives Conference, 2003, pp1272-1278.

[32] X. Huang and T. G. Habetler, “Analysis of air gap eccentricity in closed-loop drive-connected induction motors,” IEEE International on Electric Machines and Drives Conference, 2003, pp1443-1447.

[33] H. Nejjari and M. E. H. Benbouzid, “Monitoring and diagnosis of induction motors electrical faults using a current Park’s vector pattern learning approach,” IEEE Transactions on Industry Applications, Vol. 36, No. 3, May/June 2000, pp730-735.

[34] A. J. M. Cardoso and E. S. Saraiva, “Computer-aided detection of airgap eccentricity in operating three-phase induction motors by Park’s vector approach,” IEEE Transactions on Industry Applications, Vol. 29, No. 5. Sept./Oct. 1993, pp897-901.

[35] A. Murray and J. Penman, “Extracting useful higher order featues for condition monitoring using artificial neural networks,” IEEE Transactions on Signal Processing, Vol. 45, No. 11, Nov. 1997, pp2821-2828.

[36] P. V. Goode and M-Y Chow, “Using a neural/fuzzy system to extract heuristic knowledge of incipient faults in induction motors: part I-methodology,” IEEE Transactions on Industrial Electronics, Vol. 42, No. 2, April 1995, pp131-138.

[37] P. V. Goode and M-Y Chow, “Using a neural/fuzzy system to extract heuristic knowledge of incipient faults in induction motors: part II-application,” IEEE Transactions on Industrial Electronics, Vol. 42, No. 2, April 1995, pp139-146.

[38] A. Bernieri, G. Betta, and C. Liguori, “On-line fault detection and diagnosis obtained by implementing neural algorithm on a digital signal processor,” IEEE Transactions on Instrumentation and Measurement, Vol. 45, No. 5, October 1996, pp894-899.

[39] Z. Ye, B. Wu, and A. R. Sadeghian, “Induction motor mechanical fault online diagnosis with the application of artificial neural network,” IEEE Applied Power Electronics Conference, 2001, pp1015-1020.

[40] M. E. H. Benbouzid and H. Nejjari, “A simple fuzzy logic approach for induction motors stator condition monitoring,” IEEE International Electric Machines and Drives Conference, 2001, pp634-639.

[41] G. Betta, M. D’Apuzzo, and A. Pietrosanto, ”A knowledge-based approach to instrument fault detection and isolation,” IEEE Transactions on Instrumentation and Measurement, Vol. 44, No. 6, Dec. 1995, pp1009-1016.

[42] A. J. Ellison and S. J. Yang, “Effects of rotor eccentricity on acoustic noise from induction machines,” Proceedings of IEE, 118, (1), 1971, pp174-184. [43] S. P. Verma and R. Natarajan, “Effects of eccentricity in induction motors,” International Conference of Electric Machines, 1982, pp930-933.

[44] K. J. Binns and W. T. Barnard, “ Some aspects of the use of flux and vibration spectra in electrical machines,” Proceedings of Conference on Applications on time-series analysis, University of Southampton, Southampton, UK, 1977, pp71.1-71.12.

[45] C. M. Riley, B. K. Lin, T. G. Habetler, and R. R. Schoen, “A method for sensorless on-line vibration monitoring of induction machines,” IEEE Transactions on Industry Applications, Vol. 34, No. 6, Nov./Dec. 1998, pp1240-1245.

[46] C. M. Riley, B. K. Lin, T. G. Habetler, and Gerald B. Kliman, “Stator current harmonics and their causal vibrations: a preliminary investigation of sensorless vibration monitoring applications,” IEEE Transactions on Industry Applications, Vol. 35, No. 1, Jan./Feb. 1999, pp94-99.

[47] X. Huang, T. G. Habetler, and R. G. Harley, “Detection of rotor eccentricity faults in closed-loop drive-connected induction motors using an artificial neural network,” IEEE Power Electronics Specialist Conference, 2004. [48] X. Huang and T. G. Habetler, “Detection of mixed air gap eccentricity in closedloop drive-connected induction motors,” IEEE International Symposium on Diagnostics for Electric Machines, Power Electronics and Drives, 2003, pp312- 316.

[49] J. R. Cameron, W. T. Thomson, and A. B. Dow, “Vibration and current monitoring for detecting airgap eccentricity in large induction motors,” Proceedings of IEE, Vol. 133, Pt. B, No. 3, May 1986, pp155-163.

[50] E. Wiedenbrug, G. Frey, and J. Wilson, “Impulse testing as a predictive maintenance tool,” IEEE International Symposium on Diagnostics for Electric Machines, Power Electronics and Drives, 2003, pp13-19. [51] Baker Instrument, “Digital surge / DC HiPot / resistance tester D3R/D6R/D12R users manual,” Baker Instrument Manual, 2000.

[52] J. Stack, “Fault signature detection for rolling element bearings in electric machines,” Ph.D. Dissertation, Georgia Institute of Technology, U.S., 2002.

[53] R. M. Tallam, “Current-based sensorless detection of stator winding turn faults in induction machines,” Ph.D. Dissertation, Georgia Institute of Technology, U. S., 2001.

[54] R. R. Obaid, “Detection of rotating mechanical asymmetries in small induction machines,” Ph.D. Dissertation, Georgia Institute of Technology, U.S., 2002.

[55] R. Schoen, “On-line current-based condition monitoring of three-phase induction machines,” Ph.D. Dissertation, Georgia Institute of Technology, U.S., 1994.

[56] N. Mohan, “Electric drives-an integrative approach,” year 2001 edition, published by MNPERE, 2001.

[57] G. Ellis, “Control system design guide: using your computer to understand and diagnose feedback controllers,” second edition, published by Academic Press, 2000.

[58] S. Haykin, “Neural networks: a comprehensive foundation,” second edition, published by Prentice Hall, 1999.

[59] Ansoft Corporate, “Maxwell® 2D field simulator,”Ansoft Corp. Manual, 2002.

[60] W. le Roux, R. G. Harley, and T. G. Habetler, “Rotor fault analysis of a permanent magnet synchronous machine,” International Conference on Electric Machines, Bruges, Belgium, 2002.

[61] N. A. Al-Nuaim and H. A. Toliyat, “A novel method for modeling dynamic airgap eccentricity in synchronous machines based on modified winding function approach,” IEEE Transactions on Energy Conversion, Vol. 13, No. 2, June, 1998, pp156-162.

[62] H. A. Toliyat, T. A. Lipo, and J. C. White, “Analysis of a concentrated winding induction machines for adjustable speed drive applications,” IEEE

Transactions on Energy Conversion, Vol. 6, No. 4, December, 1991, pp679-683.

[63] M. Haji and H. A Toliyat, “Pattern recognition-a technique for induction machines rotor fault detection ‘broken bar fault’”, International Conference on Electric Machines and Drives Conference, 2001, pp899-904.

[64] M. Haji and H. A. Toliyat, “Pattern recognition-a technique for induction machines rotor fault detection ‘eccentricity and broken bar fault’,” Industrial Applications Society Annual Meeting, 2001, pp1572-1578.

[65] G. B. Kliman and D. Song, “Remote monitoring of DC motor sparking by wavelet analysis of the current,” IEEE Symposium on Diagnostics for Electric Machines, Power Electronics and Drives, 2003, pp25-27.